Revista Mexicana de Astronomía y Astrofísica, Volumen 2, Enero 1977

AN ATLAS OF STELLAR SPECTRA. I

HAROLD L. JOHNSON

Instituto de Astronomía
Universidad Nacional Autónoma de México

and

Steward Observatory
University of Arizona

Received 1976 October 1

RESUMEN

Se da en este trabajo la primera parte de un nuevo Atlas de Espectros Estelares, ilustrándolo con diecisiete estrellas. El rango espectral se extiende en el infrarrojo más allá de diez mil angstroms; en el azul para algunos espectros, en 4000 Å y para otros en 4800 Å, aproximadamente. Todos los espectros se han corregido por extinción atmosférica y se han transformado (aproximadamente) a una base de igual flujo por unidad de frecuencia. Los anchos equivalentes de las líneas de hidrógeno de cuatro estrellas se han calculado y tabulado (ver Tablas 1-4). La descripción completa de los procedimientos y técnicas empleadas en la producción de estos espectros se dará en el segundo artículo de esta serie.

ABSTRACT

The first part of a new Atlas of Stellar Spectra is given here. In this paper are shown the spectra of 17 stars; all of the spectra include wavelengths beyond 10000 Å, and some are printed so far as 4000 Å in the blue. The spectra have been corrected for atmospheric extinction and have been transformed (approximately) to an equal-flux-per-unit-frequency basis. The equivalent widths of the hydrogen lines of four of the stars have been computed and tabulated. A complete description of the procedures and techniques used for the production of these spectra will be given in the second paper of this series.

Key words: FOURIER SPECTROSCOPY — NARROW BAND PHOTOMETRY — STARS (INDIVIDUAL)

This publication is the first in a series which will impart the stellar spectra obtained with a newly-developed Michelson spectrophotometer system. Included in this publication are a total of 17 spectra, all obtained during three nights in November 1975 on the 90-inch Steward Observatory telescope. A silicon photodiode was used as the radiation detector, allowing the coverage in one simultaneous spectrum of the entire wavelength range from 4000 Å to beyond 10000 Å. These 17 spectra were merely the first 17 to be reduced and the selection of stars here must not be taken as indicative of the extent of the whole program. We have another 25 stars on magnetic tape waiting for reduction, and we intend that the number of stars which will be observed in the manner illustrated here will be approximately 100.

The Michelson spectrophotometer system is not limited, however, to the present resolution nor to the use of silicon photodiodes. In the future, this program will include observations taken at higher and lower resolutions (depending upon the expected use of the spectra), and other detectors will be used. The spectrophotometer itself is capable of 0.5 cm^{-1} resolution and will operate efficiently over the full wavelength range out to nearly 6 micrometers in the infrared.

The resolution of the spectra reproduced here is 3.855 cm^{-1}, which corresponds to 3.855 Å at 10000 Å and 1.928 Å at 5000 Å. Since they are the uninterpolated output of a discrete Fourier transform, these spectra differ significantly from those produced by a spectrum scanner. They consist, in fact, of tables of spectral intensities as a function of frequency. Each entry represents the integrated flux over a frequency range of 3.855 cm^{-1}, centered on the tabulated frequency. A considerable amount of care was taken in the observations and data-reduction procedures to be sure that the data are photometrically linear (with zero intensity at the zero line in each graph) and that each individual spectral element is actually statistically independent of all the others. A second paper in this series, discussing in great detail the instrumentation and data reduction, will be also published in this Journal.

Without further justification here (because that justification will appear in the next paper), we state that these spectra consist of a series of spectral blocks, each 3.855 cm^{-1} wide, each of which is independent of all others except, of course, for the correlation introduced by the stellar spectrum itself (the observational data). Since there are about 4000 spectral elements in the wavelength range from 4000 Å to 10000 Å, it is quite valid to describe this work as "4000-color photometry" —a new photometric system which has narrow-band, square-topped filters 3.855 cm^{-1} wide, with no significant "tails" on either side. This "4000-color photometry" can be corrected for atmospheric extinction by standard photometric techniques (with due attention to the extinction coefficients and extinction law for spectral elements in regions of high atmospheric absorption). It can, furthermore, be placed on an absolute basis by comparison with the 13-color photometry of Johnson and Mitchell (1975). All of the spectra proffered in this paper have been corrected for atmospheric extinction and have been put (approximately) on a constant-flux-per-unit-frequency system. This means that (except for certain blue stars whose spectra were tilted as described in the descriptions of the figures) a horizontal straight line on the spectral plots represents constant flux per unit frequency interval. From this point, the absolute flux at any wavelength may be obtained by use of the known absolute calibrations for these stars (Johnson and Mitchell 1975).

At this point in time, the absolute calibration of the 4000-color photometry (or spectroscopy) is only approximate ($\pm$ 10%). Greater precision will be possible when a larger sample of stars, observed on more than 3 nights, is available. The user of these spectra should understand, however, that the quoted $\pm$ 10% error of the absolute calibration does not apply to adjacent or nearby spectral elements (the plotted noise blocks represent this uncertainty) but means merely that the average value of a number of spectral elements may differ in absolute calibration from another such block of elements two to four thousand Angstroms distant.

In principle, these spectra should be plotted as points, or as histograms. Point plots, however, are very difficult for a person to interpret visually, while histograms present a peculiar appearance to most astronomers, who are more accustomed to the type of continuous spectrum produced by spectrum scanners. As a compromise, we have plotted the point-by-point spectra, with straight lines connecting the points. This procedure is illustrated in Figure 1, which exhibits on a greatly expanded scale the Hβ line of α Cygni. The diamonds call attention to, and enclose, the individual points. All of the stellar spectra are plotted in this manner (except, of course, the diamonds are omitted).

The computation of the equivalent widths of spectral features is particularly easy with these photometric spectra. We have written an interactive computer program for computing equivalent widths directly from the data file in the computer memory.

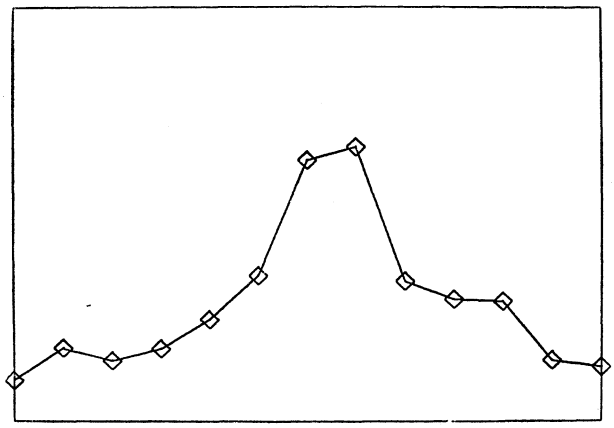

FIG. 1. The Hβ line of α Cygni greatly expanded, so as to show the individual data points and the straight lines connecting them. The diamonds enclose the individual data points.

The program allows the astronomer full control of the choice of continuum position and plots each continuum choice, along with the relevant spectral data, on an oscilloscopic display. When the astronomer is satisfied that the continuum choice is correct, he tells the computer to calculate the equivalent width of the feature. As examples of the results of this procedure, the measured equivalent widths of the hydrogen lines in four stellar spectra are listed in Tables 1 - 4. Many other features could have been measured, and such measures will indeed be contained in following interpretative papers. We emphasize that these computations were made using the data file in the computer; they were not derived from the plotted spectra.

In addition to the equivalent widths, the program also computes the wavelength of each measured line; these are the wavelengths listed in Tables 1-4. From a comparison of the lines measured in both α Cygni and ζ Orionis, the probable error of a single wavelength measure an ony line is $\pm$ 1.05 Å. From the means of all measured lines common to these two stars the difference in radial velocity is 33 $\pm$ 9 km s^{-1}, compared with the difference of 23 km s^{-1} from the Catalog of Bright Stars (Hoffleit 1964). Full details will be included in the following paper.

TABLE 1

THE MEASURED EQUIVALENT WIDTHS AND WAVELENGTHS OF THE HYDROGEN LINES OF α CYGNI.

	Å	1/cm	Å
LINE	LAMBDA	EQUIVALENT	WIDTHS
P7	10049.3	3.39	3.43
P8	9544.3	3.04	2.77
P9	9229.8	3.48	2.97
P10	9014.9	3.20	2.60
P11	8862.5	4.03	3.17
P12	8751.6	4.20	3.22
P13	8660.3	5.35	4.01
P14	8599.2	4.63	3.43
P15	8544.1	5.14	3.75
P16	8503.3	4.75	3.43
P17	8469.9	3.96	2.84
P18+0	8441.2	5.01	3.57
P19	8415.0	2.91	2.06
P90	8392.1	2.55	1.79
P21	8374.5	1.97	1.38
P22	8359.5	1.44	1.01
P23	8346.1	.79	0.55
P24	8334.1	.72	0.50
P25	8323.4	.68	0.47
P26	8314.1	.50	0.35
P27	8306.1	0.37	0.26
B3	6560.7	3.06	1.32
B4	4860.5	12.51	2.95
B5	4340.2	17.34	3.27
B6	4100.0	16.33	2.76
B7+CA	3967.5	25.31	3.98

TABLE 2

THE MEASURED EQUIVALENT WIDTHS AND WAVELENGTHS OF THE HYDROGEN LINES OF α PEGASI.

	Å	1/cm	Å
LINE	LAMBDA	EQUIVALENT	WIDTHS
P7	10049.2	11.35	11.46
P8	9544.5	13.69	12.47
P9	9224.2	14.89	12.67
P10	9019.4	13.56	11.03
P11	8869.6	13.44	10.58
P12	8755.6	11.62	8.91
P13	8668.1	9.56	7.18
P14	8602.0	6.11	4.52
P15	8548.2	4.82	3.52
P16	8506.1	2.82	2.04
P17	8471.5	1.08	0.78
B3	6562.2	24.65	10.62
B4	4860.9	59.55	14.07
B5	4339.5	83.63	15.75
B6	4146.5	95.37	16.16

It seems likely that other astronomers will want to analyze these spectra using their own computers; we do, therefore, offer (at the cost of production and shipping) magnetic-tape copies of these spectra, as plotted. They probably will be updated soon, when better extinction coefficients and absolute calibrations are available, but the present spectra may be useful to others as they are.

There have been published a number of atlases of stellar spectra, but most of them consist of reproductions of photographic spectral plates and none cover full spectral range out to 10000 Å, and beyond. None has the photometric precision of ours. However, because the present sample of spectra is not complete and a more meaningful discussion is possible in the near future when more data have become available, we defer such references and discussions to a later paper in this series. Furthemore, such references and discussions will also appear in interpretative papers now in preparation.

The individual spectra of the 17 stars are plotted in Figures 2 - 18. As indicated in the descriptions for each figure, all of the data have been put on an

TABLE 3

THE MEASURED EQUIVALENT WIDTHS AND WAVELENGTHS OF THE HYDROGEN LINES OF ζ PEGASI.

	Å	1/cm	Å
LINE	LAMBDA	EQUIVALENT	WIDTHS
P7	10049.3	10.28	10.38
P8	9533.3	11.48	10.43
P9	9230.2	11.17	9.52
P10	9014.9	14.00	11.38
P11	8861.1	11.79	9.26
P12	8753.1	10.25	7.86
P13	8668.2	8.66	6.51
P14	8600.7	5.91	4.37
P15	8548.3	4.17	3.05
P16	8503.5	1.88	1.36
P17	8470.1	1.35	0.97
B3	6559.3	19.89	8.56
B4	4861.0	43.26	10.22
B5	4339.7	55.50	10.45
B6	4103.0	49.01	8.25

TABLE 4

THE MEASURED EQUIVALENT WIDTHS AND WAVELENGTHS OF THE HYDROGEN LINES IN ζ ORIONIS.

	Å	1/cm	Å
LINE	LAMBDA	EQUIVALENT	WIDTHS
P7	10049.2	2.72	2.74
P8	9546.1	1.71	1.56
P9	9230.1	1.73	1.47
P10	9015.1	1.72	1.40
P11	8861.1	1.74	1.37
P12	8751.9	1.66	1.27
P13	8664.2	1.59	1.19
P14	8600.8	1.34	0.99
P15	8548.4	0.91	0.67
P16	8504.9	0.73	0.53
P17	8468.9	0.40	0.29
P18	8437.2	0.28	0.20
P19	8412.5	0.34	0.24
B3 ALL	6563.9	2.31	0.99
B3 ABS	6563.8	1.83	0.79
B4	4862.1	7.91	1.87
B5	4340.8	11.07	2.09
B6	4101.3	12.50	2.10
B7	3968.8	19.33	3.05

absolute flux basis; as indicated on the figures, the bluest stars have been plotted on a different scale, precisely related to the absolute scale, merely so that the spectra will be approximately horizontal over the whole range. (Please note that θ^1 Orionis C is erroneously called θ^1 Orionis A in the figure 15; θ^1 Orionis D is called θ^1 Orionis B in figure 16).

When this program was planned originally (about 14 months ago) it was expected that the shortest wavelength that would be included would be 4800 Å —to include Hβ but no shorter wavelengths. The quartz beam-splitter and the particular silicon photodiode were selected with this limit in mind. As a result, the spectra shown here are good to 4800 Å, but the sensitivity of the detector and the efficiency of the beam-splitter both drop off as wavelength becomes shorter.

When the data were reduced, however, we found that there are actually considerable usable data shortward of Hβ in many of the stellar spectra. Because of the drop-off in sensitivity, the signal-to-noise ratio becomes much poorer at short wavelengths and it was decided not to carry out the transformation to absolute flux for wavelengths shorter than about 4800 Å. The spectrum of α Cygni exhibits the effect of this decision. The computer files, which are kept on magnetic tape, contain exactly 4096 data points covering the range in wavelength from slightly shorter than 4000 Å to beyond 10000 Å. This is true of all of the spectra, even though the shorter-wavelength regions were not plotted in all of the diagrams. Any person who requests magnetic-tape copies of these spectra will receive for all stars the full data for the entire spectral region even if, as for example in Omicron Ceti, there is nothing but noise at the shorter wavelengths.

Since November 1975, a new silicon photodiode with much enhanced blue response (and much lower dark noise) has been installed and data taken in 1976 will be of higher quality, especially shortward of 4800 Å.

All of the observations contained in this first part of the Atlas of Stellar Spectra were obtained with the Steward Observatory 90-inch telescope on the nights of November 16, 17 and 18, 1975. Dr. Santiago Tapia assisted with the observations. The Fourier transforms of the co-added interferograms were performed on the DEC-system-10 computer of the University of Arizona; the digitization from the analog tapes, the coadding of the interferograms, and all of

the data-analysis (including the production of the spectral plots for publication) were done on a special NOVA computer setup. This NOVA computer has been specially programmed for this work.

Note added in proof:

Since the spectra printed in this paper were drawn, two changes were made: 1. The atmospheric extinction corrections have been improved; and, 2. a minor error in the Fourier-transform program was corrected. This error had the effect of reducing the spectral resolution somewhat. Both changes have been incorporated into the magnetic-tape spectra that will be made available upon request.

REFERENCES

Hoffleit, D. 1964 (New Haven: Yale Univ. Press.)
Johnson, H. L. and Mitchell, R. I. 1975, *Rev. Mex. de Astron. y Astrof.* **1**, 299.

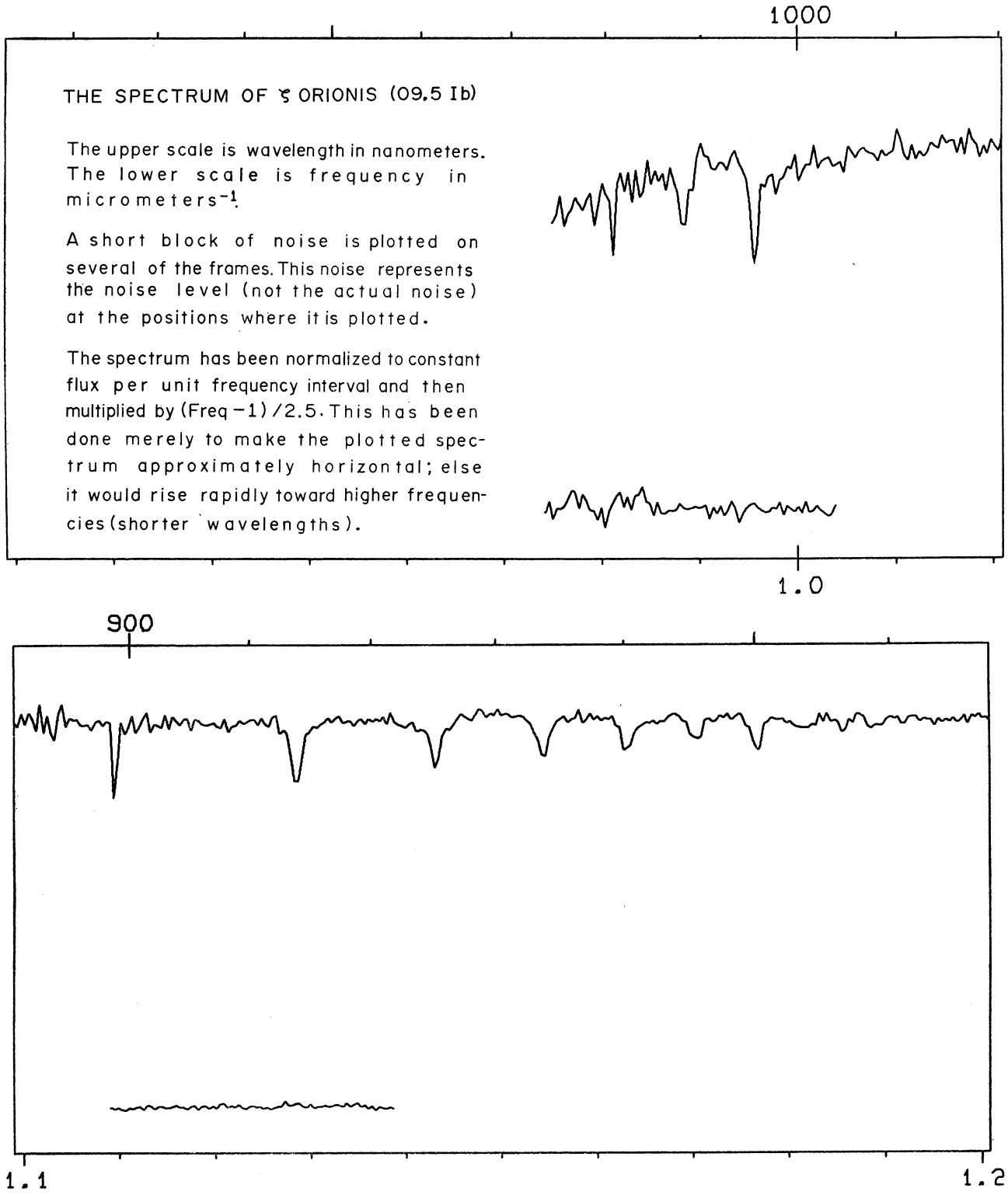

FIG. 2. The Spectrum of ζ Orionis (09.5 Ib)

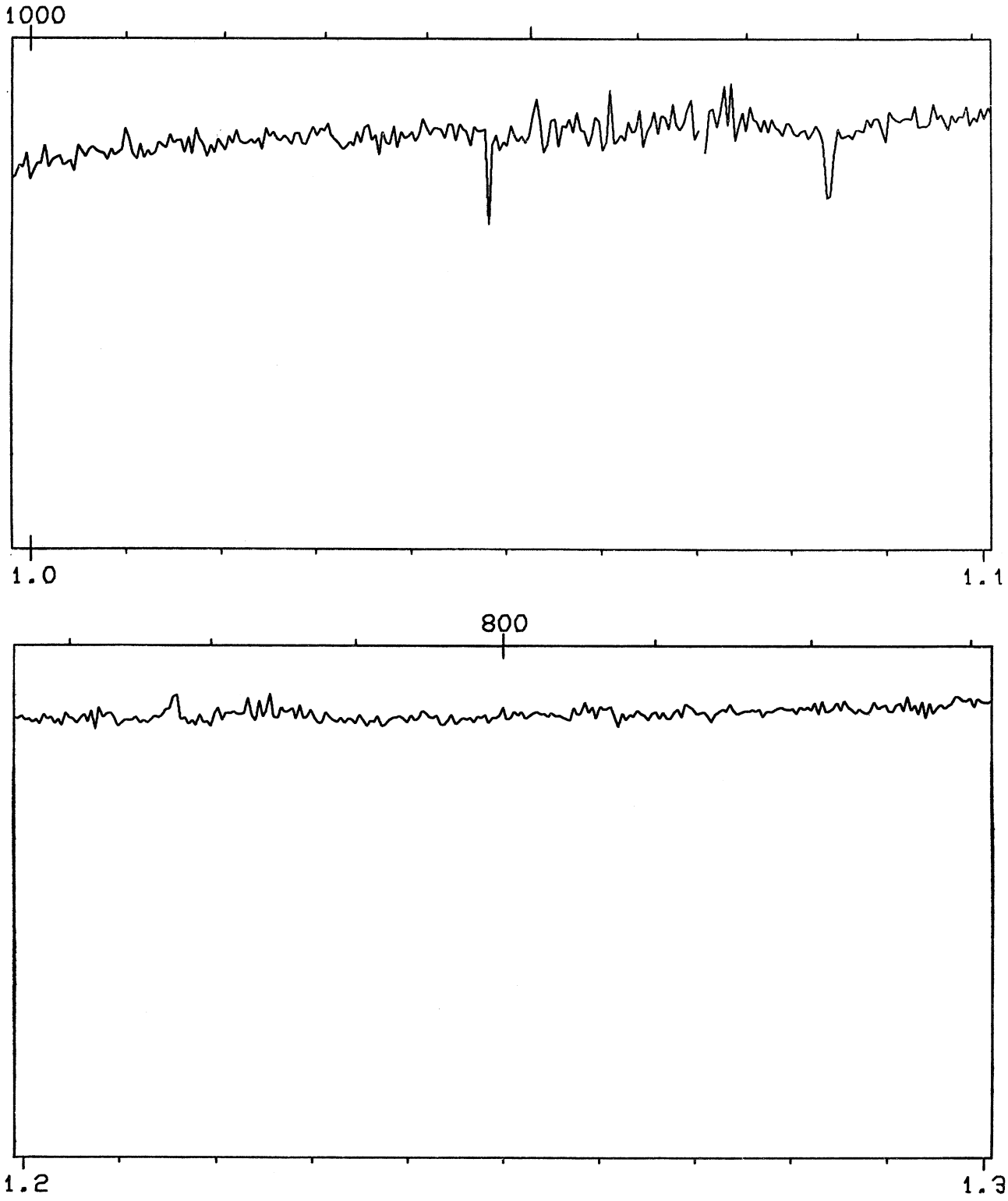

FIG. 2. The Spectrum of ζ Orionis (09.5 Ib)

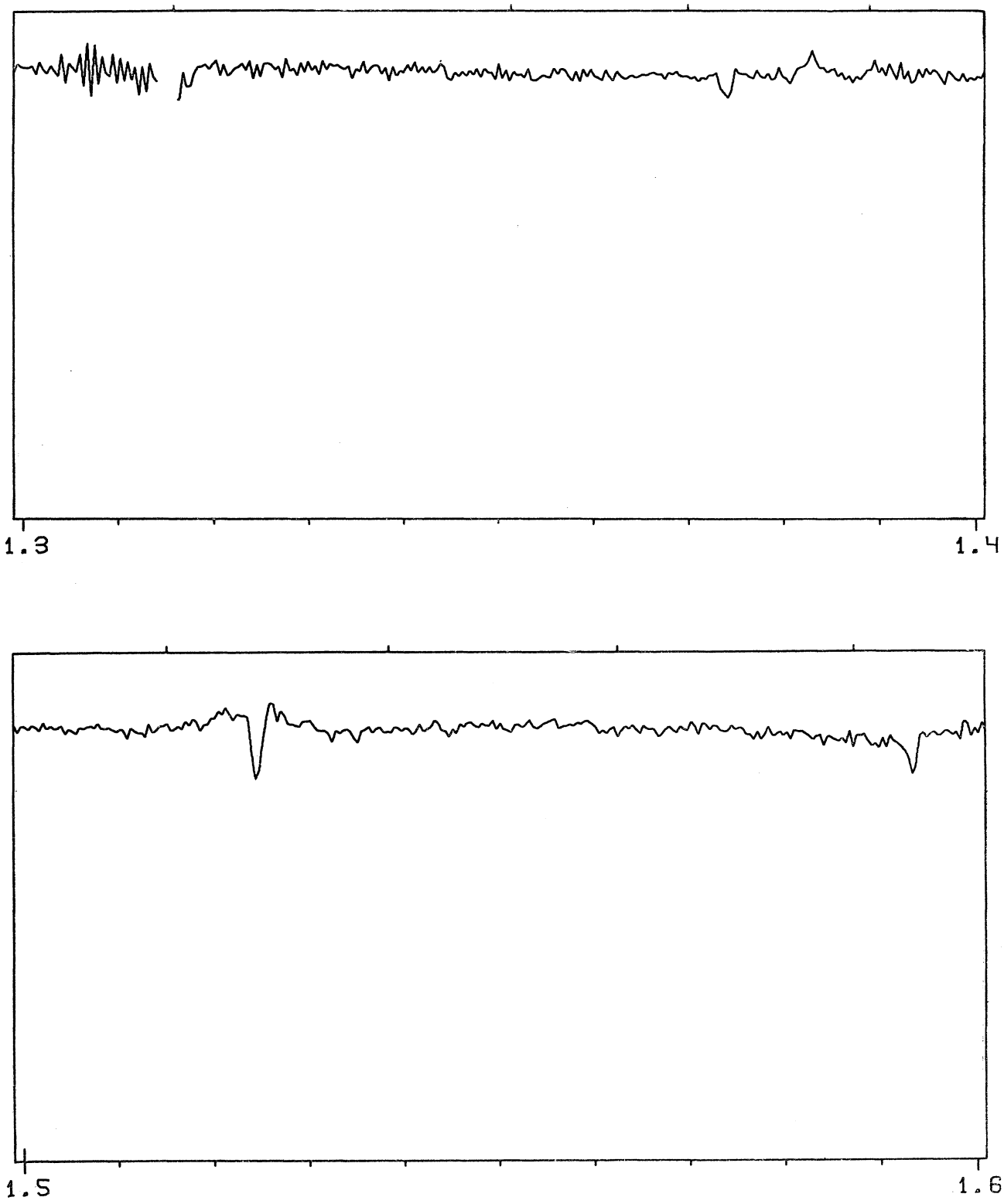

FIG. 2. The Spectrum of ζ Orionis (09.5 Ib)

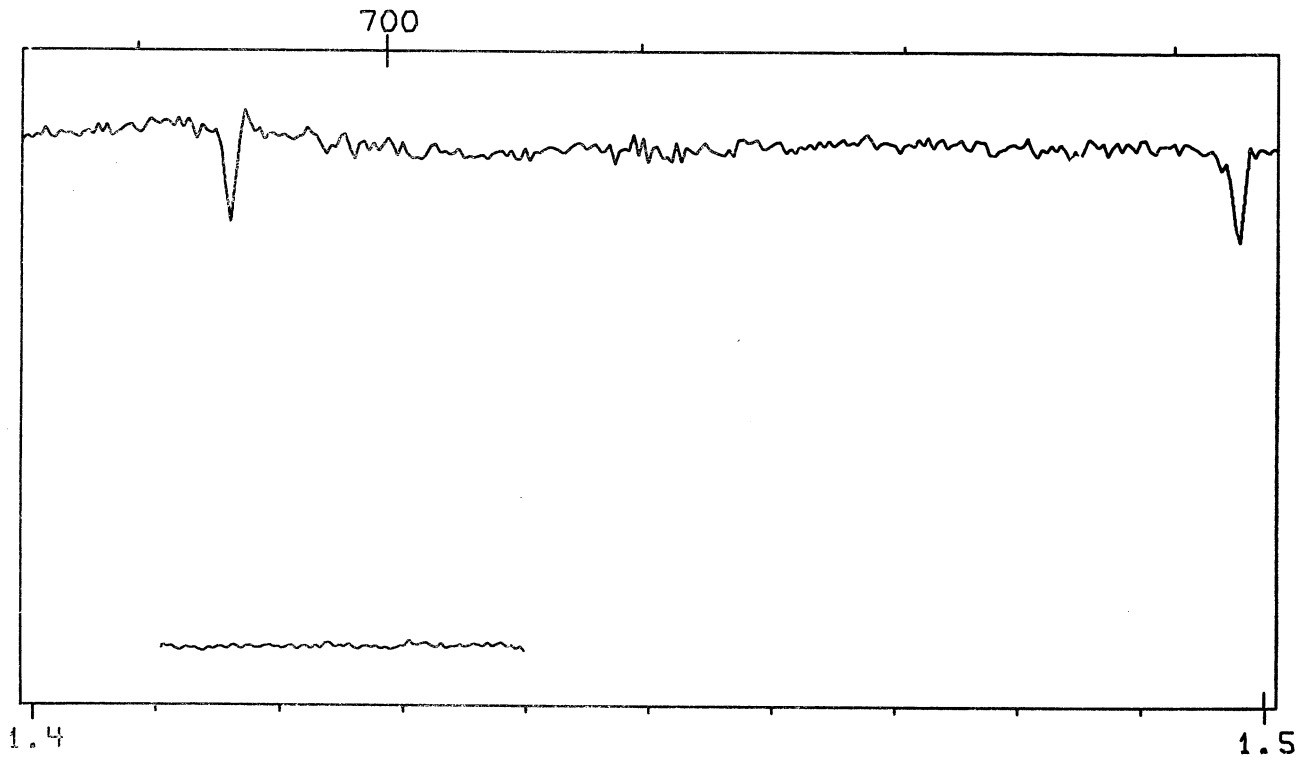

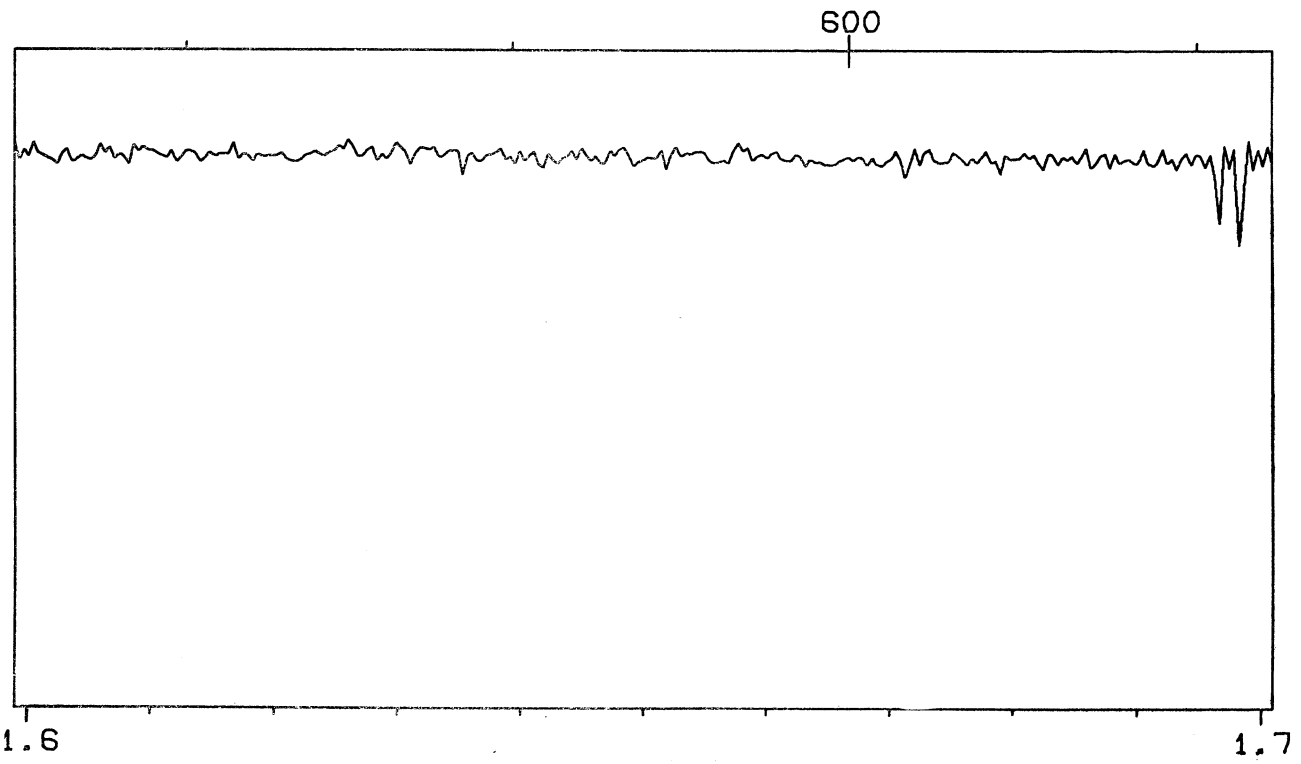

FIG. 2. The Spectrum of ζ Orionis (09.5 Ib)

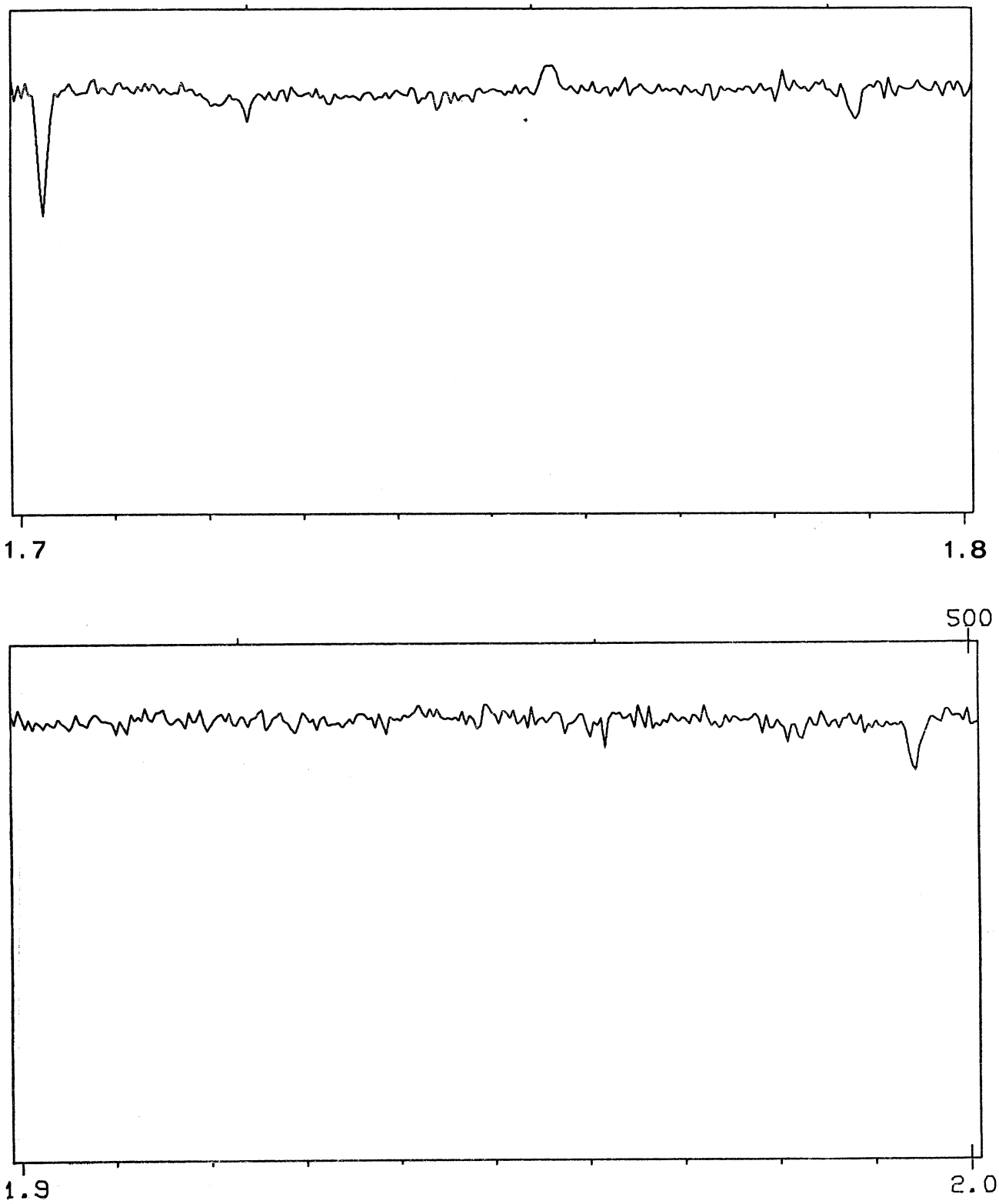

FIG. 2. The Spectrum of ζ Orionis (09.5 Ib)

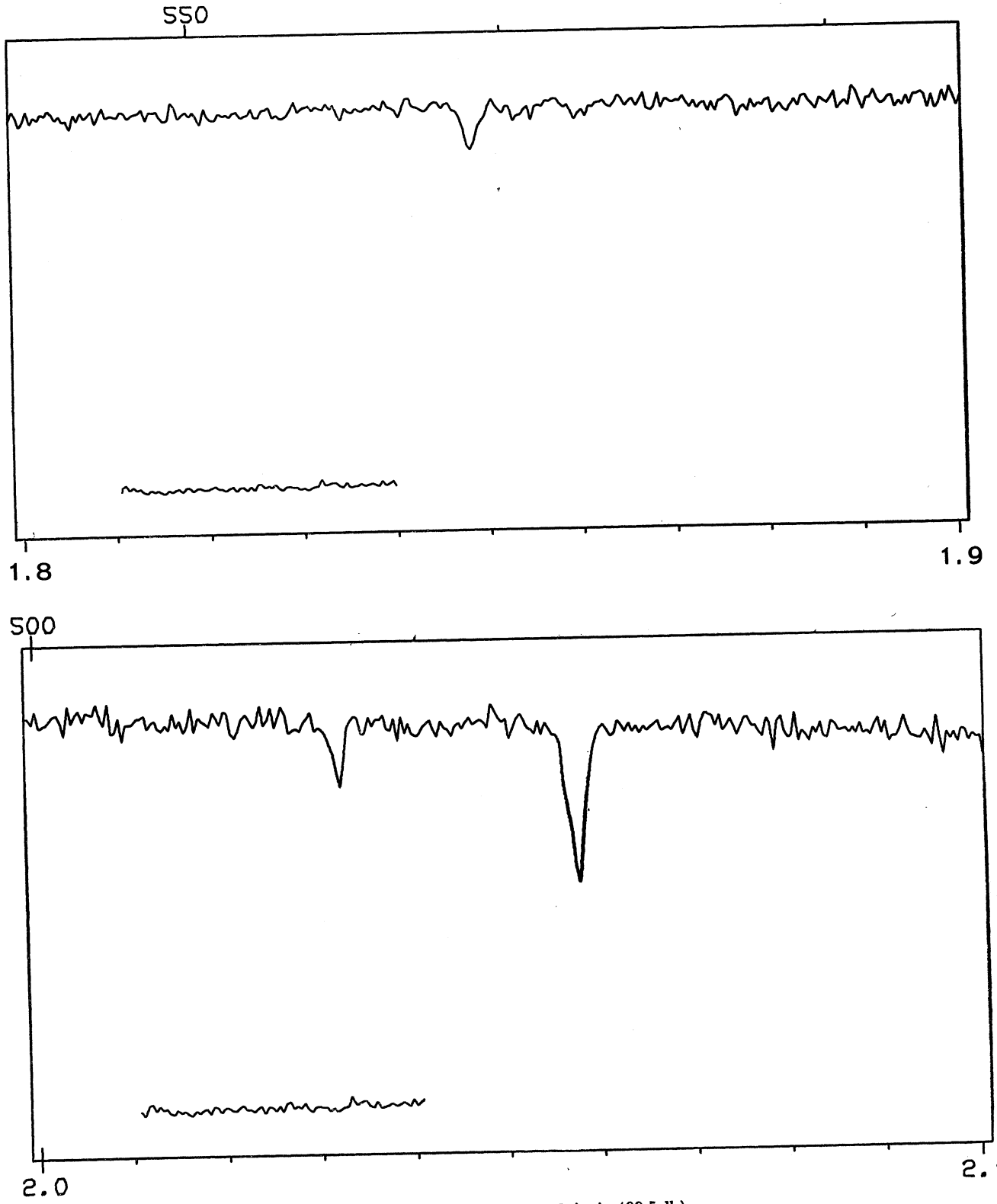

FIG. 2. The Spectrum of ζ Orionis (09.5 Ib)

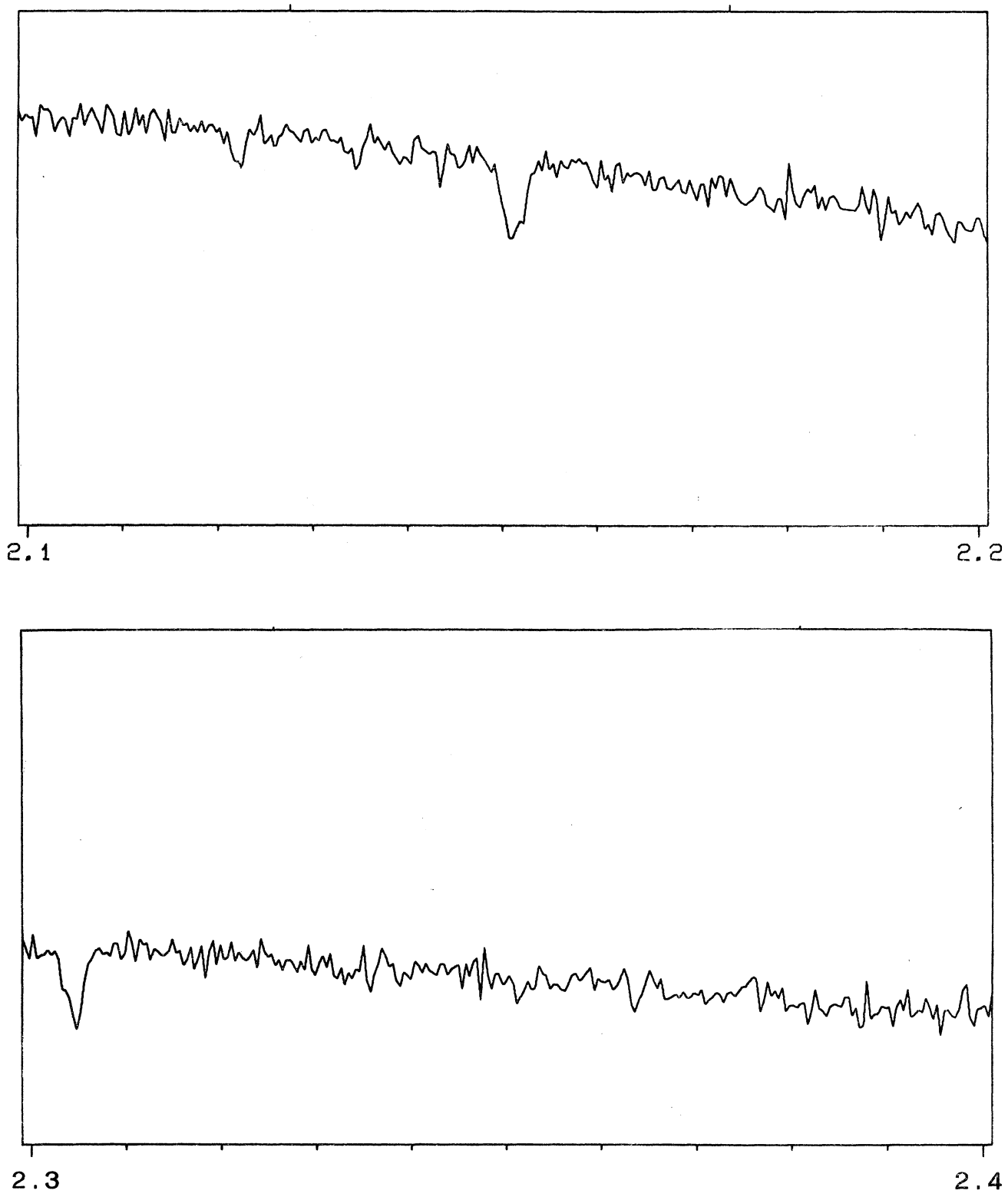

FIG. 2. The Spectrum of ζ Orionis (09.5 Ib)

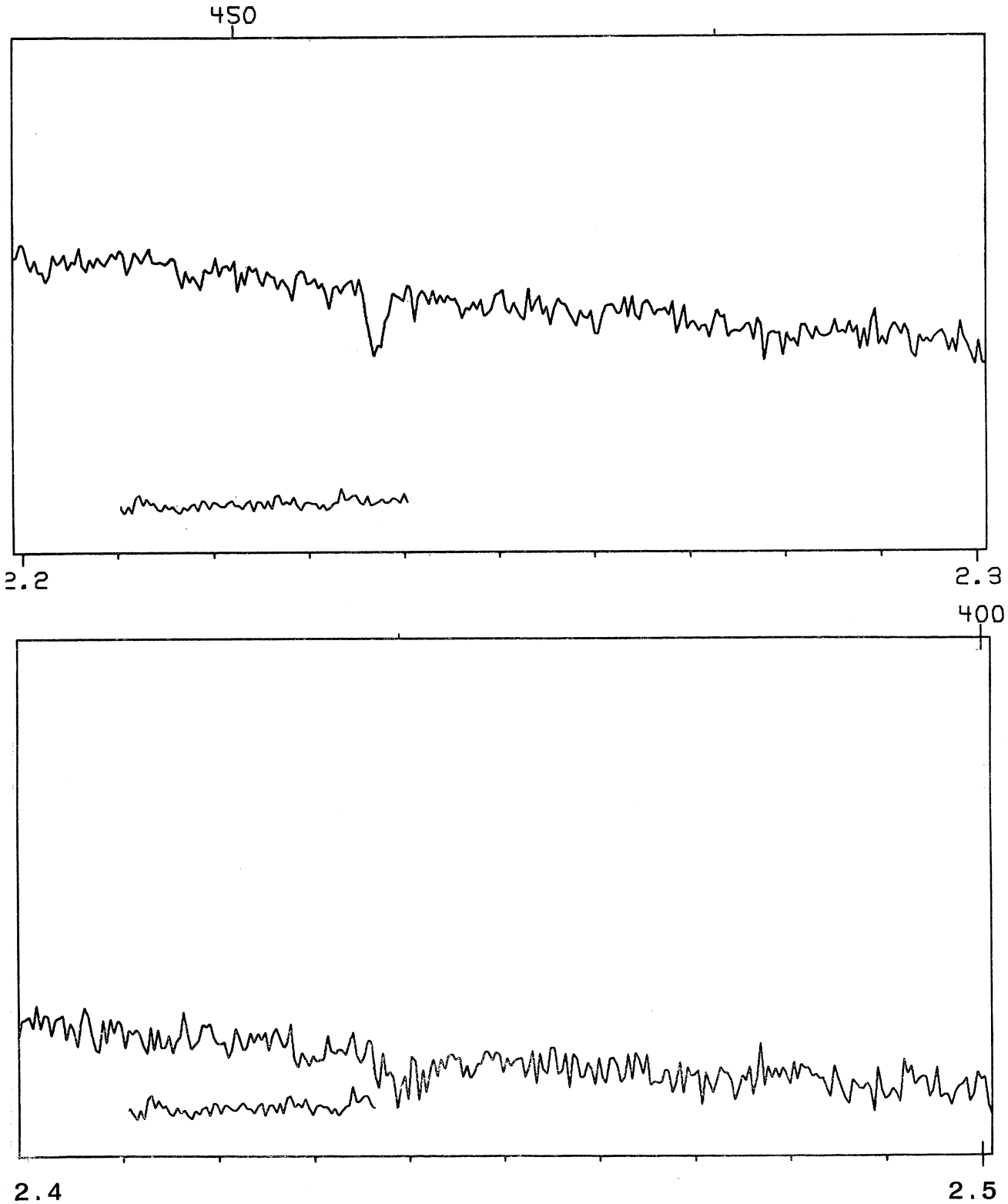

FIG. 2. The Spectrum of ζ Orionis (09.5 Ib)

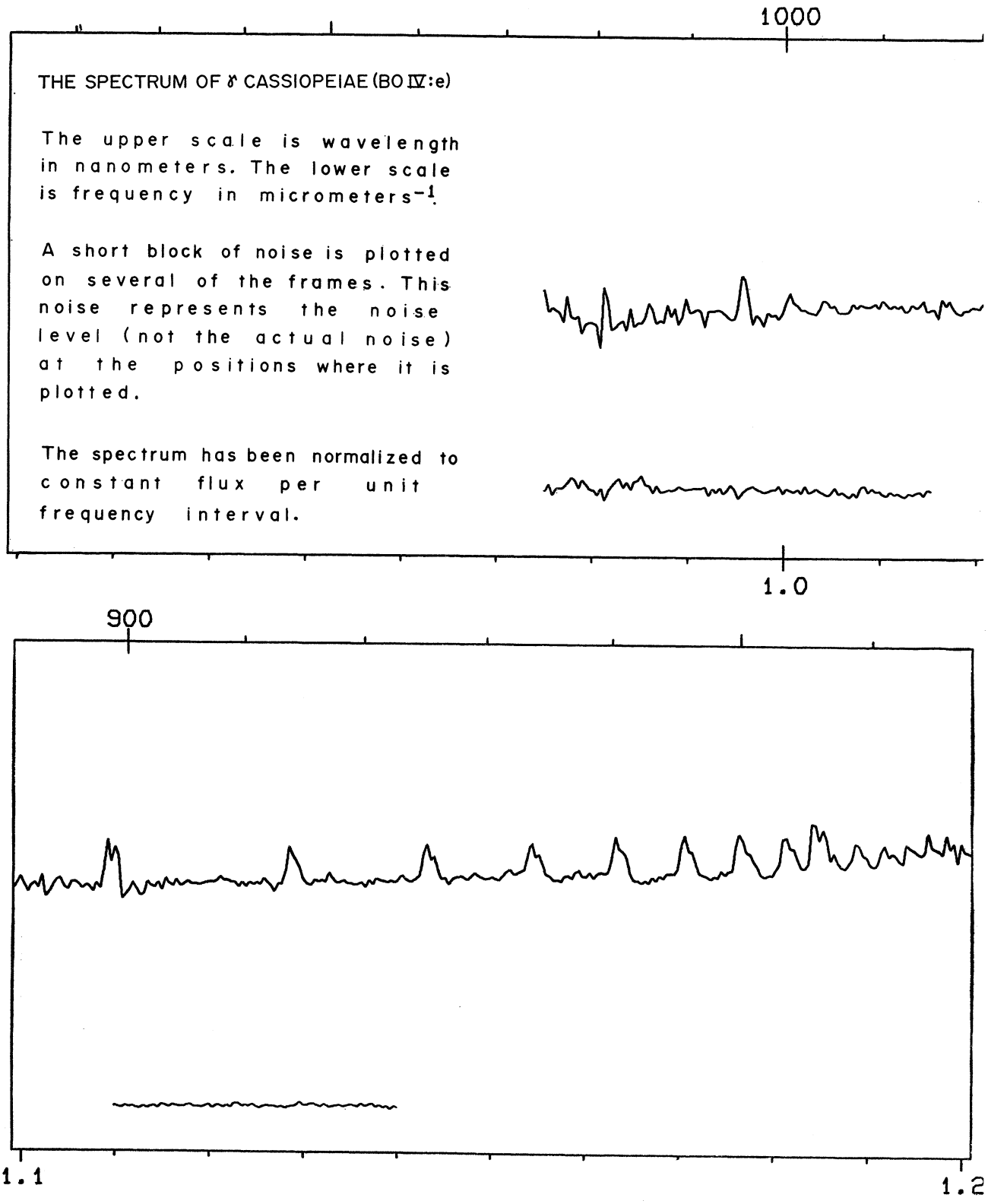

FIG. 3. The Spectrum of γ Cassiopeiae (BO IV:e)

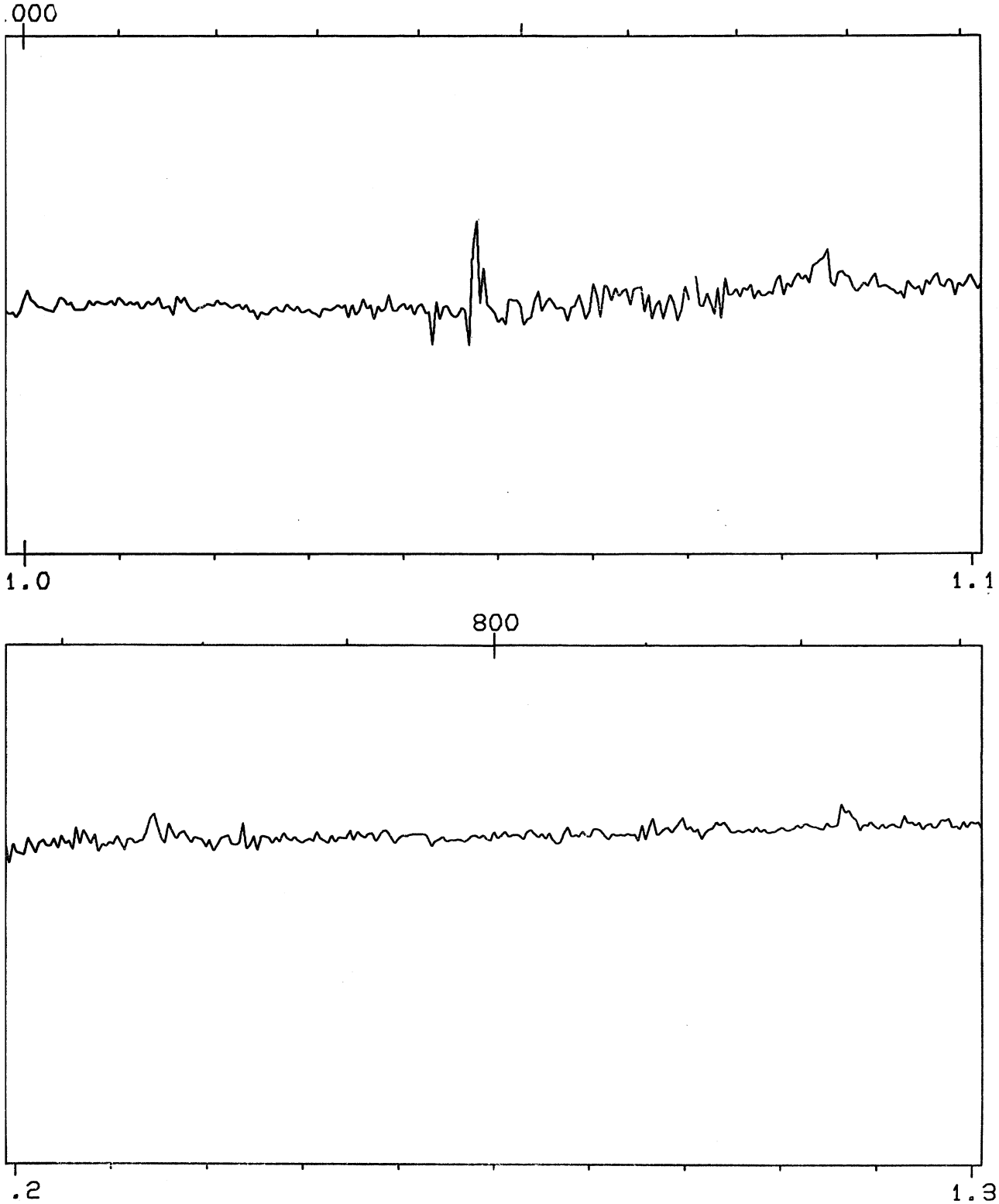

FIG. 3. The Spectrum of γ Cassiopeiae (BO IV:e)

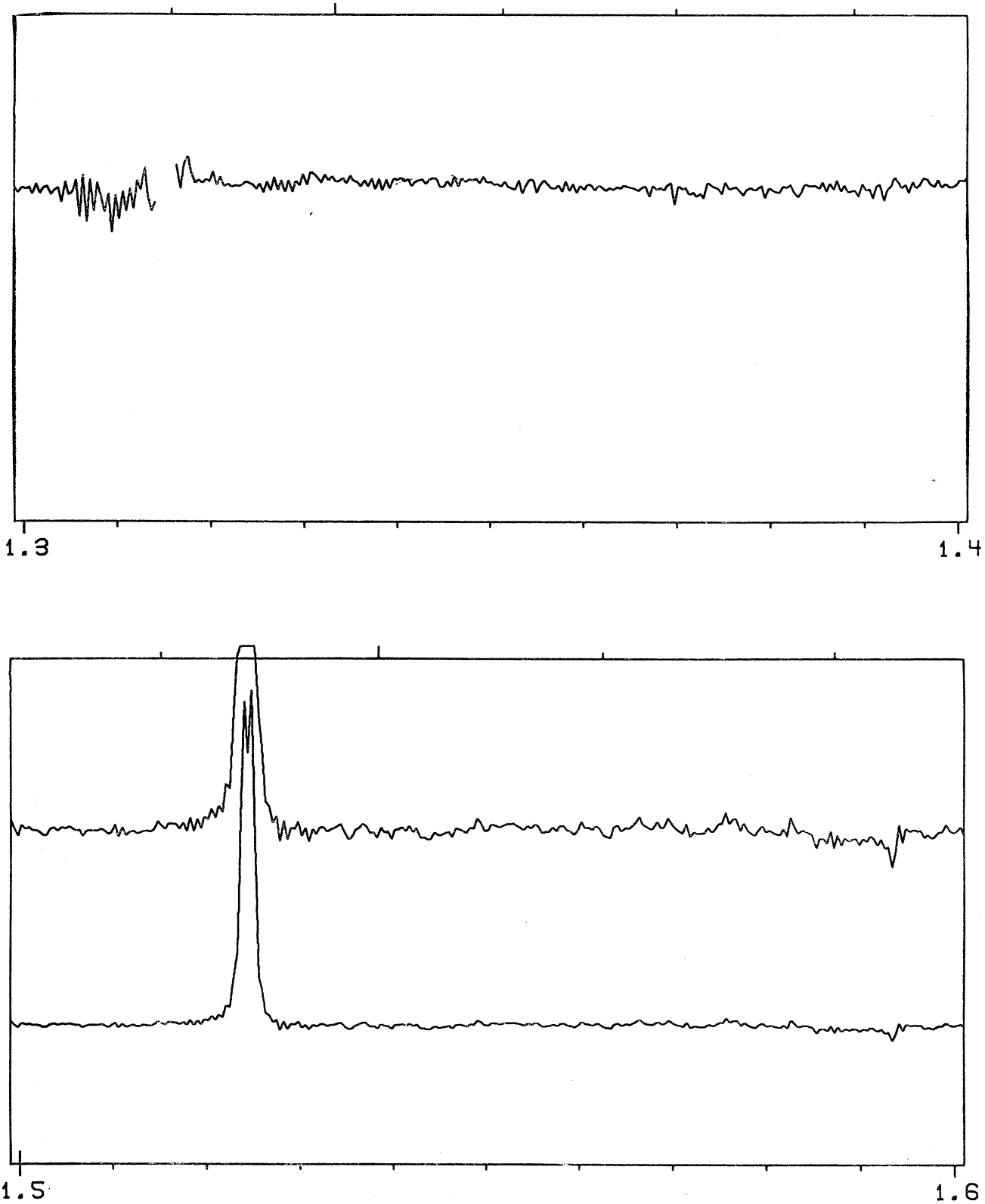

FIG. 3. The Spectrum of γ Cassiopeiae (BO IV:e)

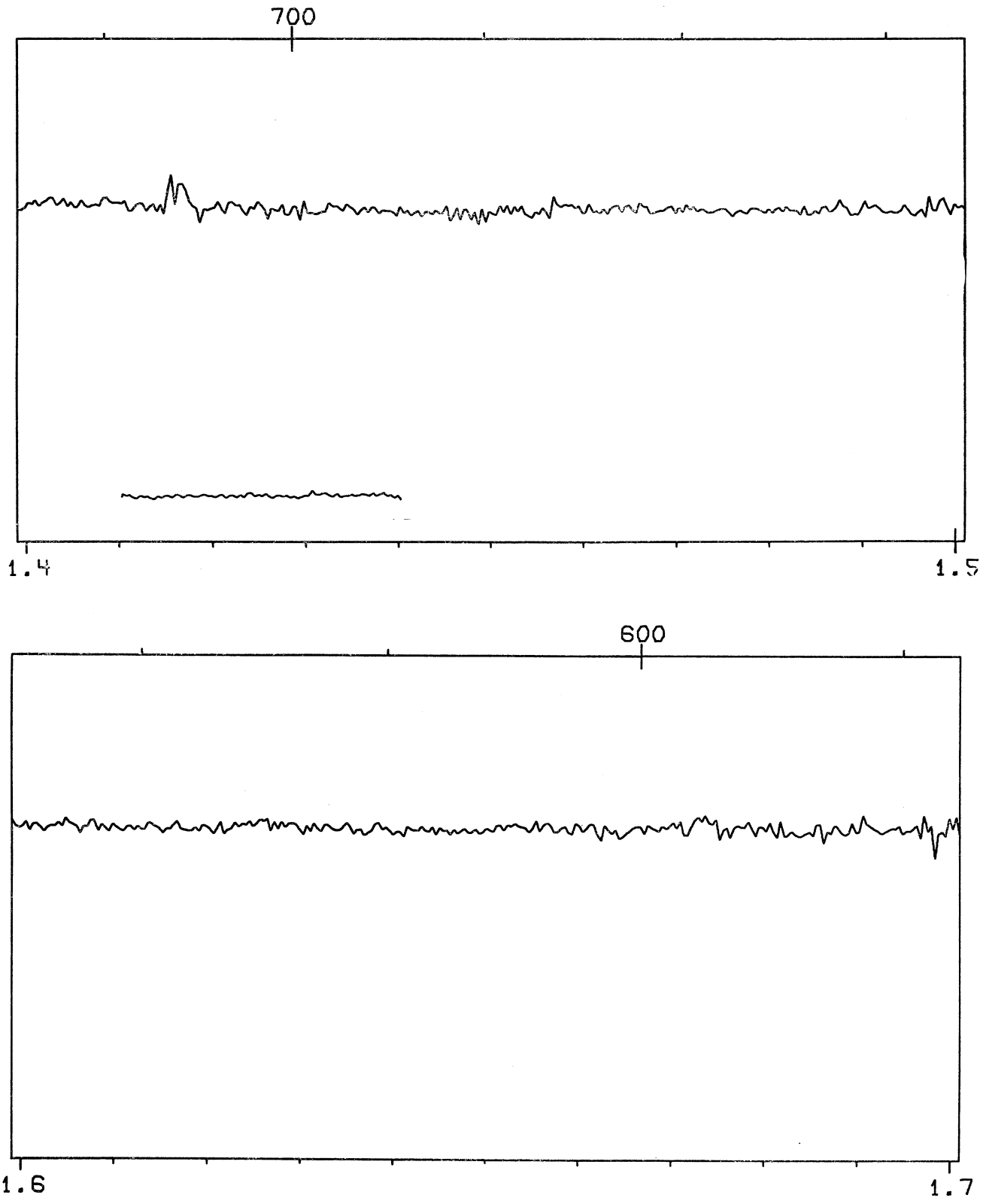

FIG. 3. The Spectrum of γ Cassiopeiae (BO IV:e)

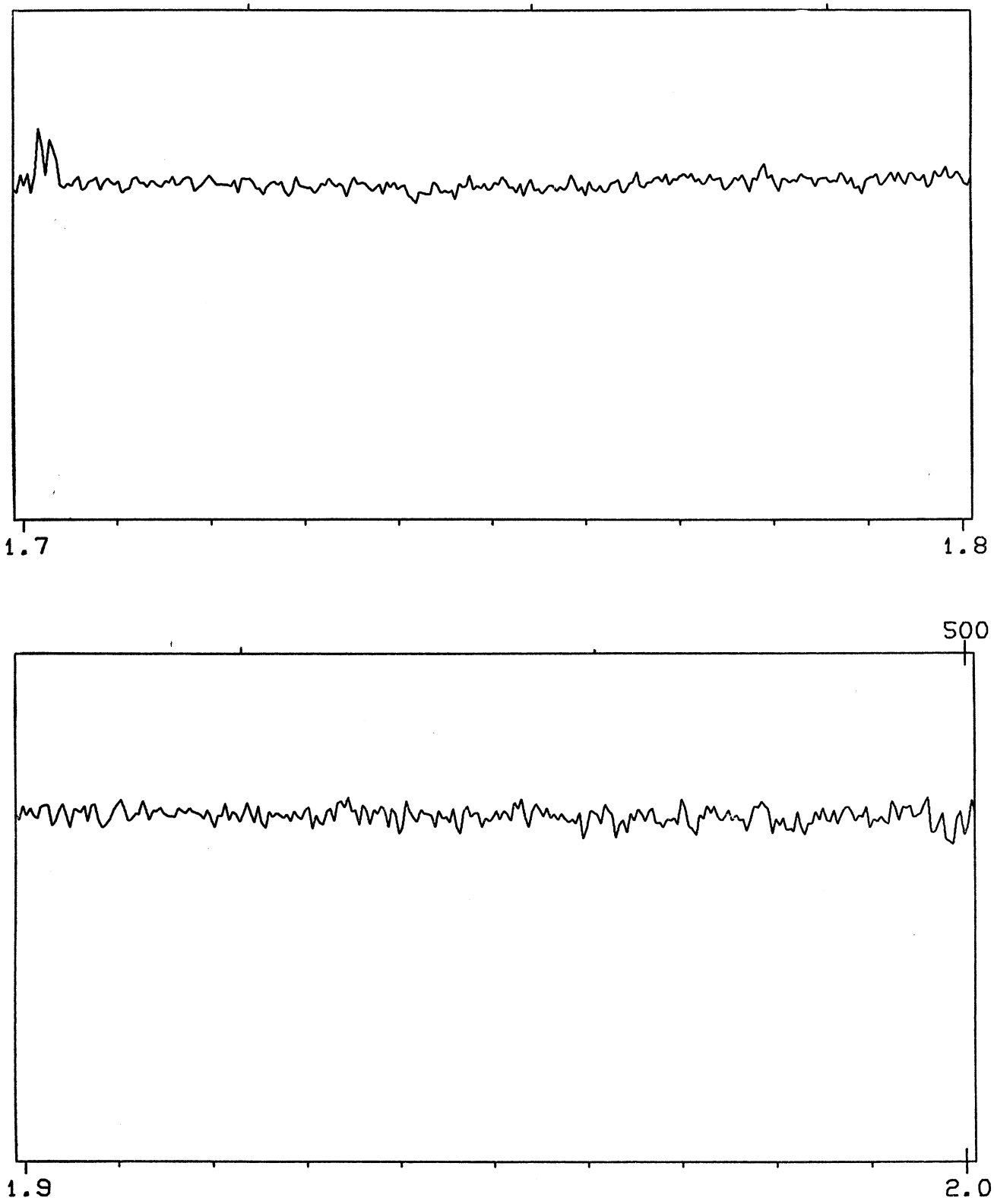

FIG. 3. The Spectrum of γ Cassiopeiae (BO IV:e)

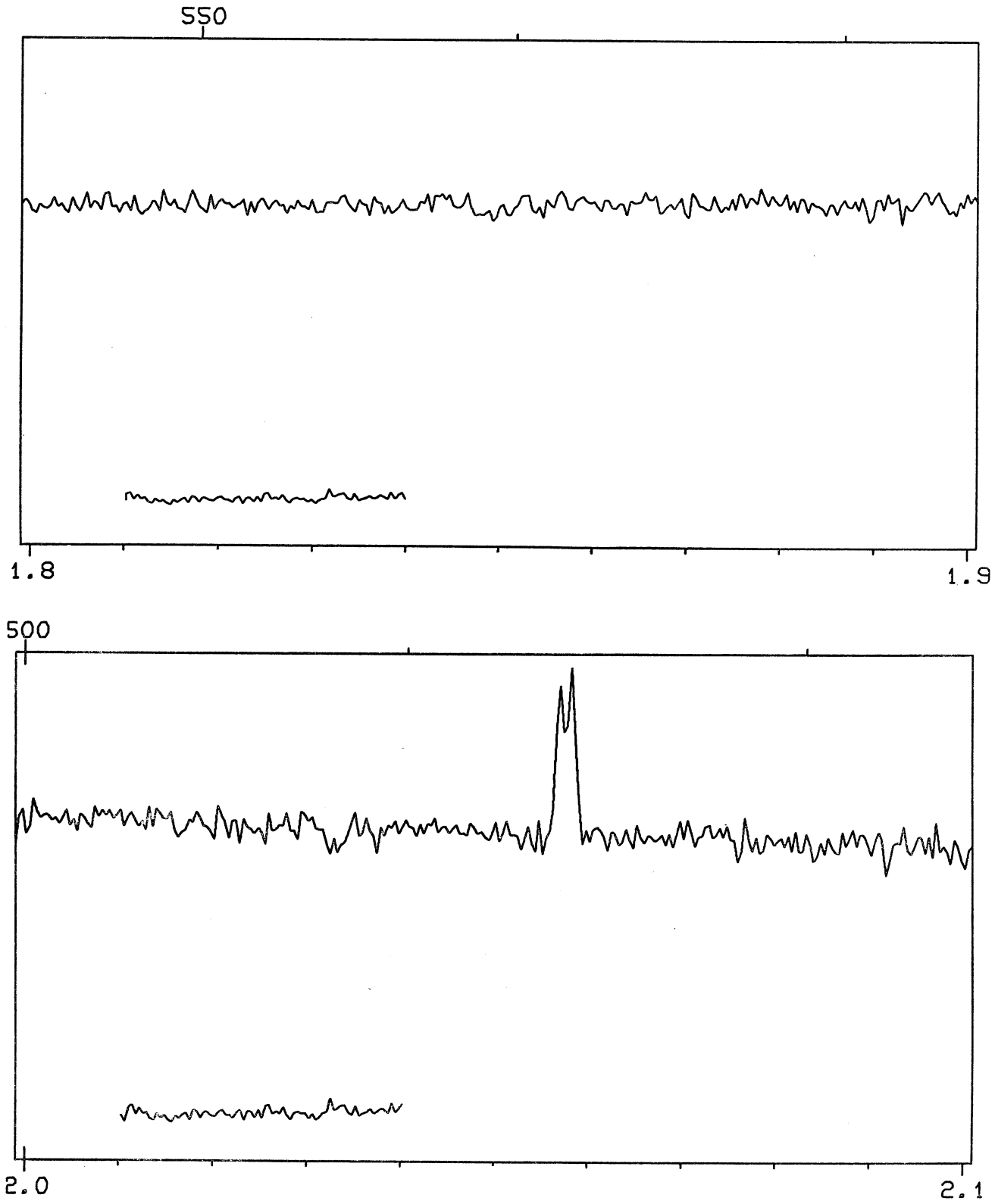

FIG. 3. The Spectrum of γ Cassiopeiae (BO IV:e)

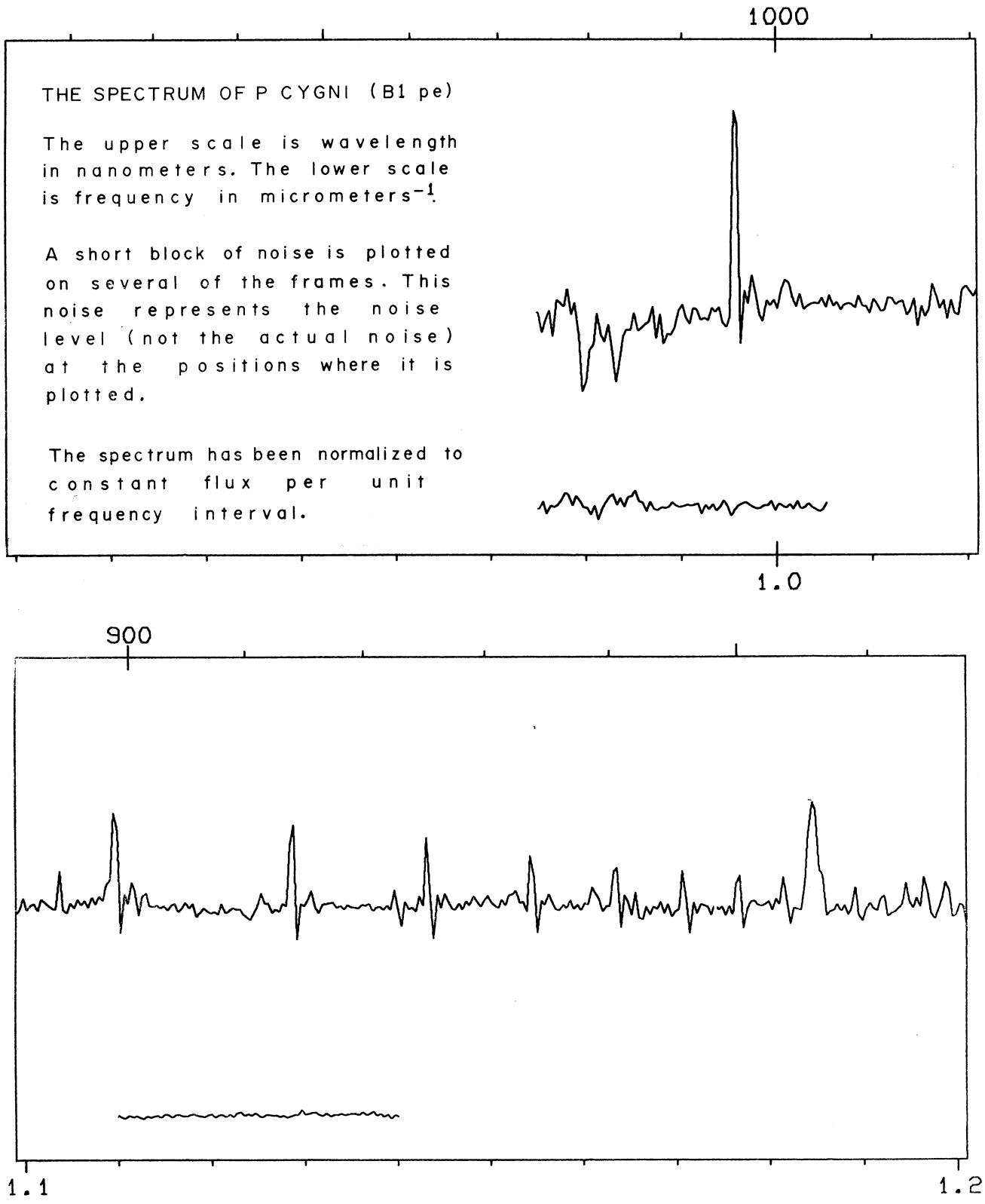

FIG. 4. The Spectrum of P Cygni (B1 pe)

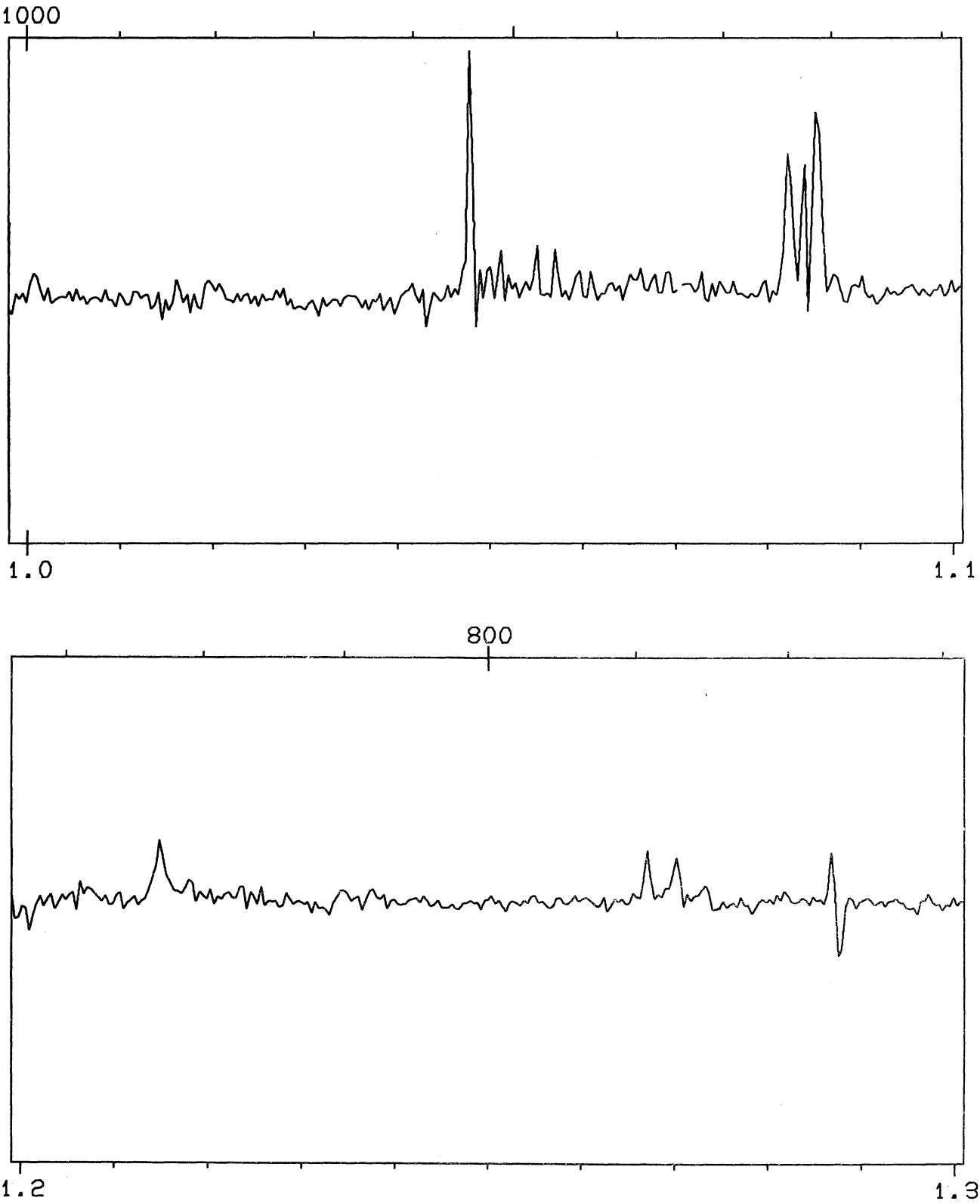

FIG. 4. The Spectrum of P Cygni (B1 pe)

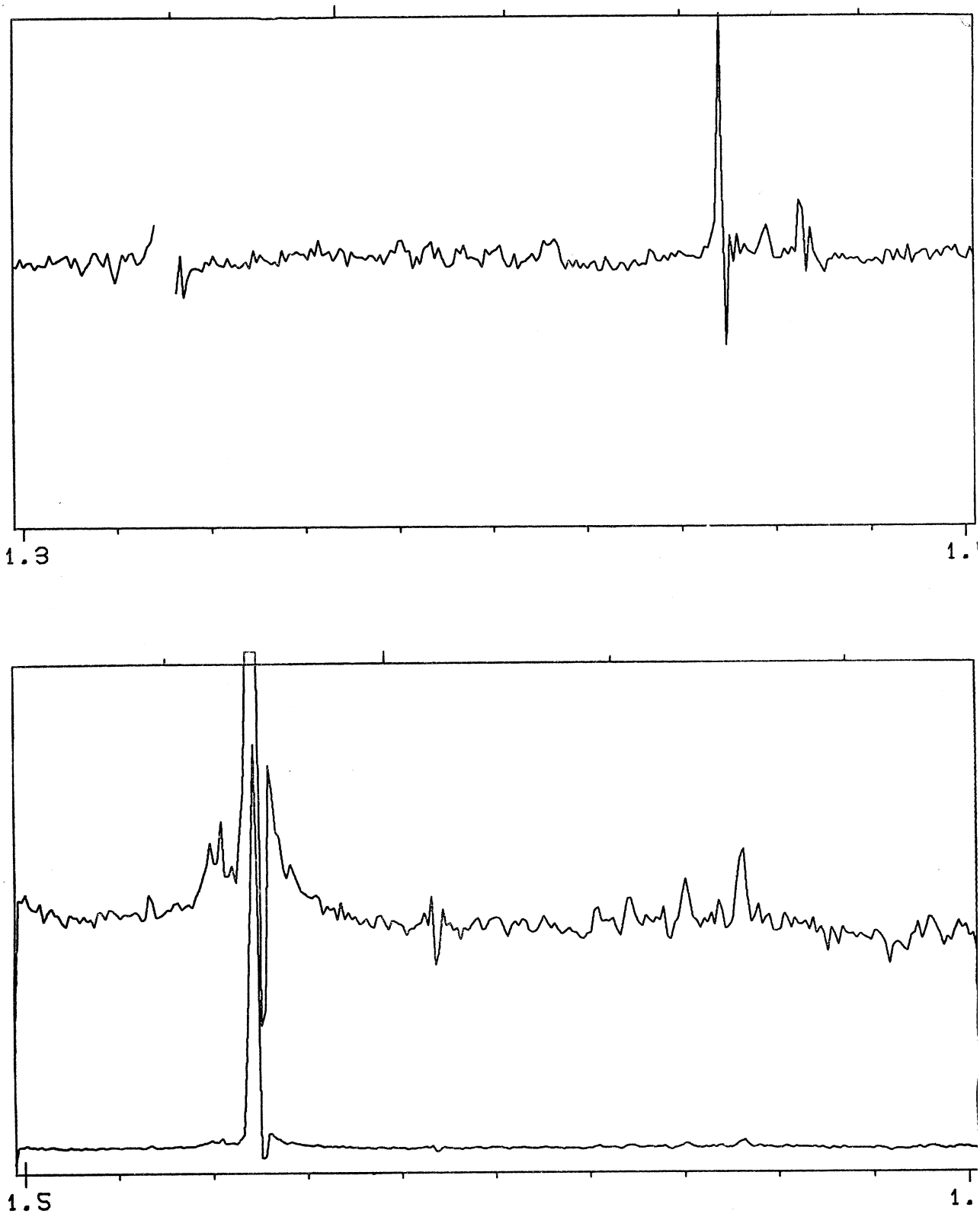

FIG. 4. The Spectrum of P Cygni (B1 pe)

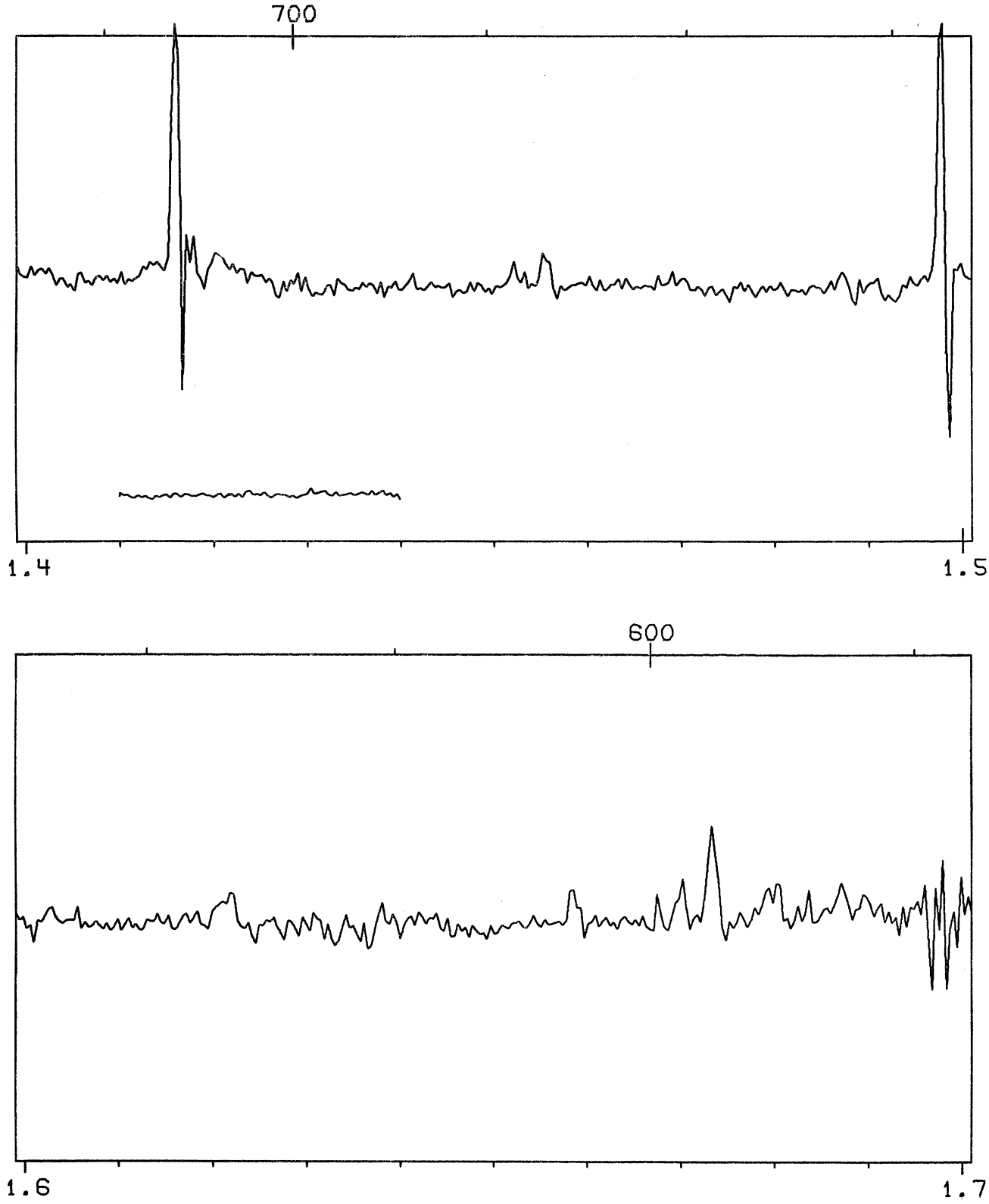

FIG. 4. The Spectrum of P Cygni (B1 pe)

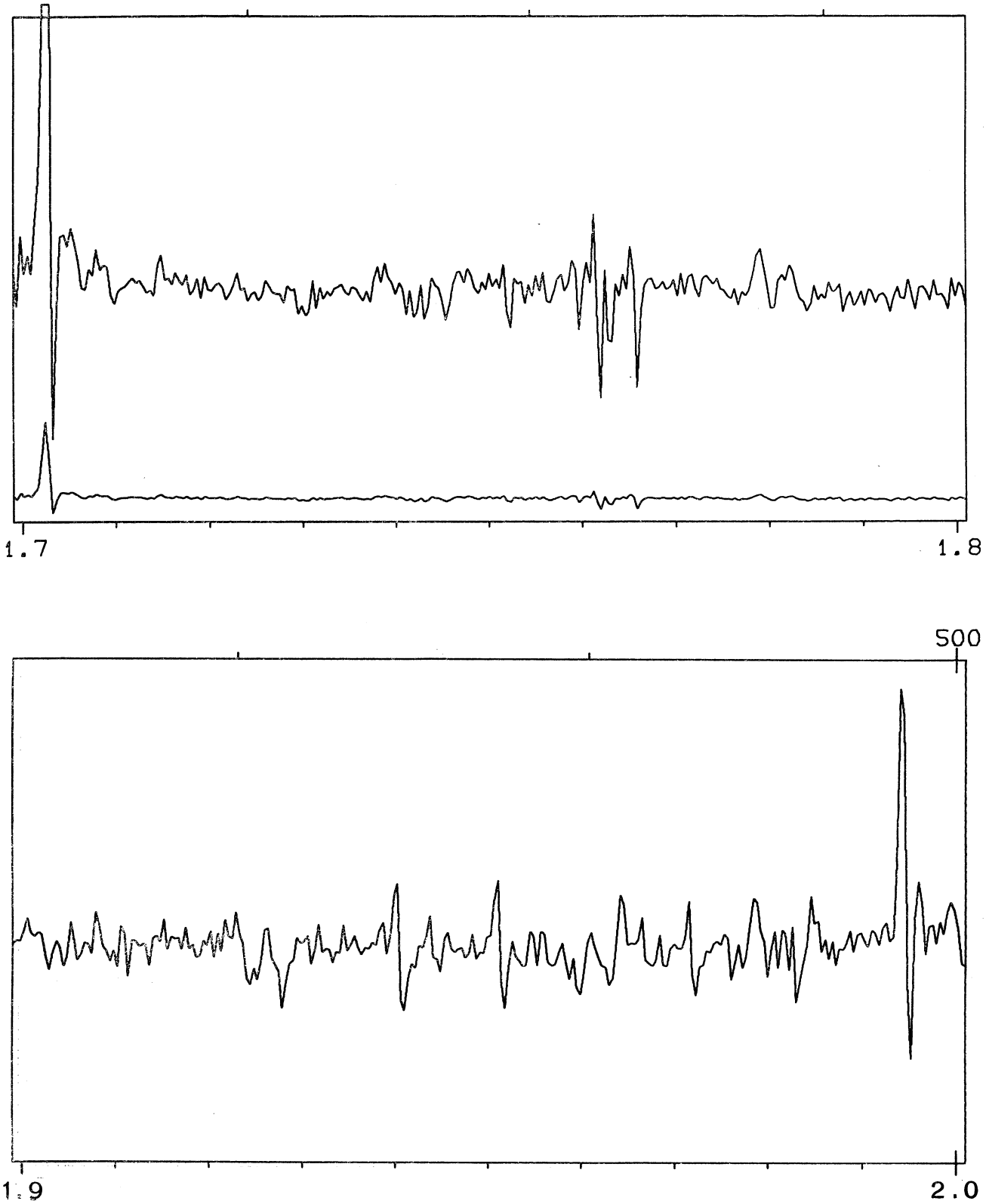

FIG. 4. The Spectrum of P Cygni (B1 pe)

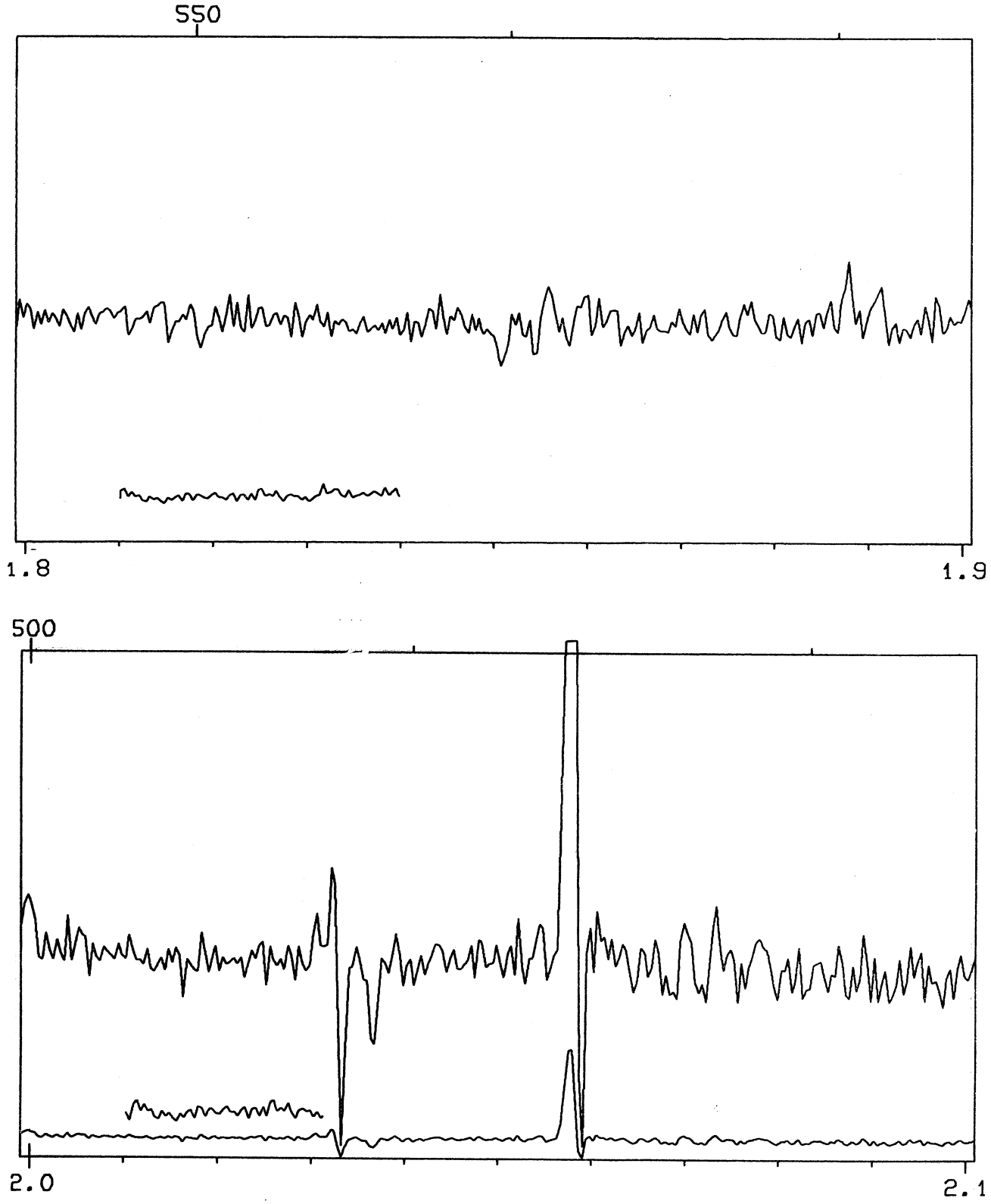

FIG. 4. The Spectrum of P Cygni (B1 pe)

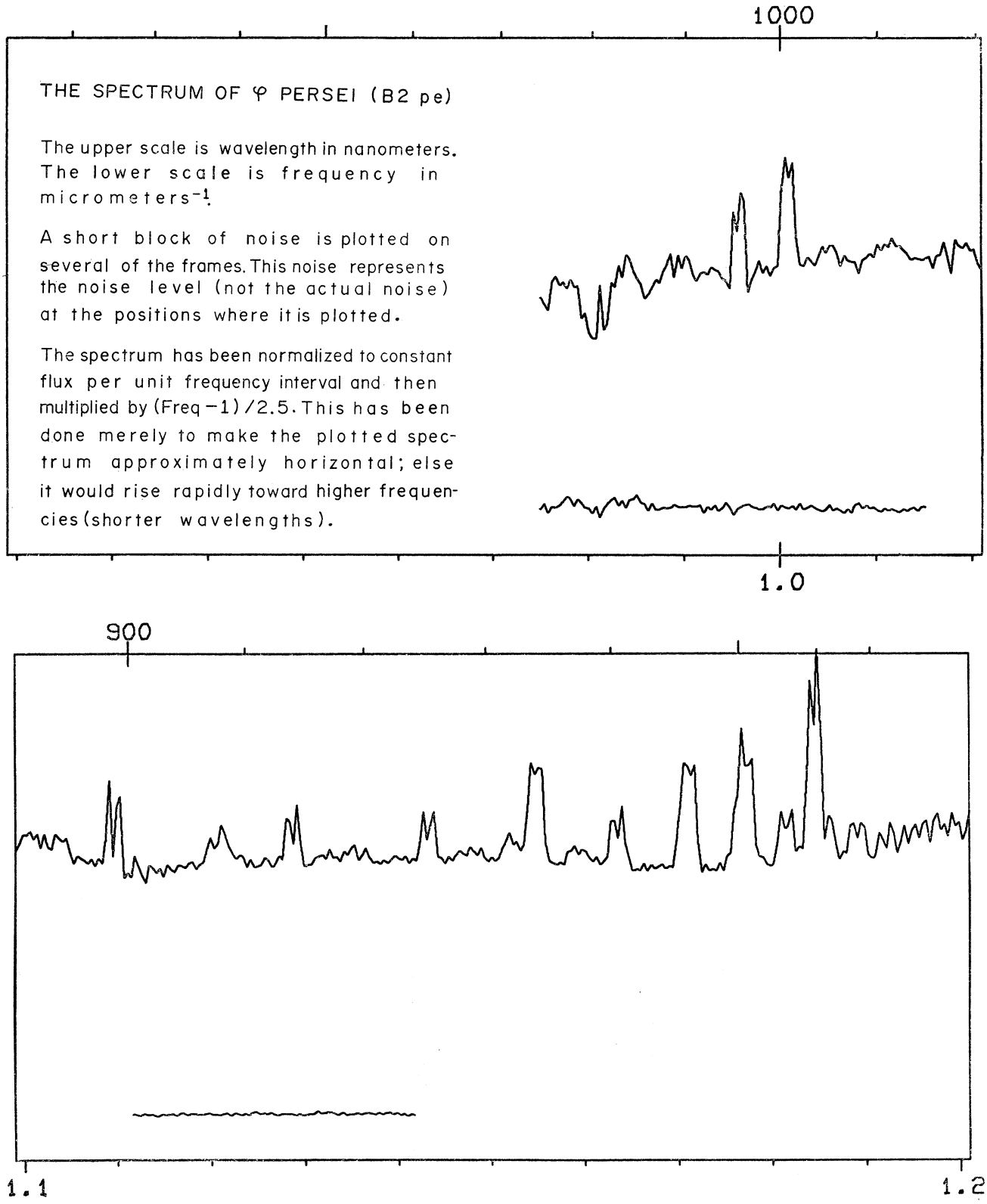

FIG. 5. The Spectrum of φ Persei (B2 pe)

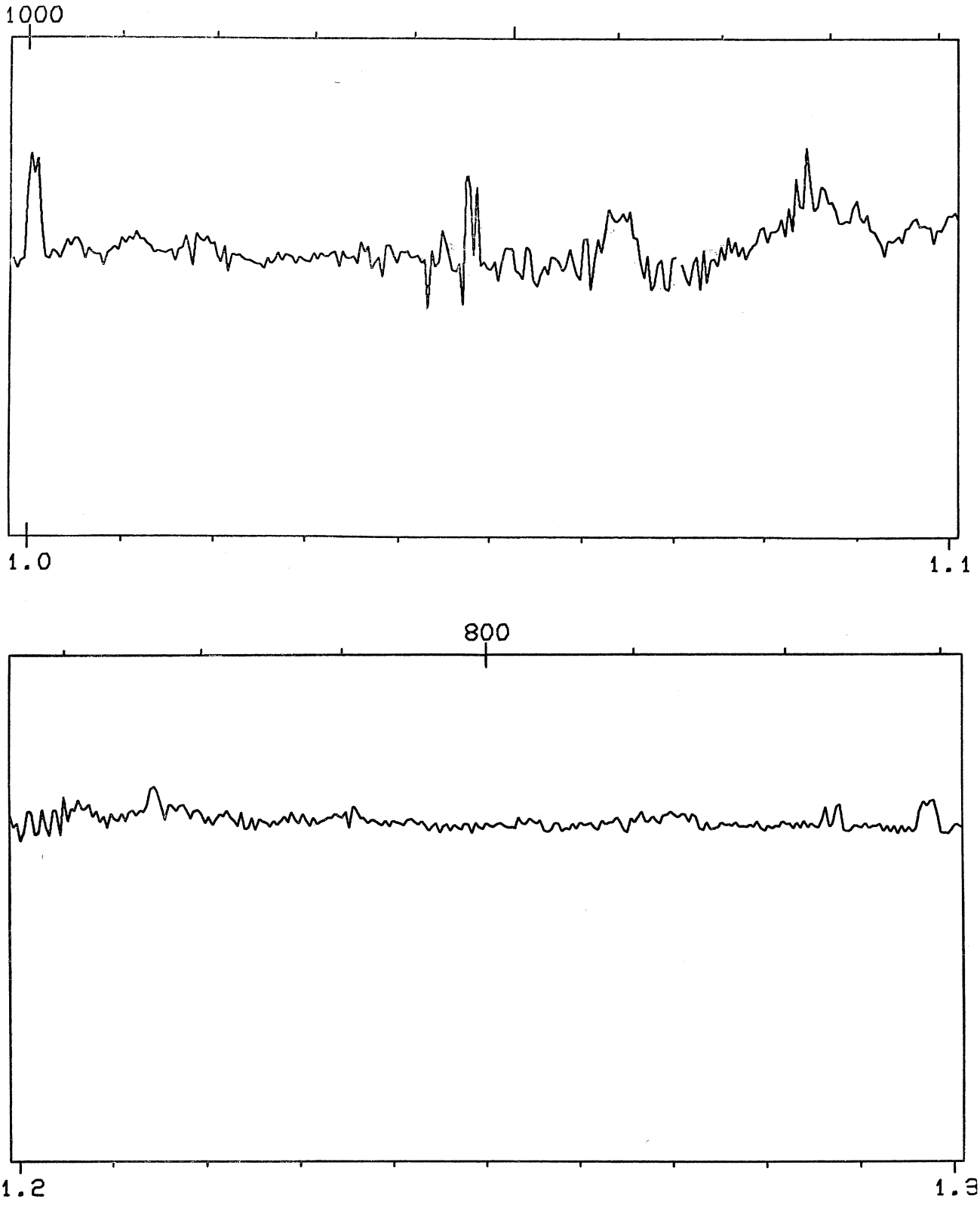

FIG. 5. The Spectrum of φ Persei (B2 pe)

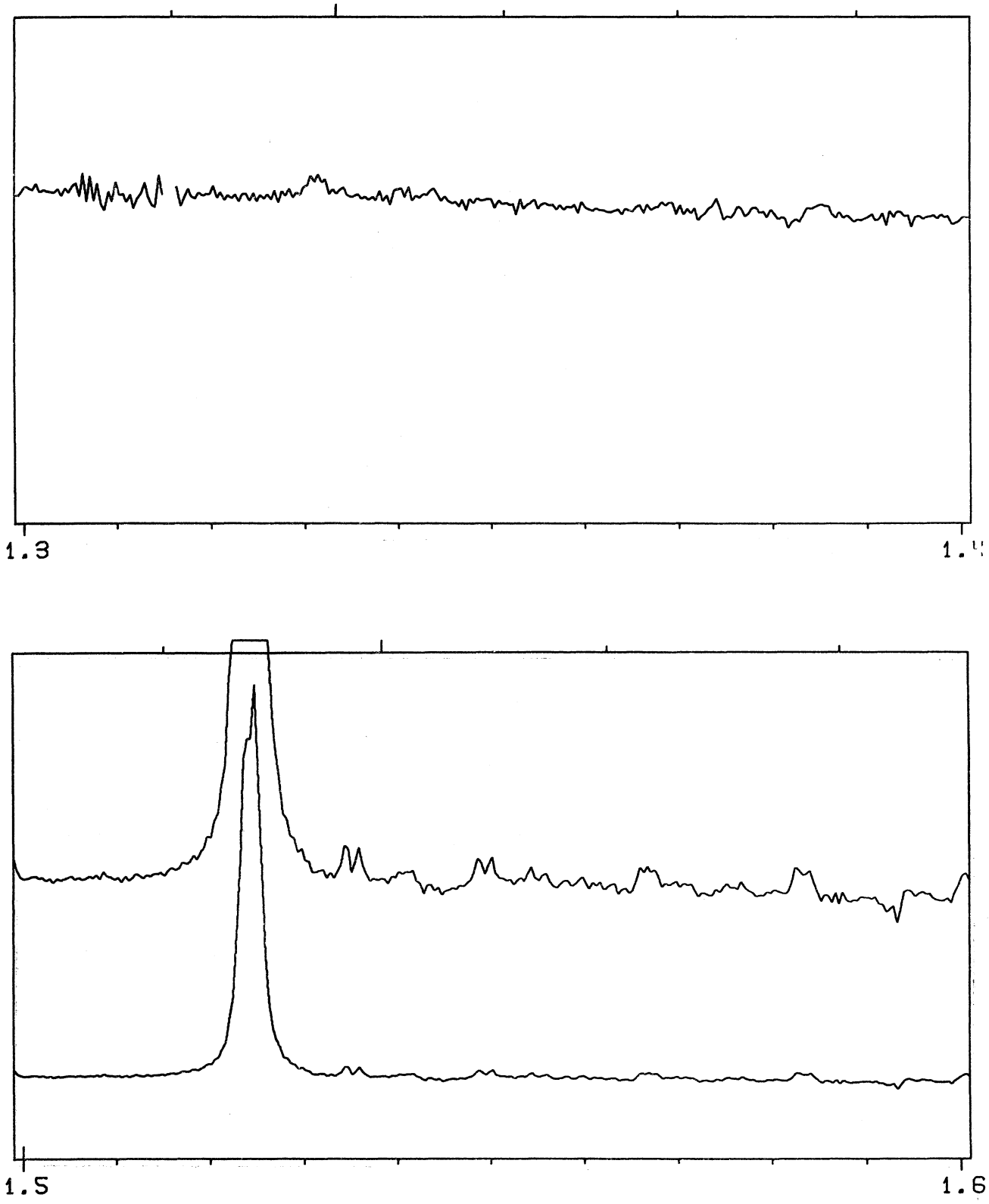

FIG. 5. The Spectrum of φ Persei (B2 pe)

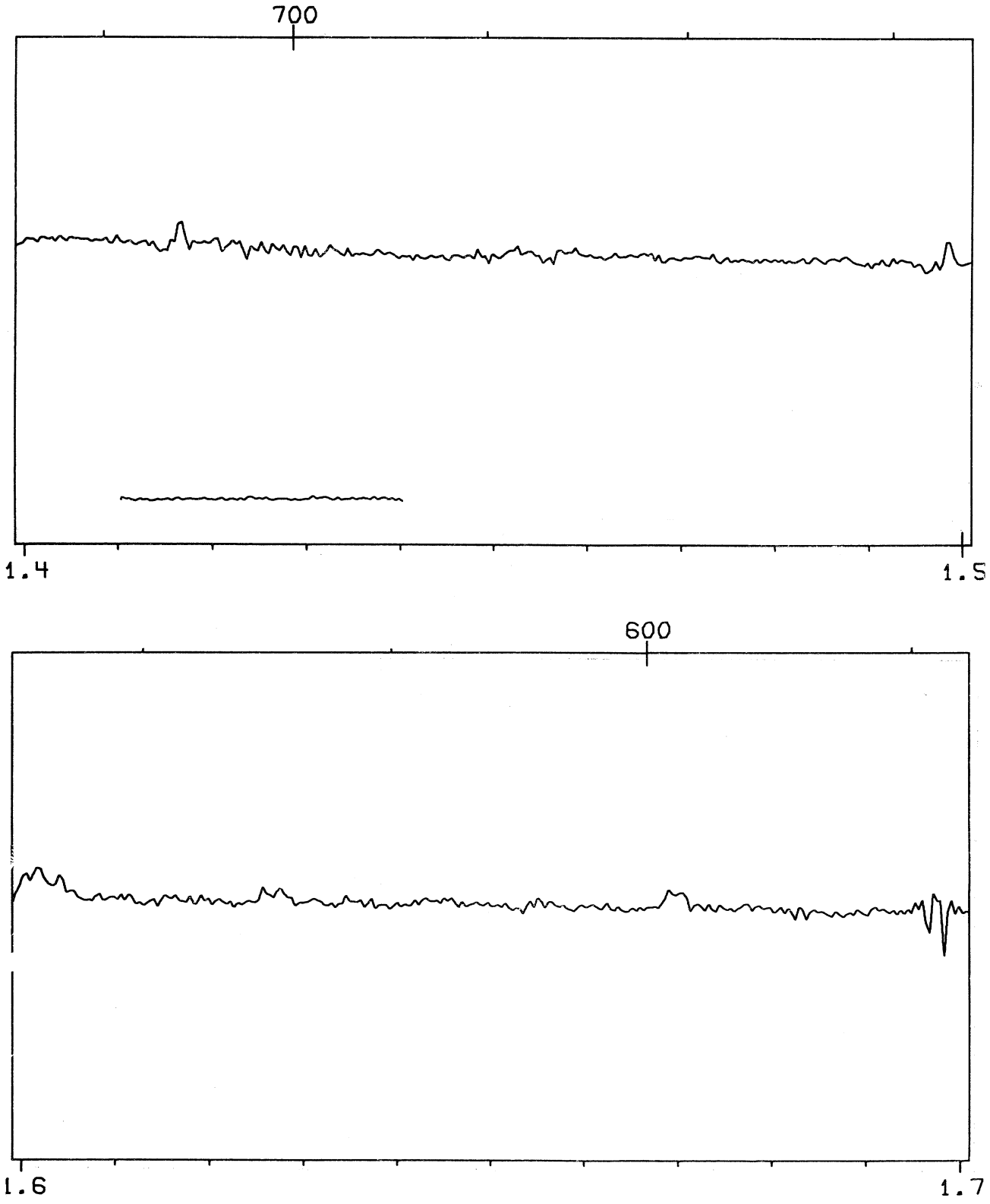

FIG. 5. The Spectrum of φ Persei (B2 pe)

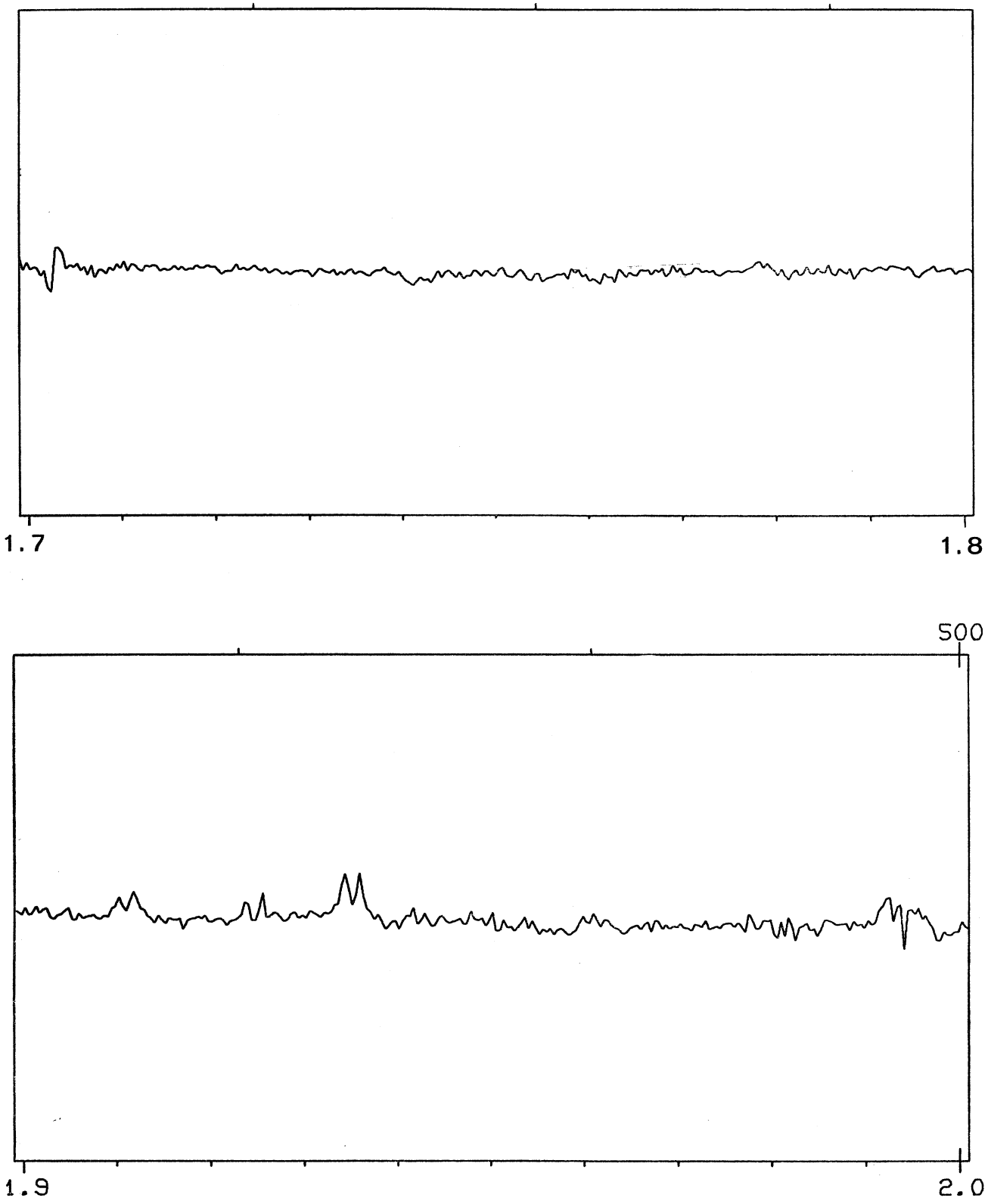

FIG. 5. The Spectrum of φ Persei (B2 pe)

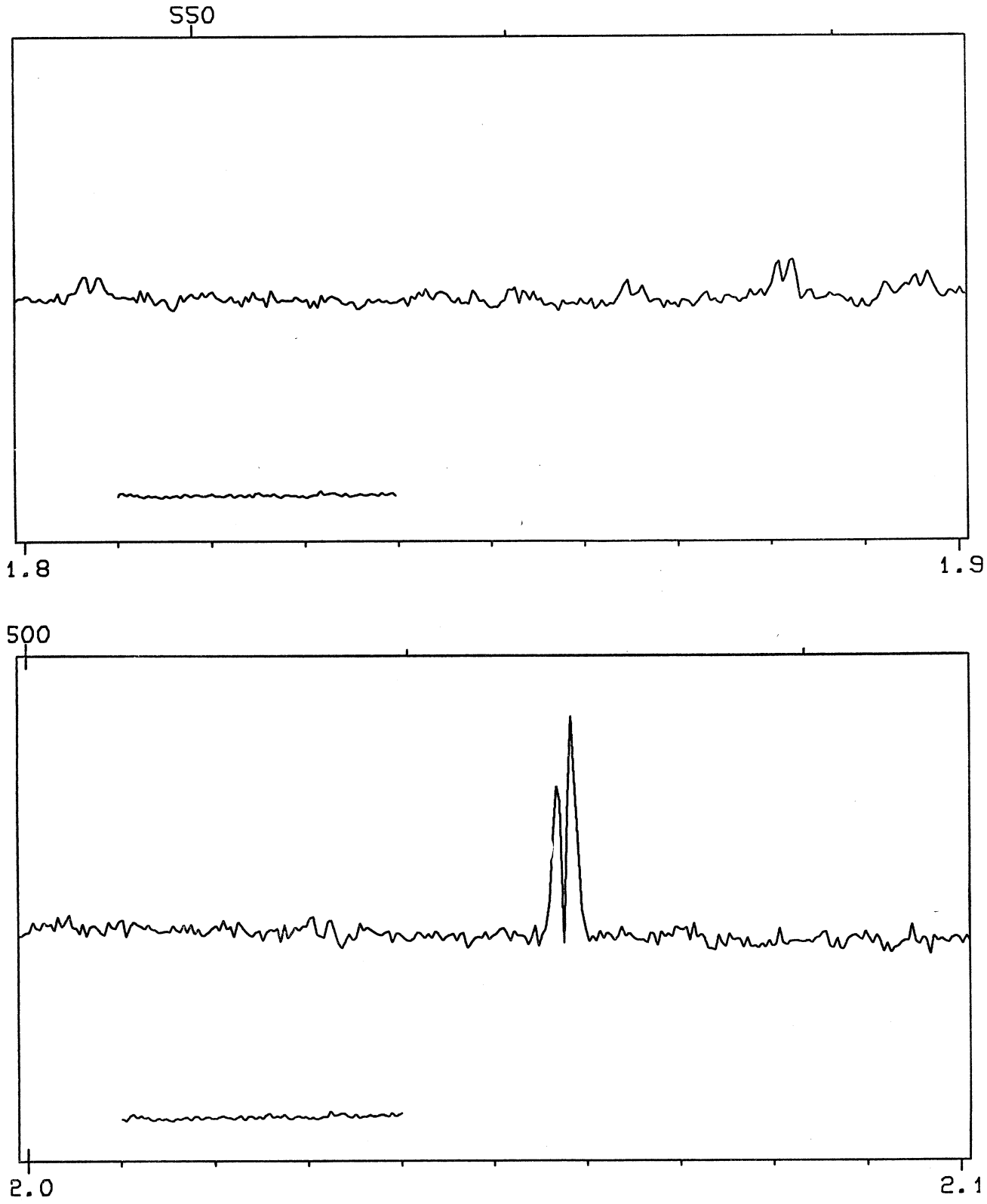

FIG. 5. The Spectrum of φ Persei (B2 pe)

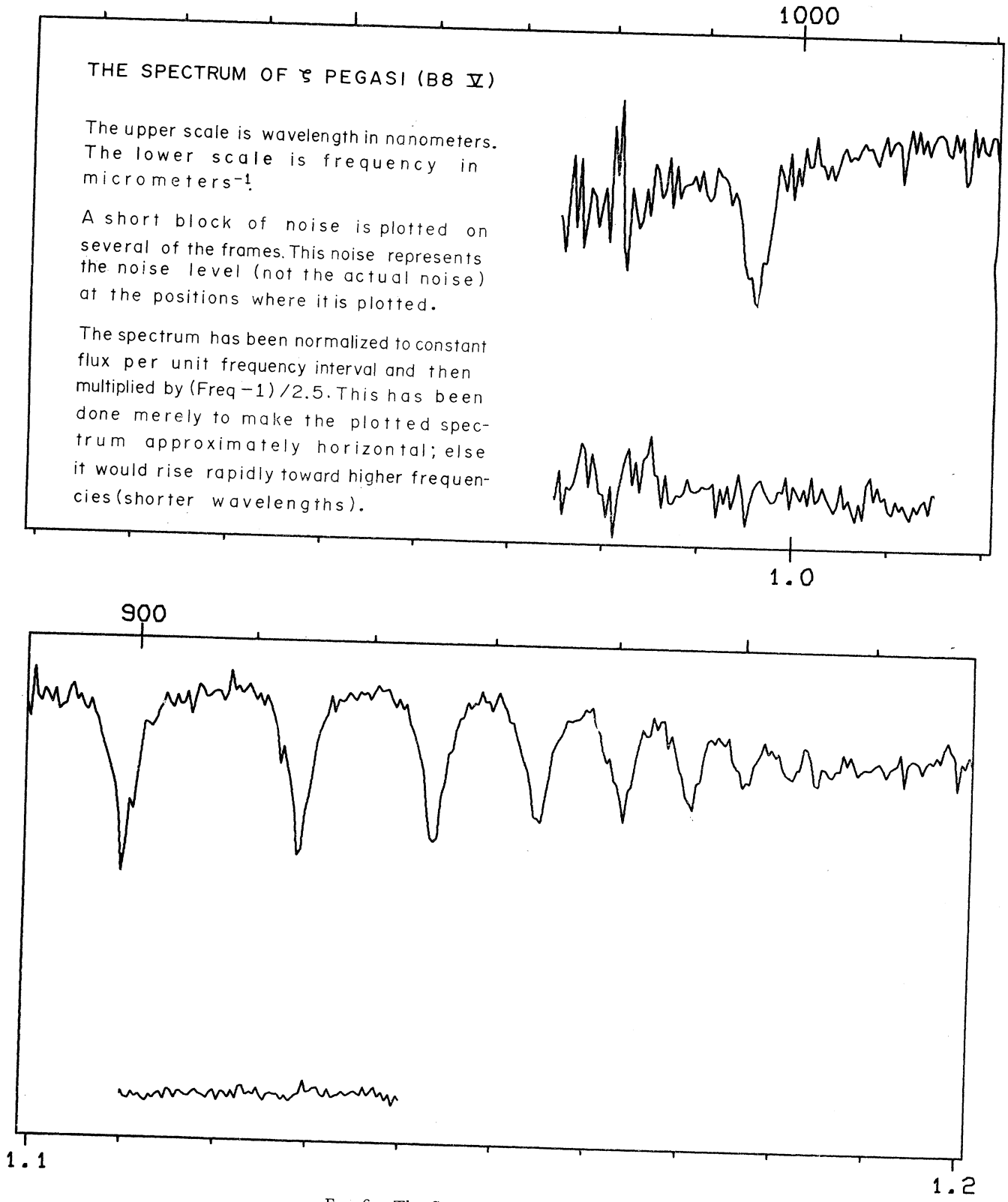

FIG. 6. The Spectrum of ζ Pegasi (B8 V)

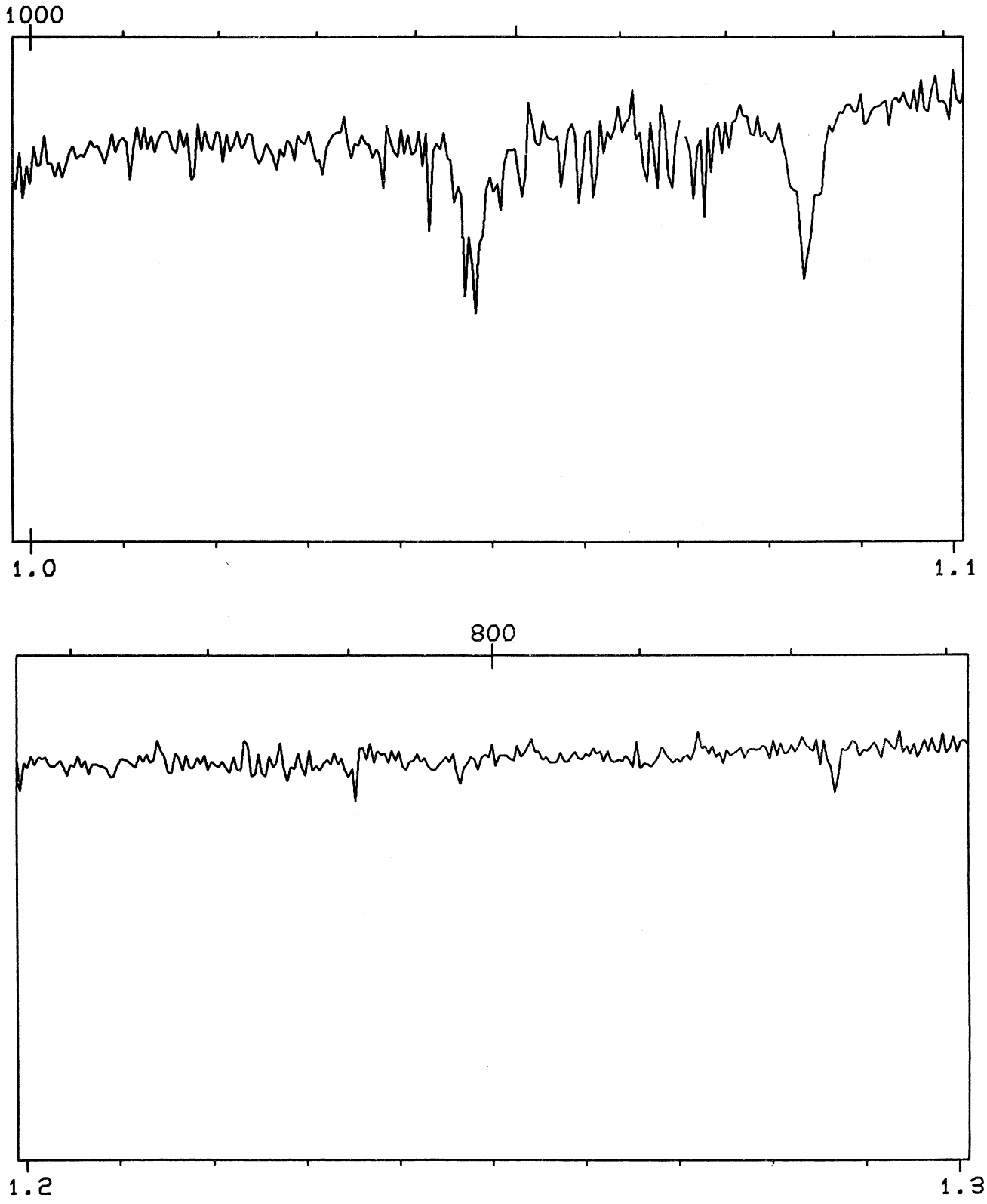

FIG. 6. The Spectrum of ζ Pegasi (B8 V)

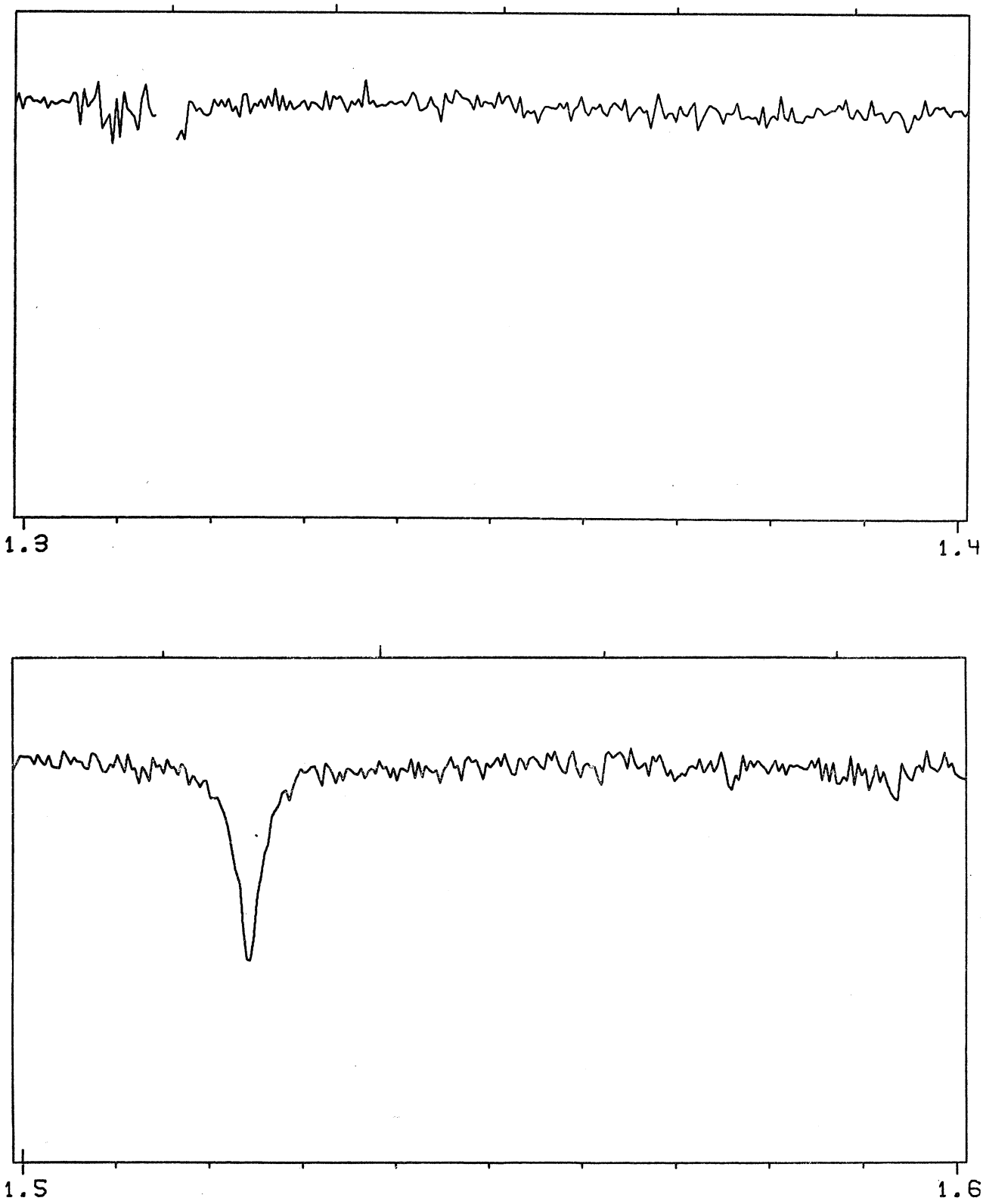

FIG. 6. The Spectrum of ζ Pegasi (B8 V)

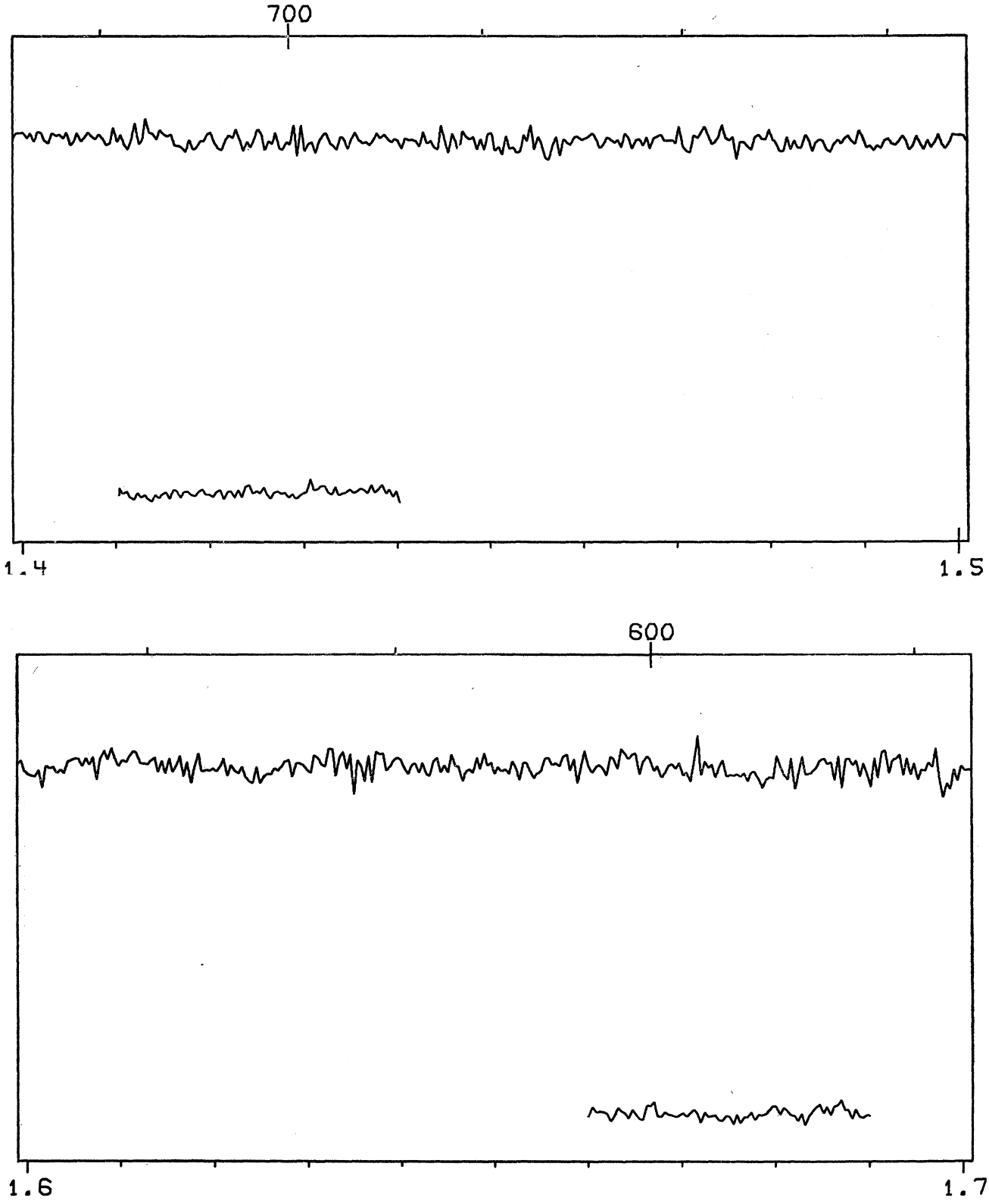

FIG. 6. The Spectrum of ζ Pegasi (B8 V)

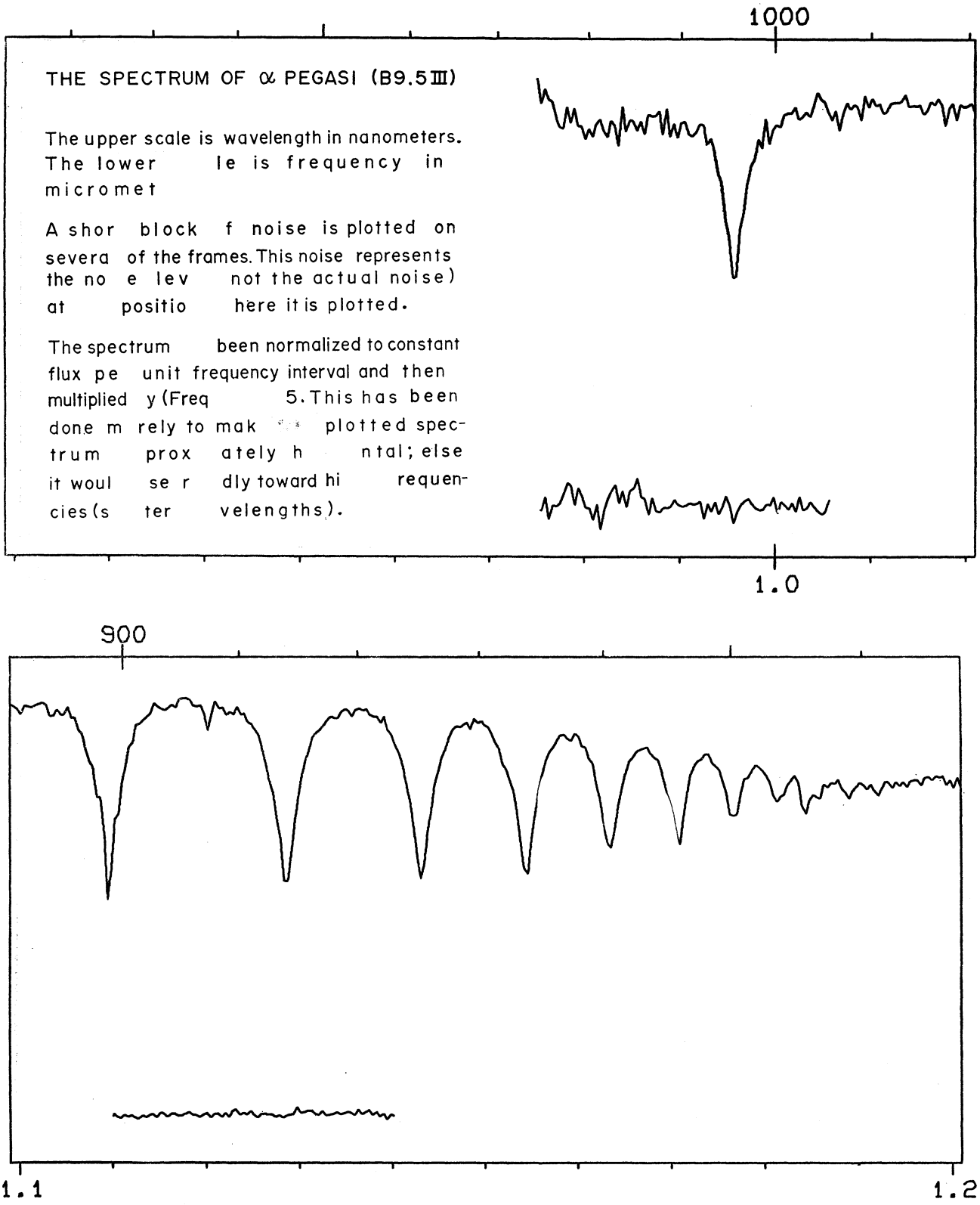

FIG. 7. The Spectrum of α Pegasi (B9.5 III)

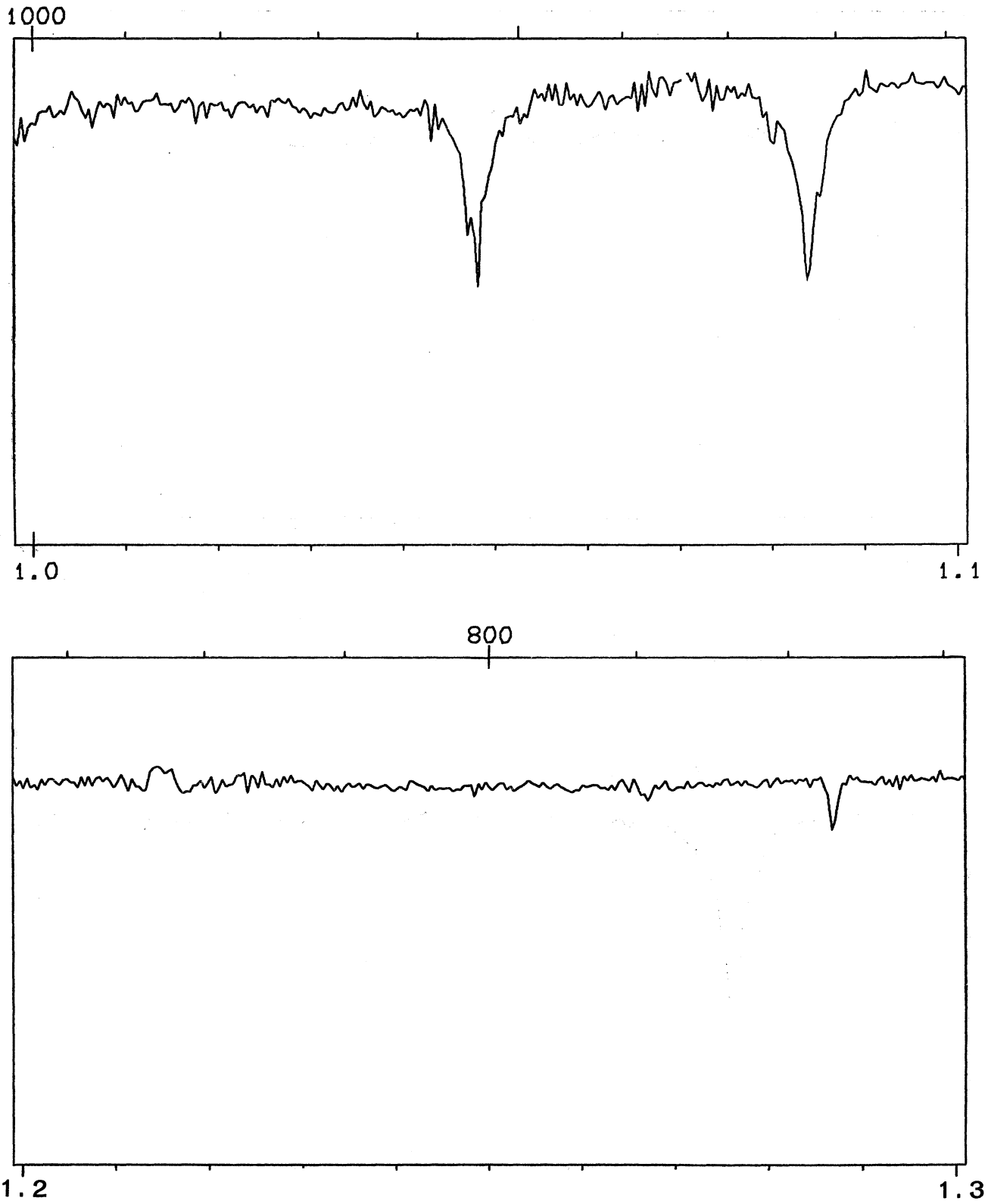

FIG. 7. The Spectrum of α Pegasi (B9.5 III)

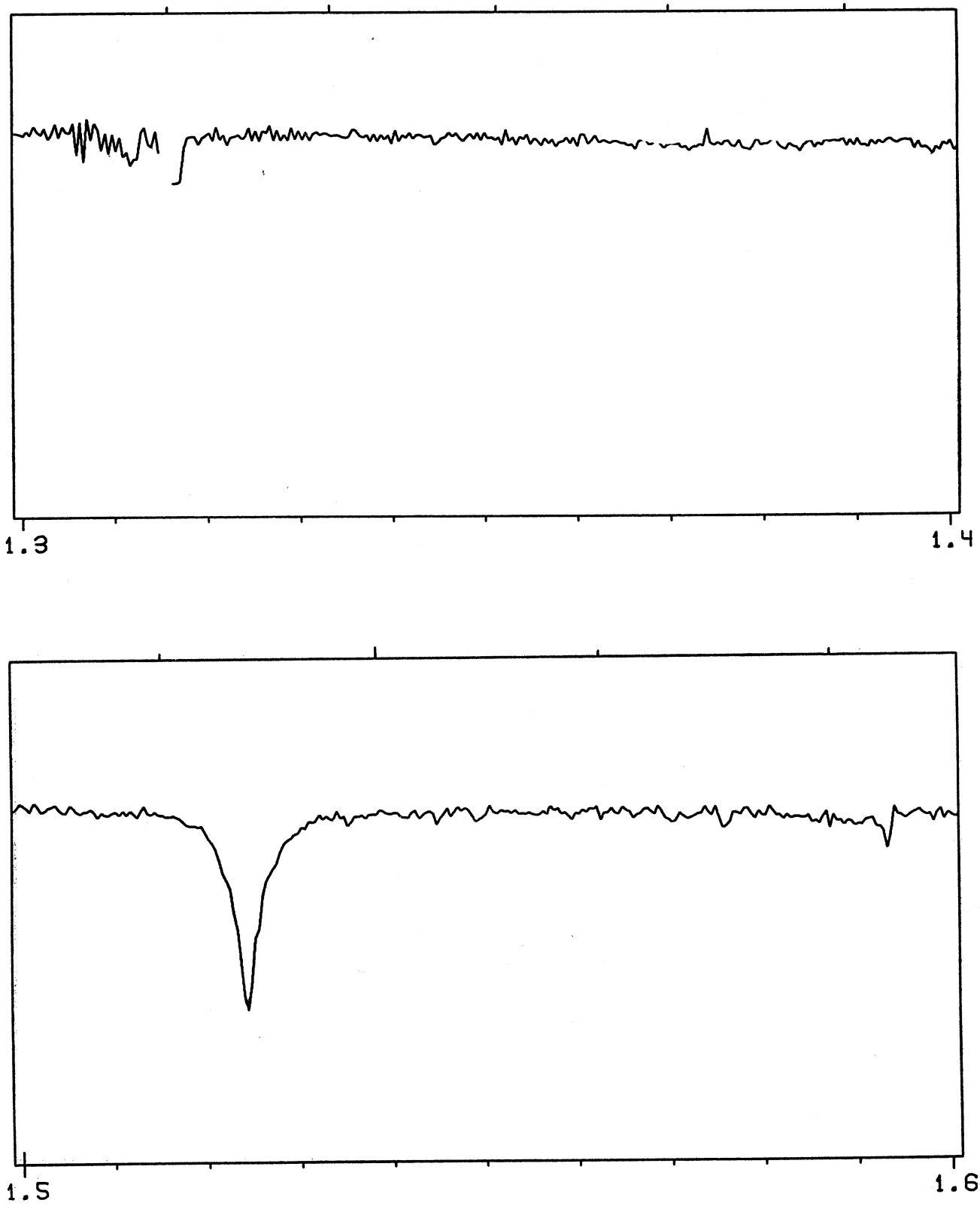

FIG. 7. The Spectrum of α Pegasi (B9.5 III)

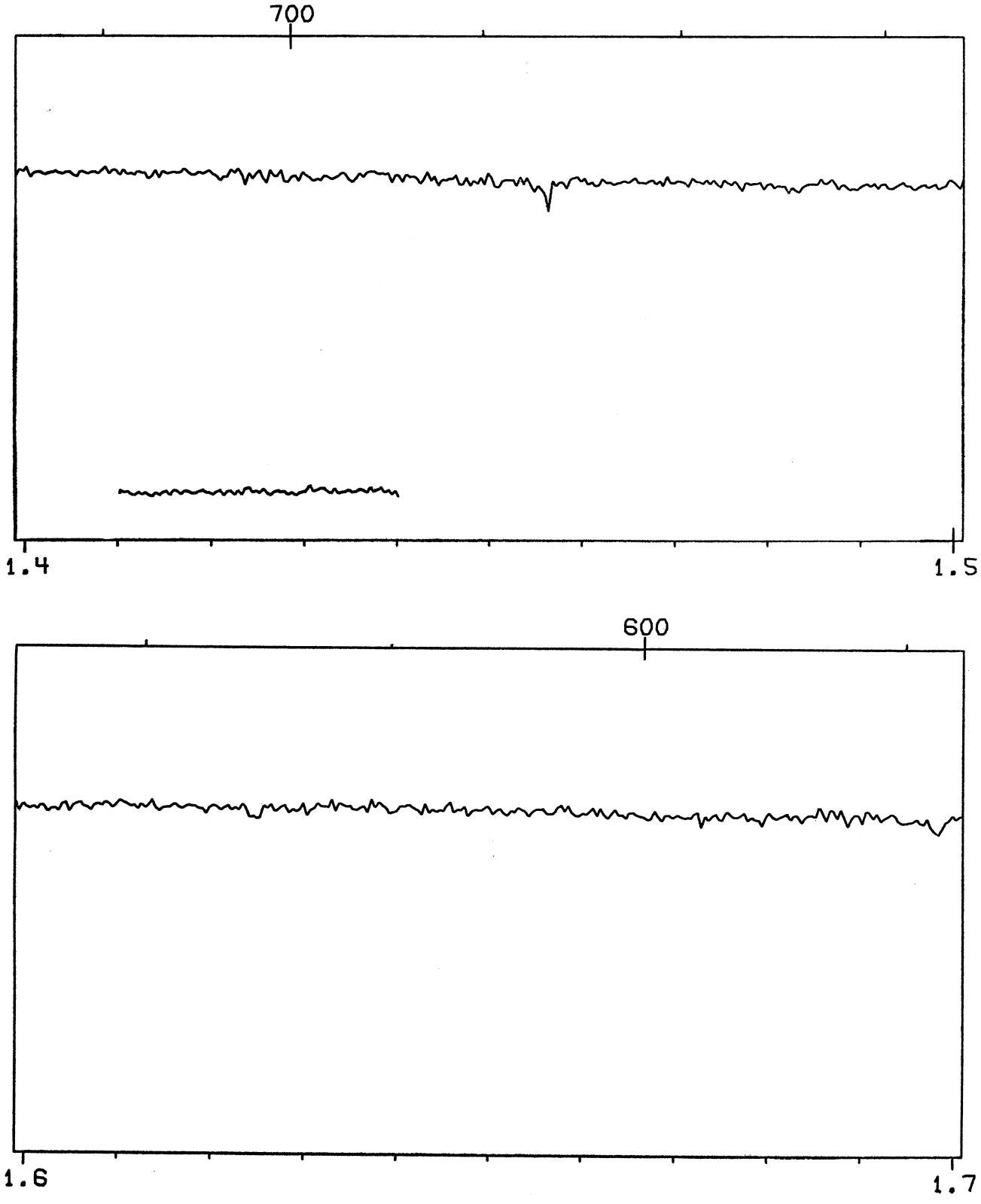

FIG. 7. The Spectrum of α Pegasi (B9.5 III)

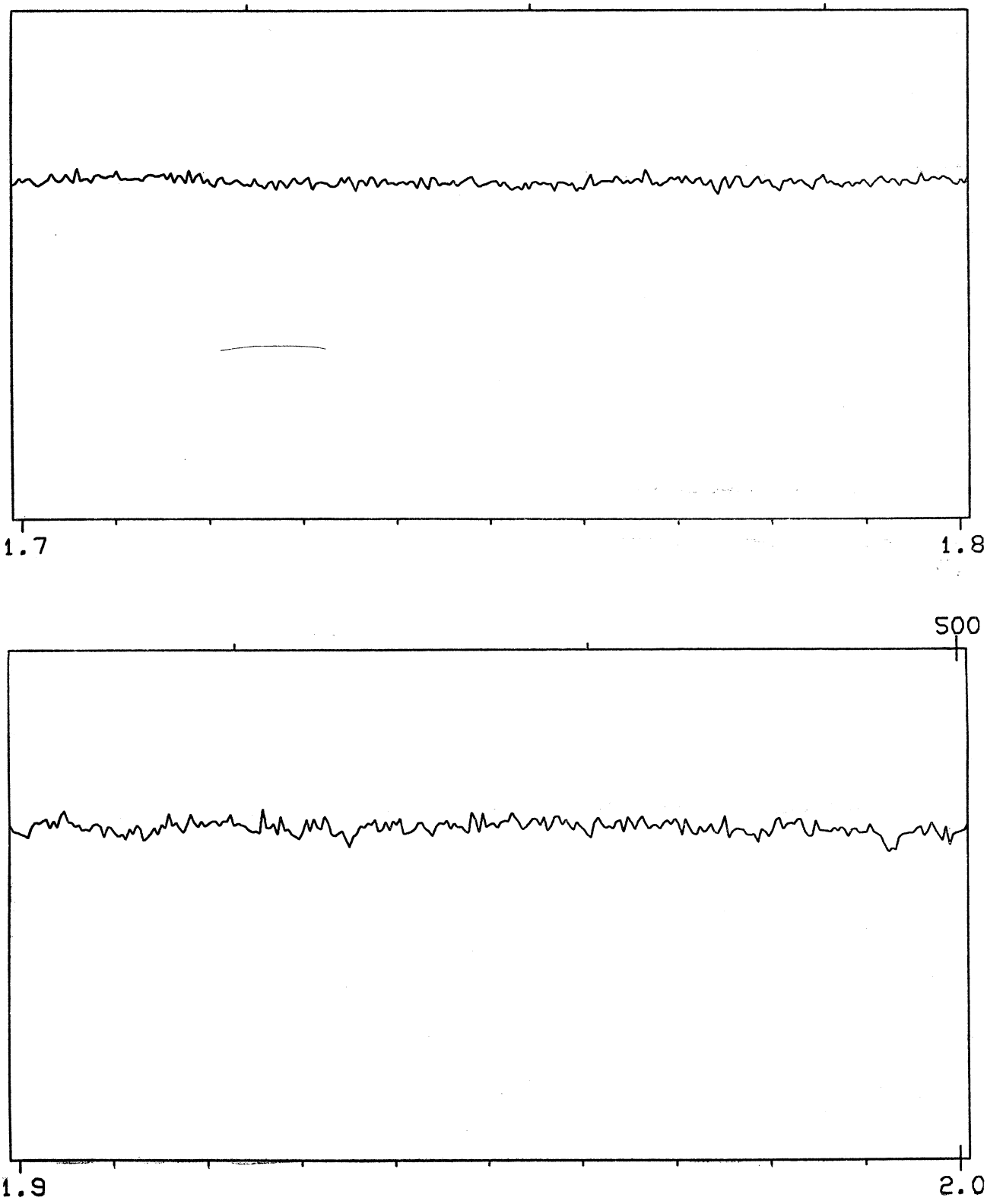

FIG. 7. The Spectrum of α Pegasi (B9.5 III)

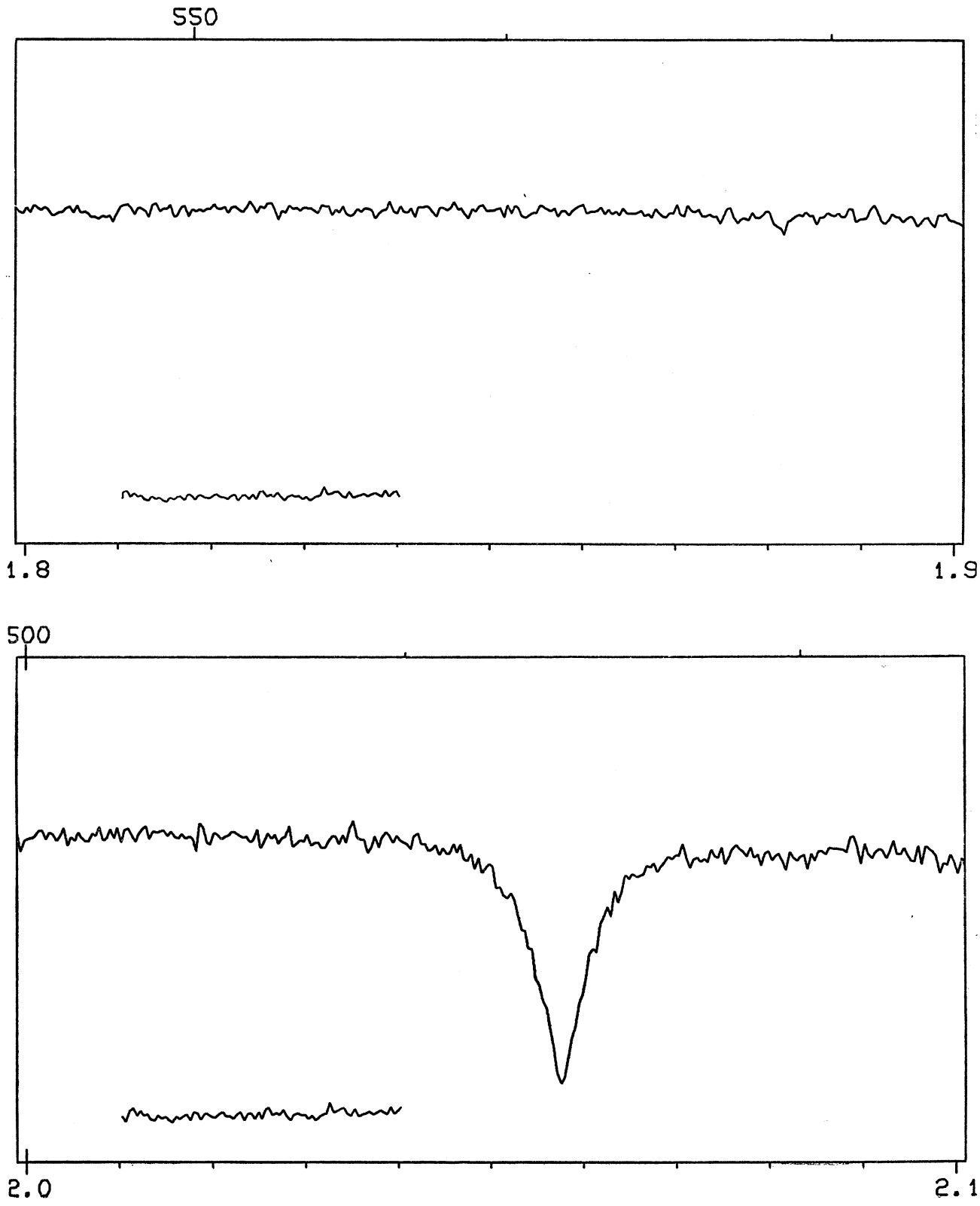

FIG. 7. The Spectrum of α Pegasi (B9.5 III)

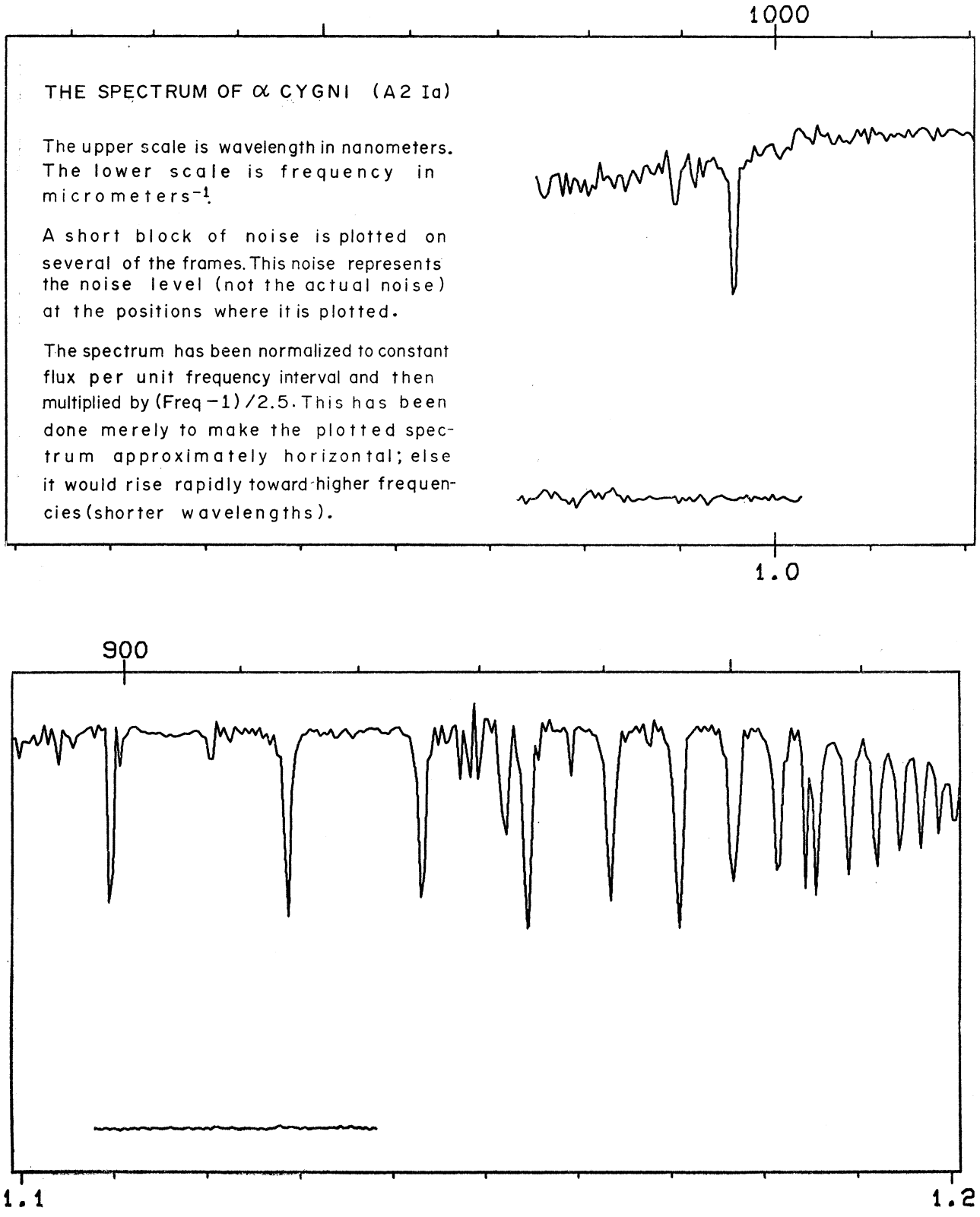

FIG. 8. The Spectrum of α Cygni (A2 Ia)

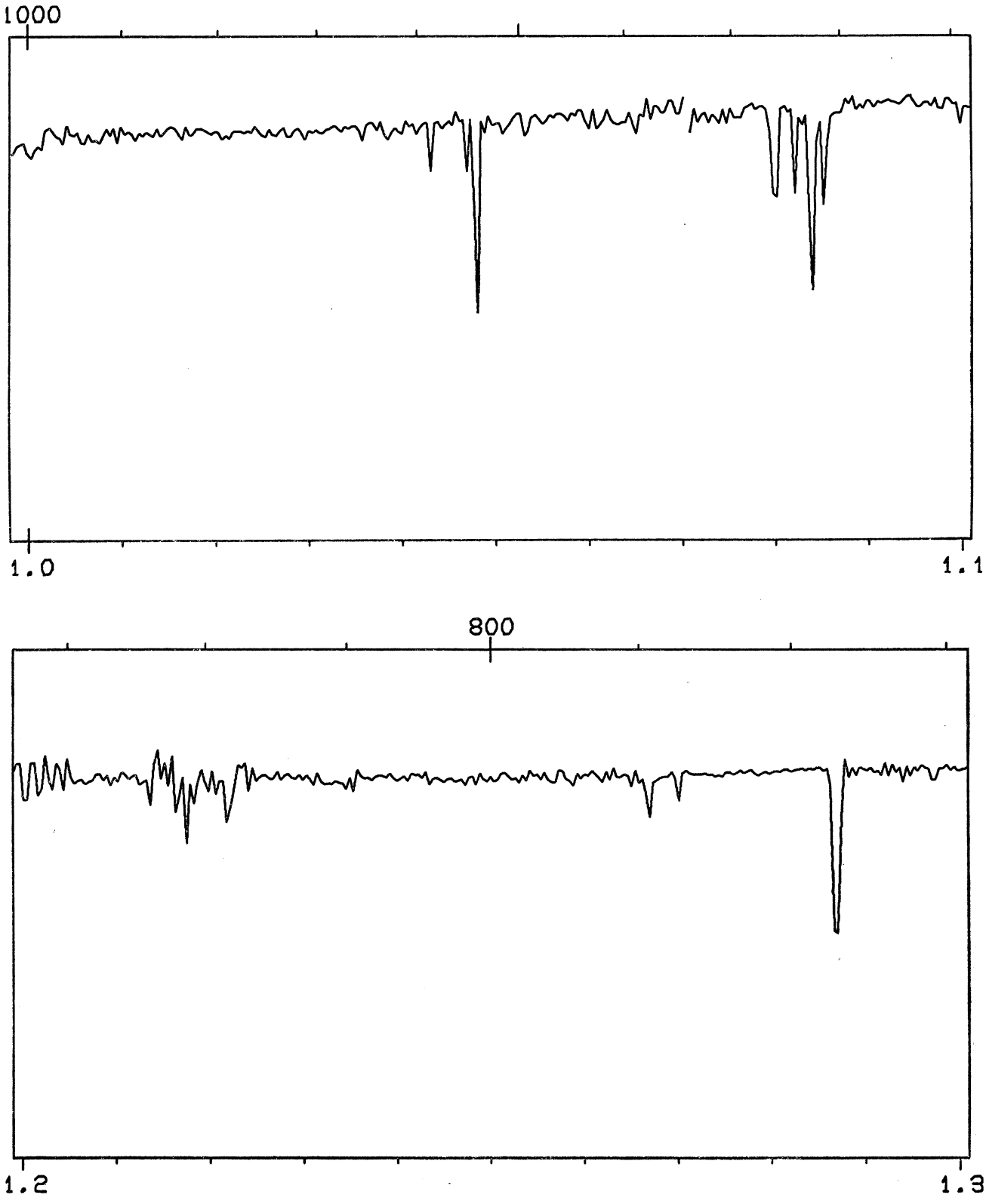

FIG. 8. The Spectrum of α Cygni (A2 Ia)

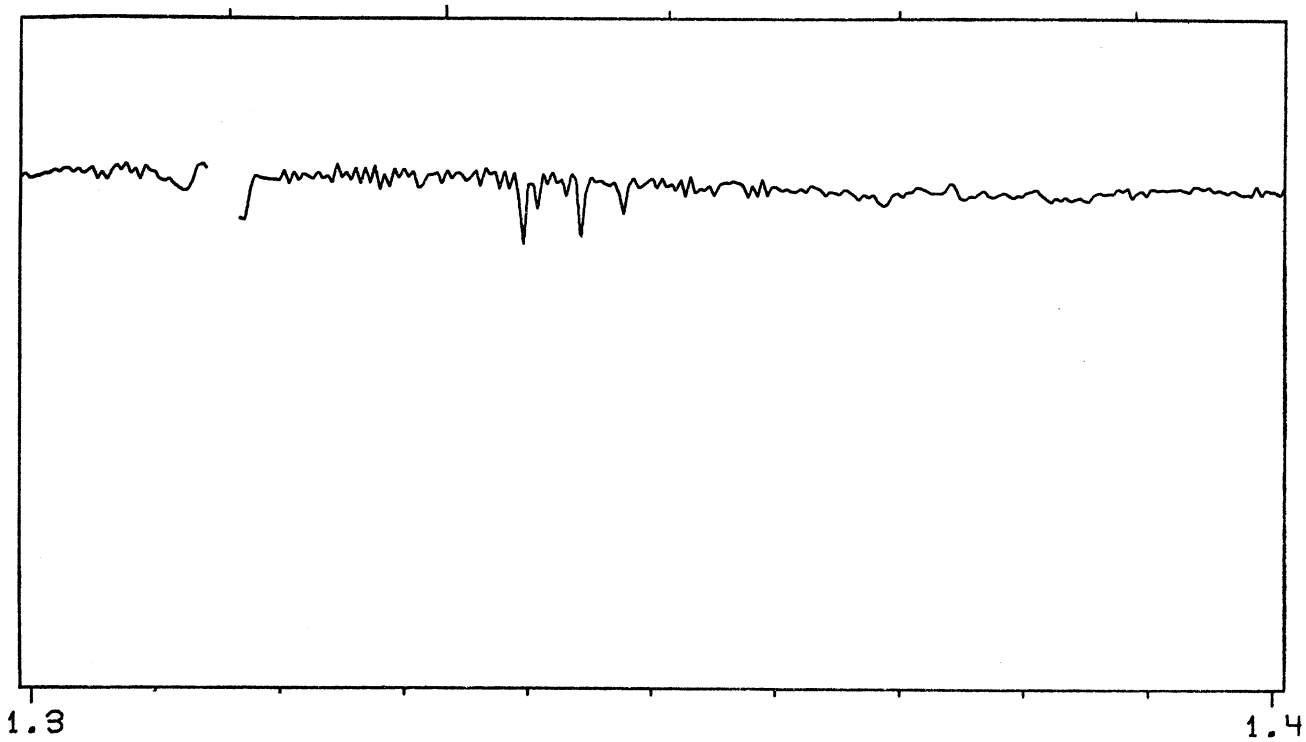

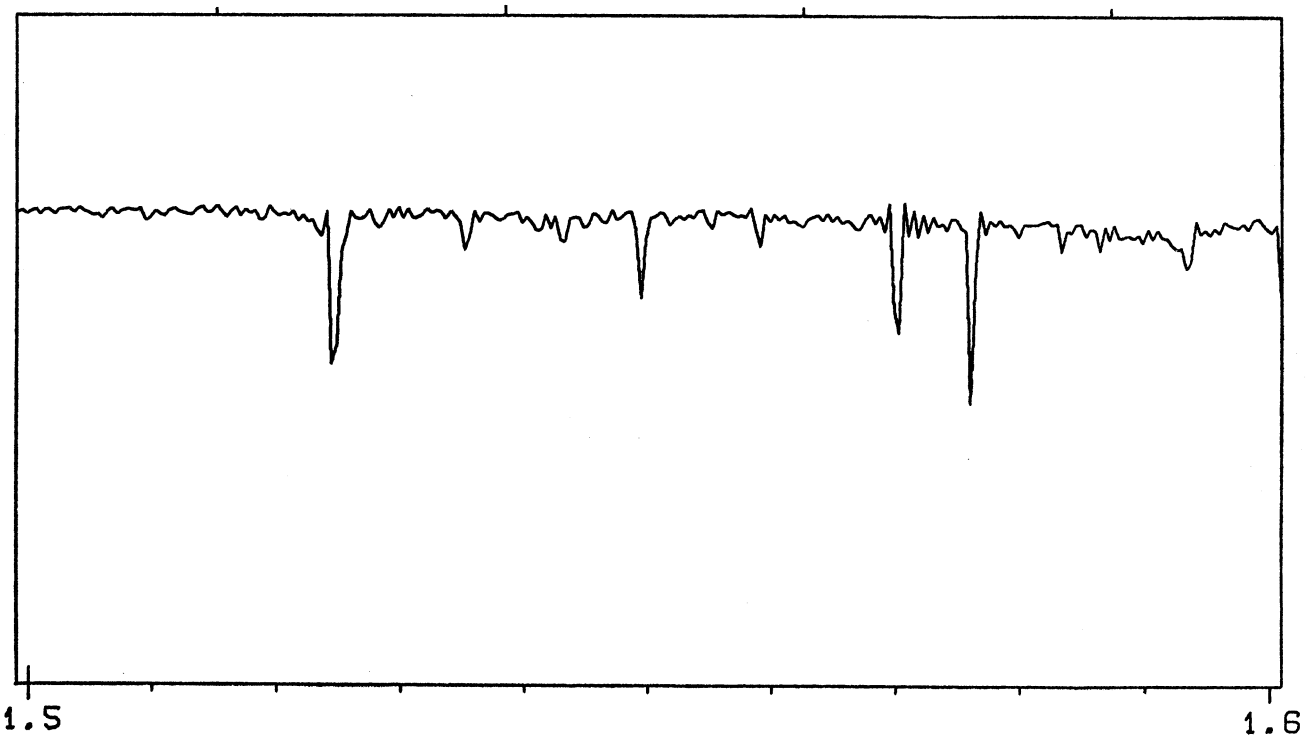

FIG. 8. The Spectrum of α Cygni (A2 Ia)

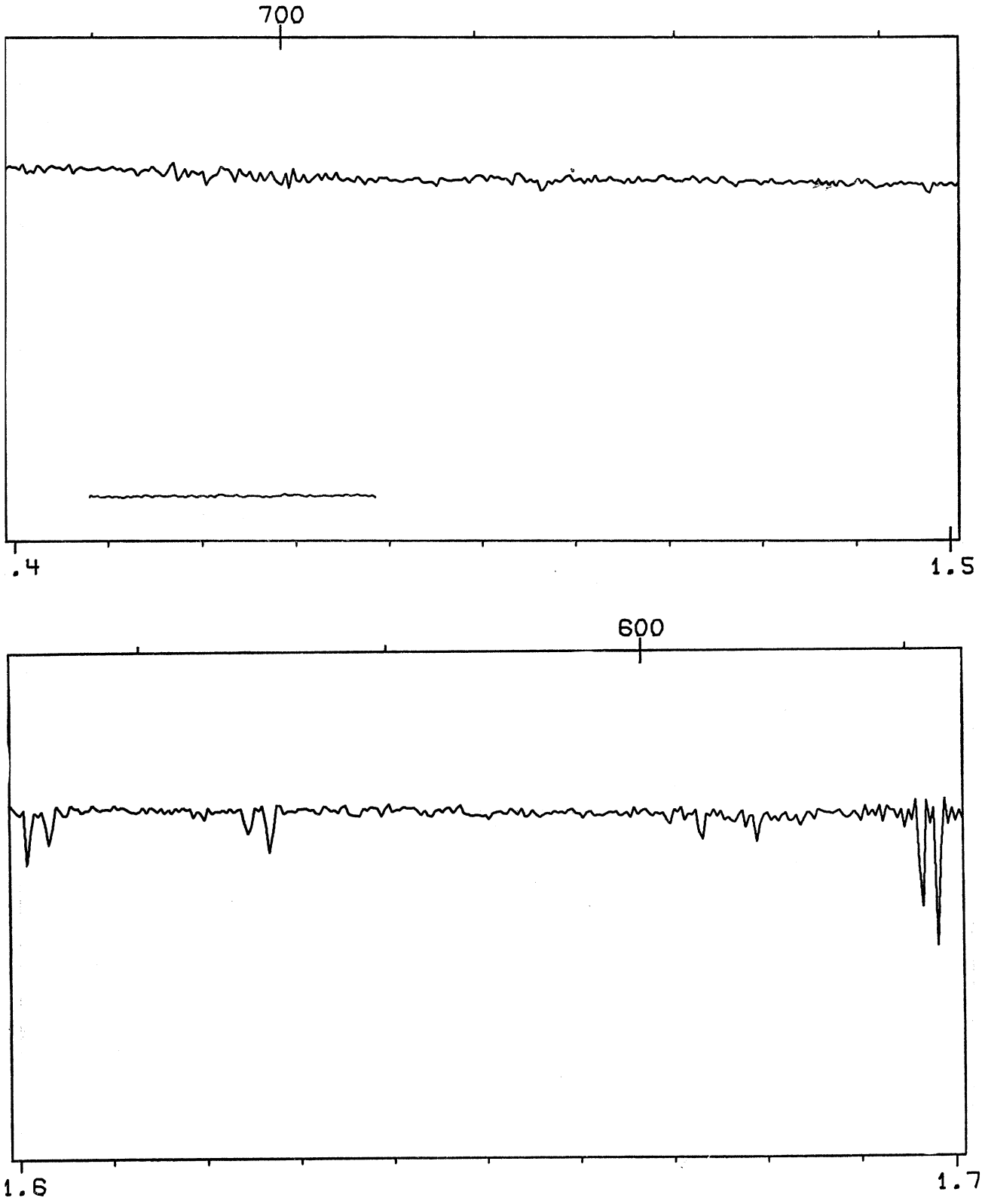

FIG. 8. The Spectrum of α Cygni (A2 Ia)

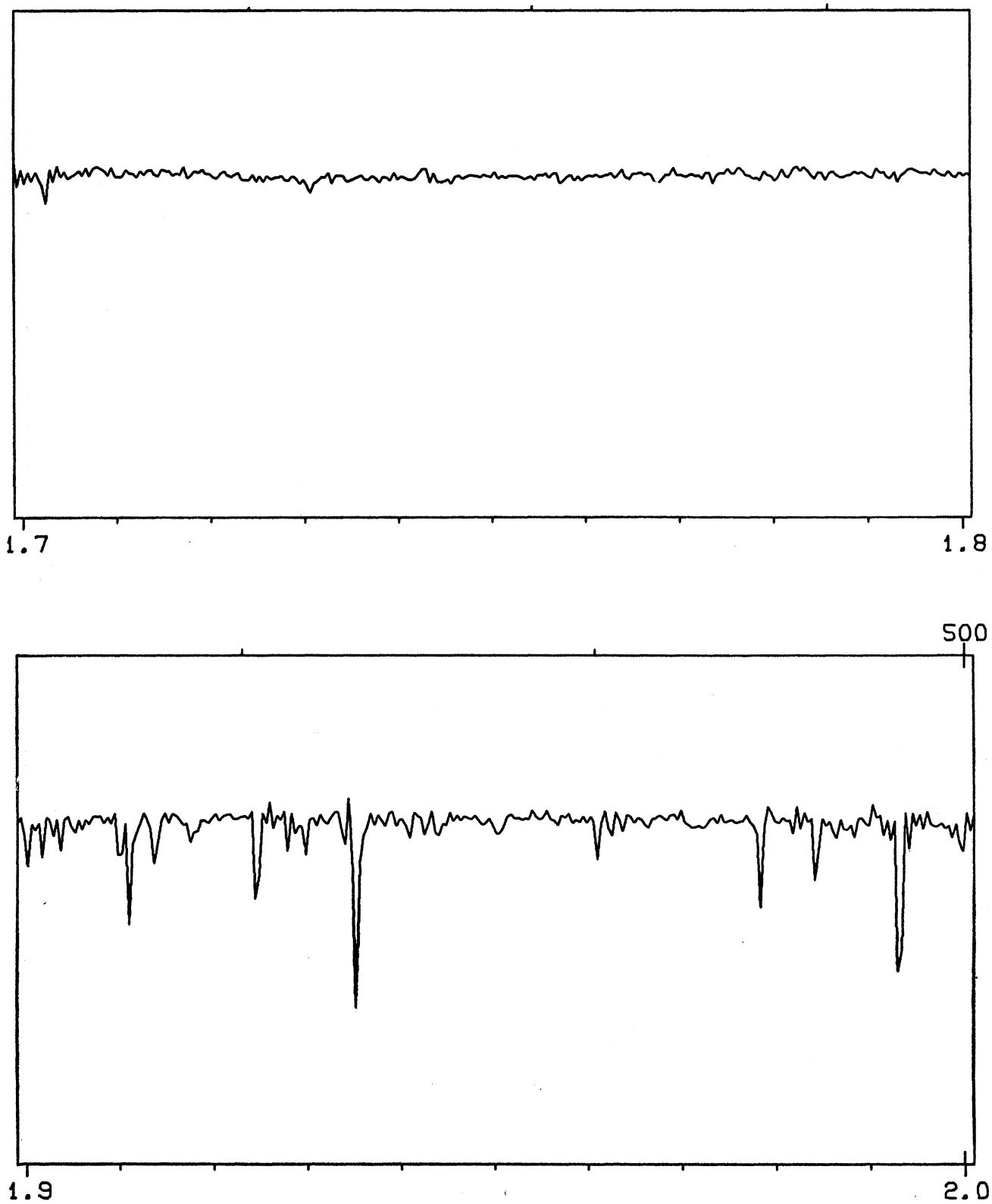

FIG. 8. The Spectrum of α Cygni (A2 Ia)

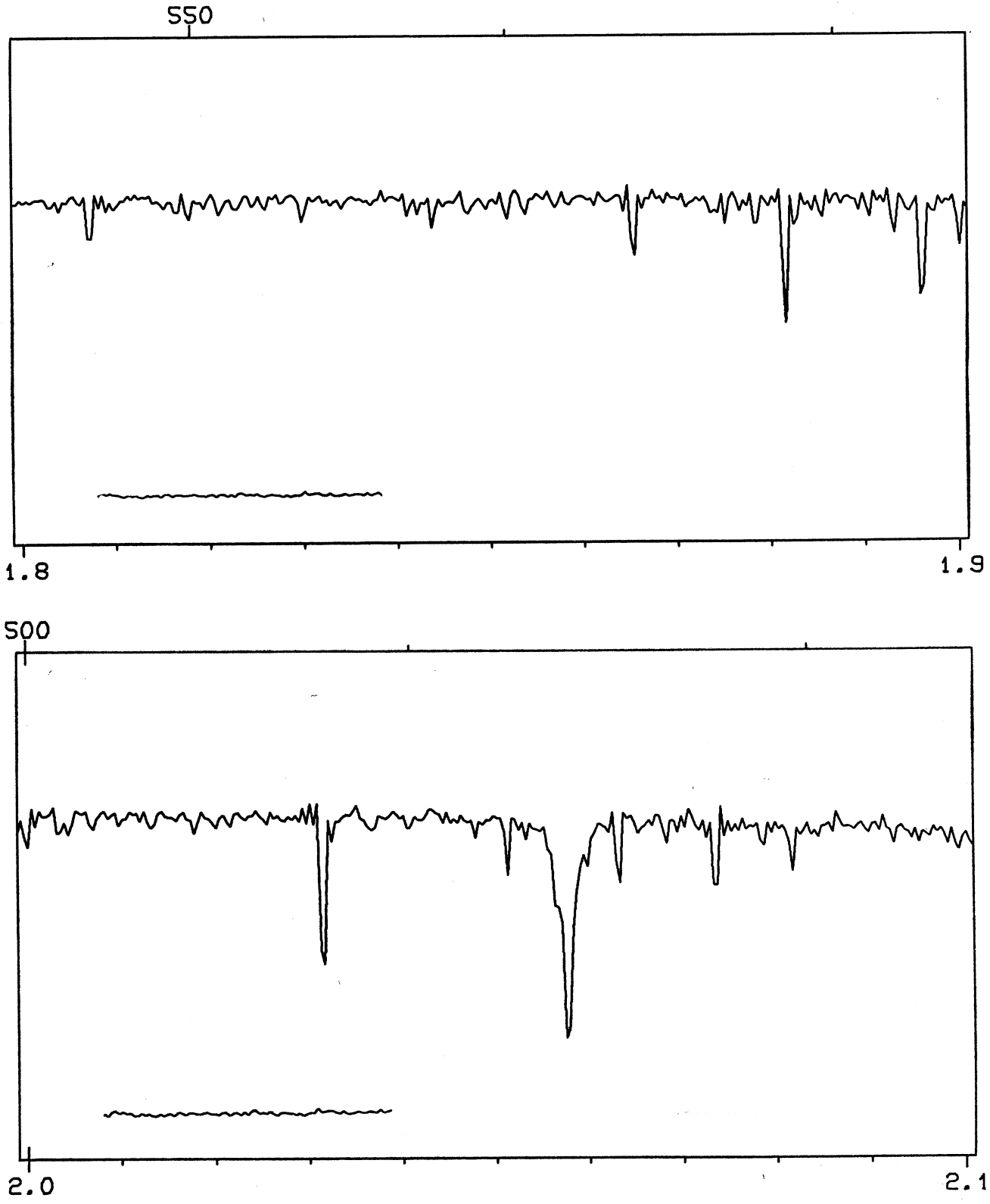

FIG. 8. The Spectrum of α Cygni (A2 Ia)

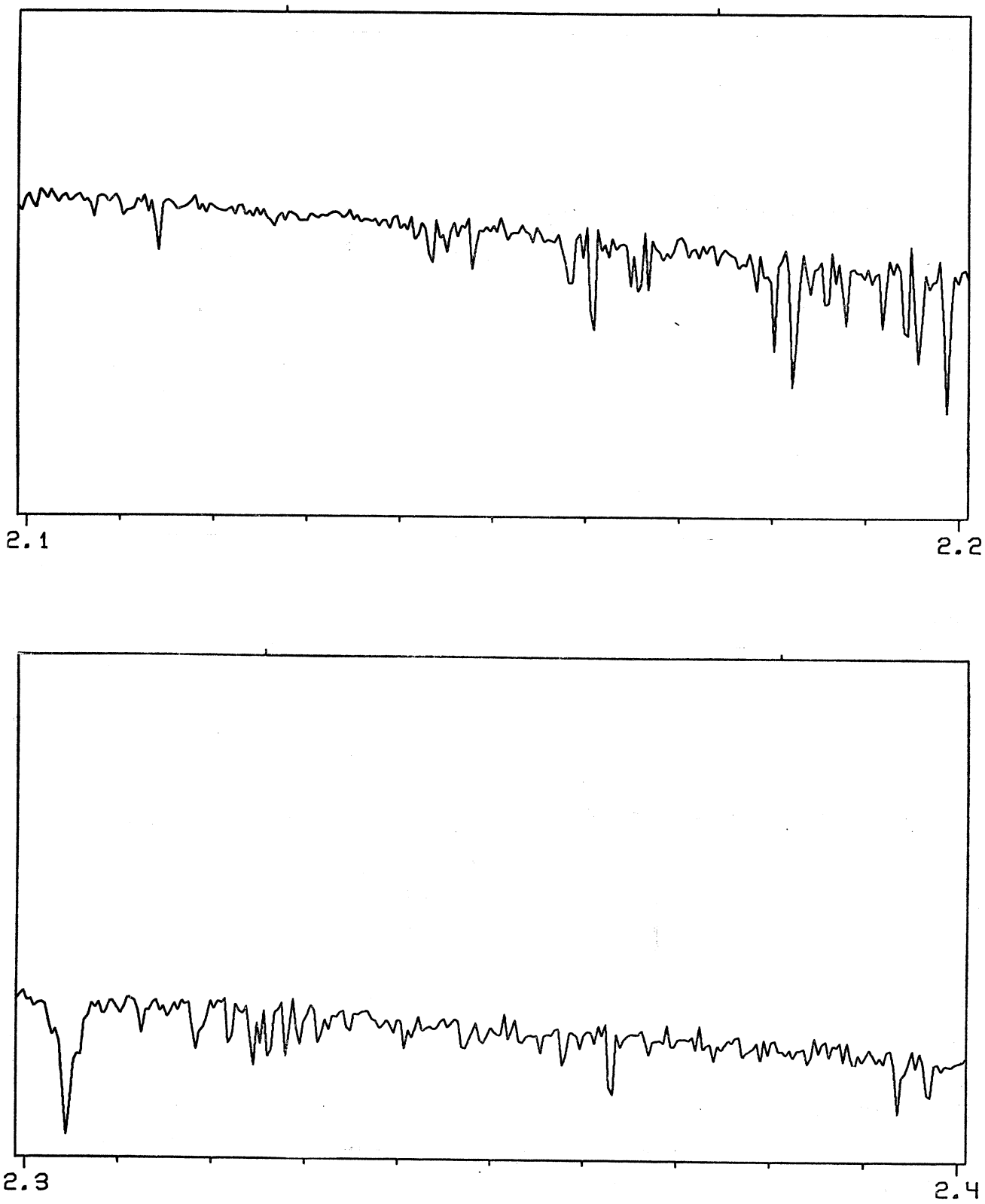

FIG. 8. The Spectrum of α Cygni (A2 Ia)

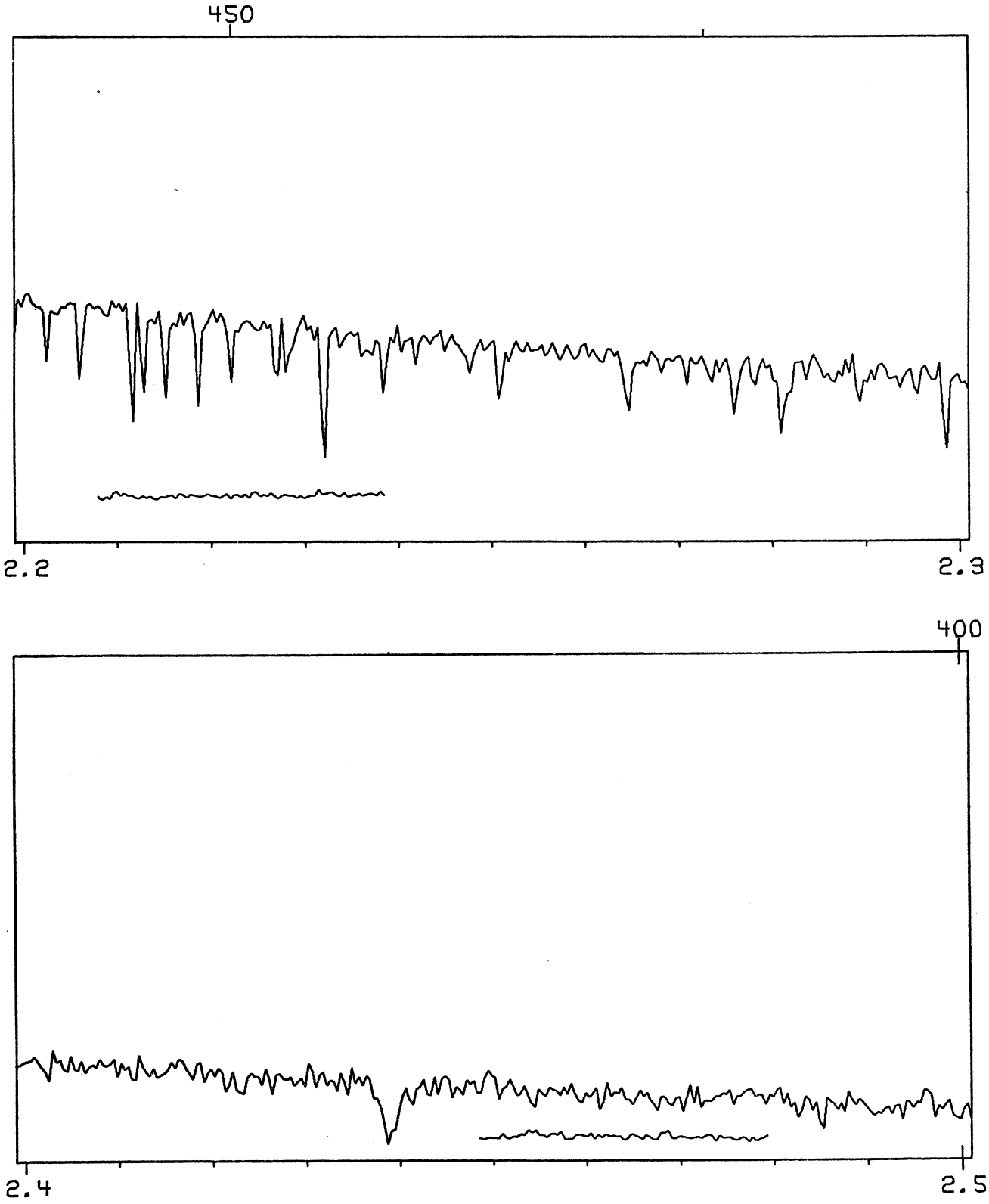

FIG. 8. The Spectrum of α Cygni (A2 Ia)

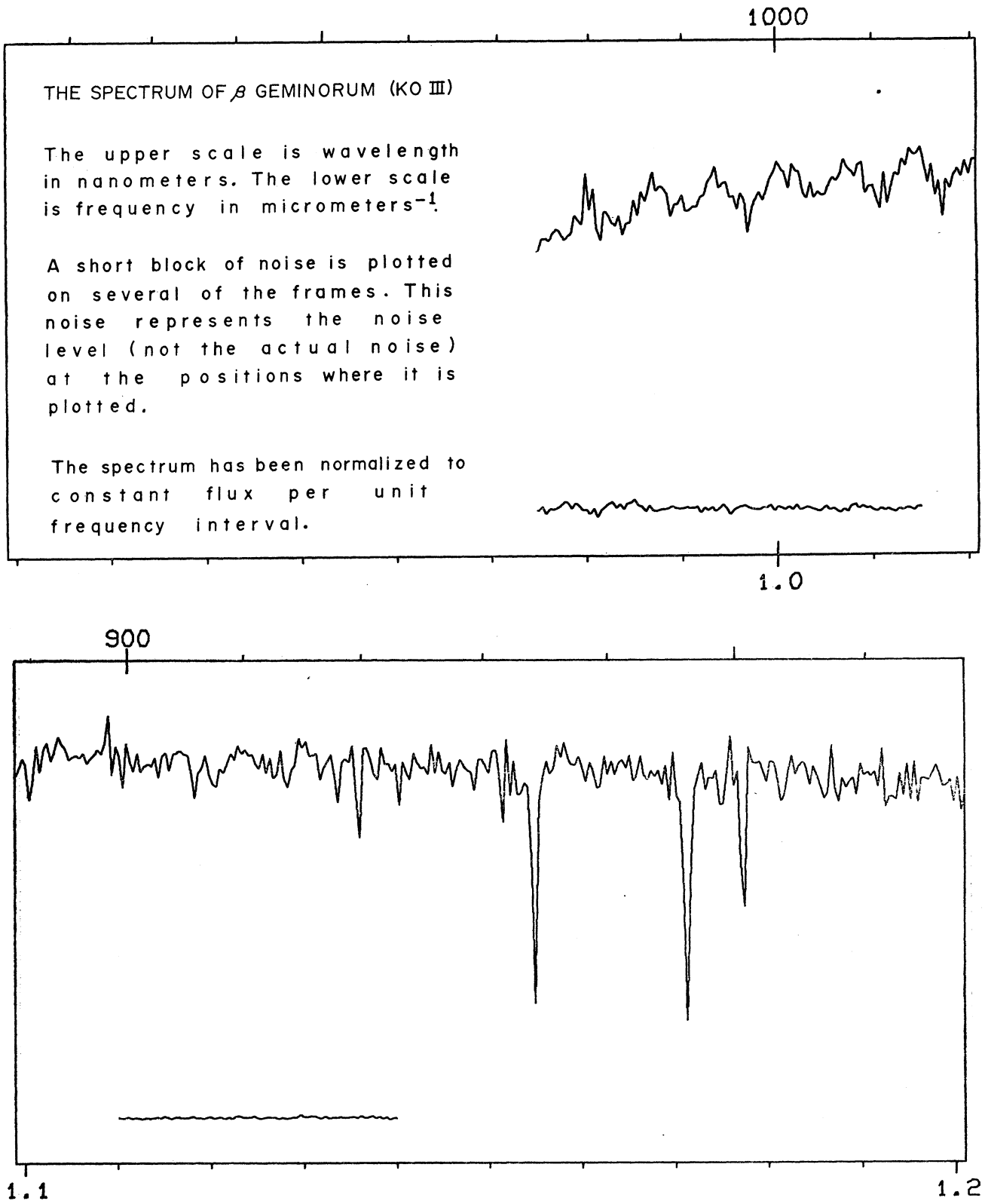

FIG. 9. The Spectrum of β Geminorum (K0 III)

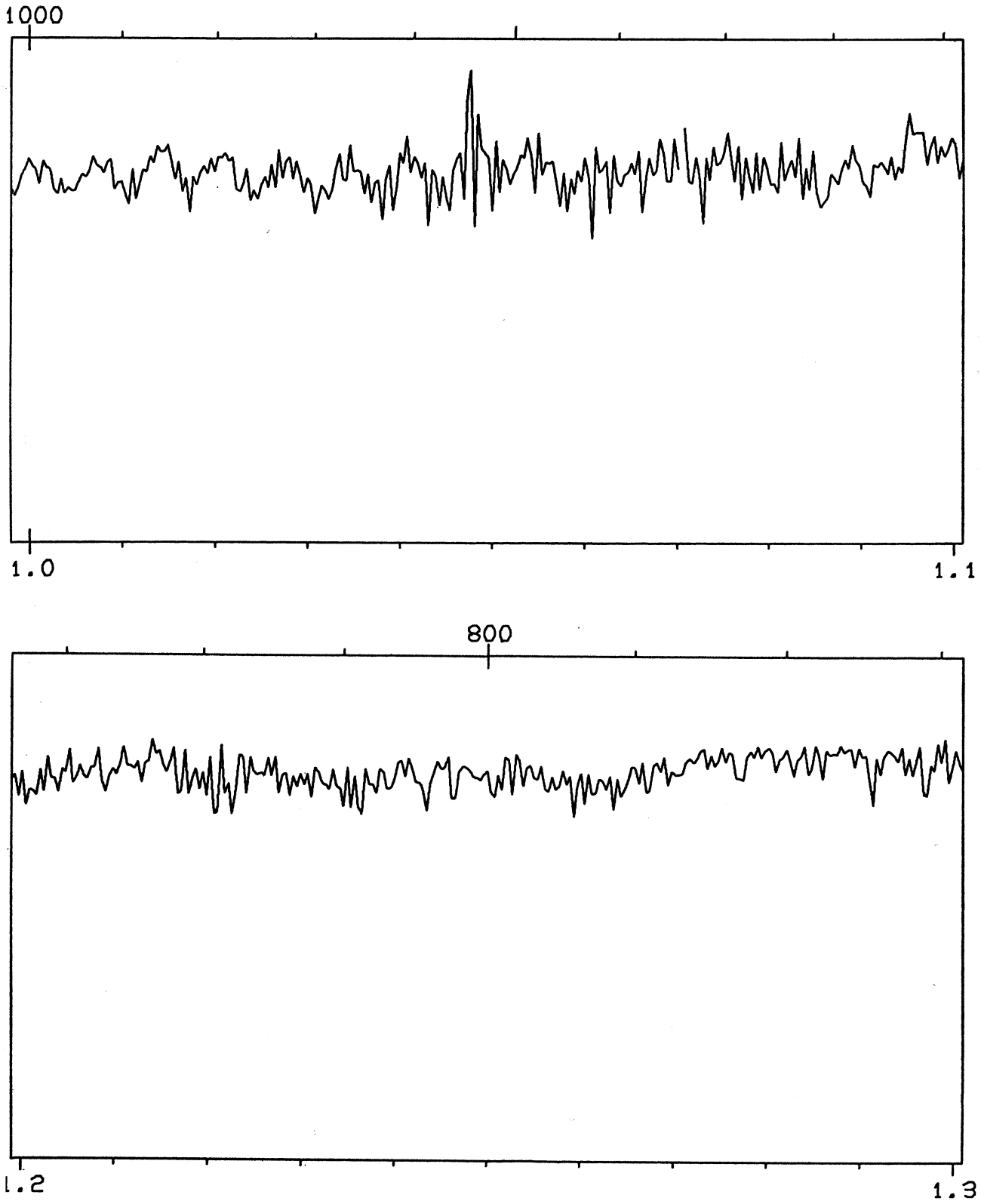

FIG. 9. The Spectrum of β Geminorum (K0 III)

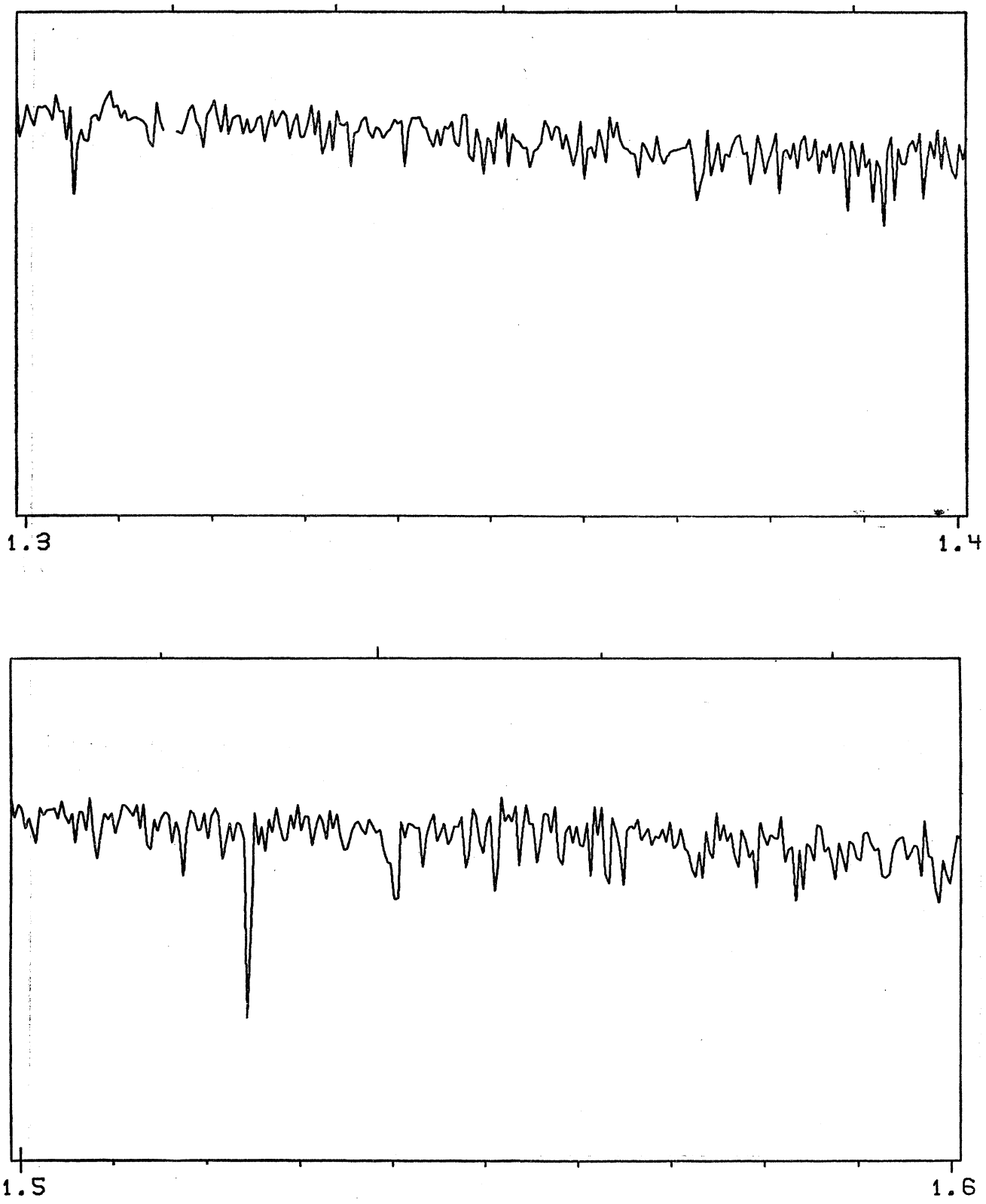

FIG. 9. The Spectrum of β Geminorum (K0 III)

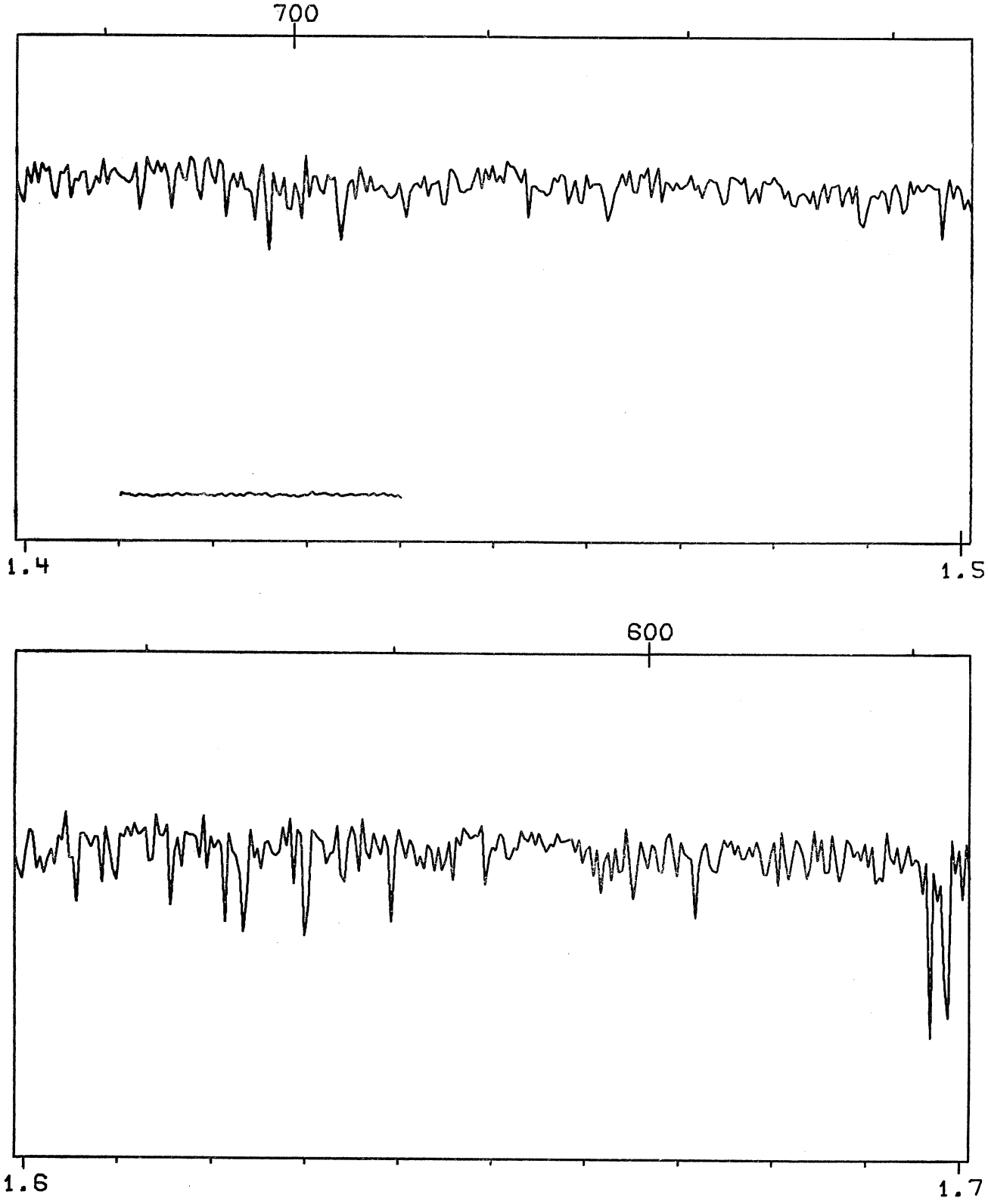

FIG. 9. The Spectrum of β Geminorum (K0 III)

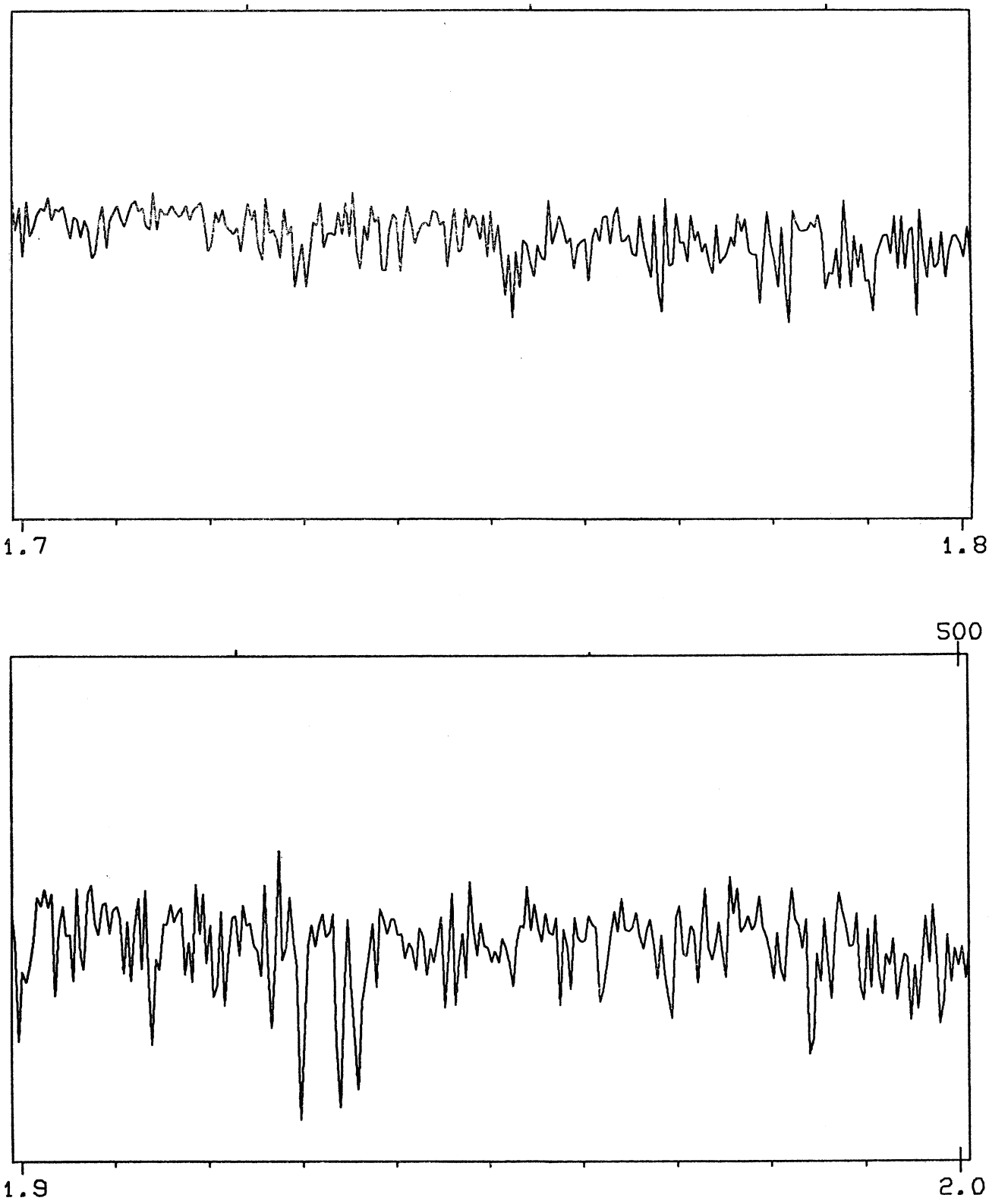

FIG. 9. The Spectrum of β Geminorum (K0 III)

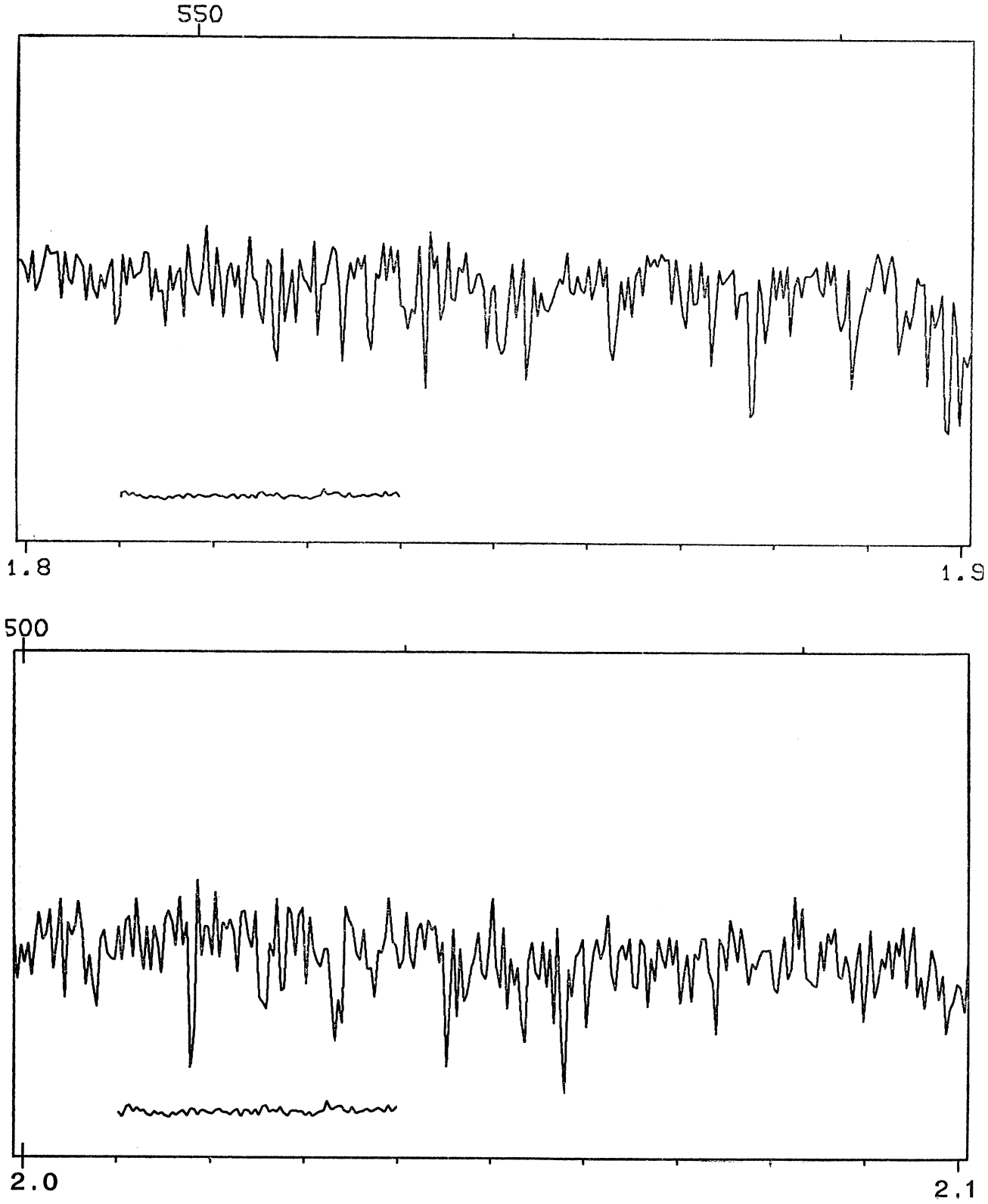

FIG. 9. The Spectrum of β Geminorum (K0 III)

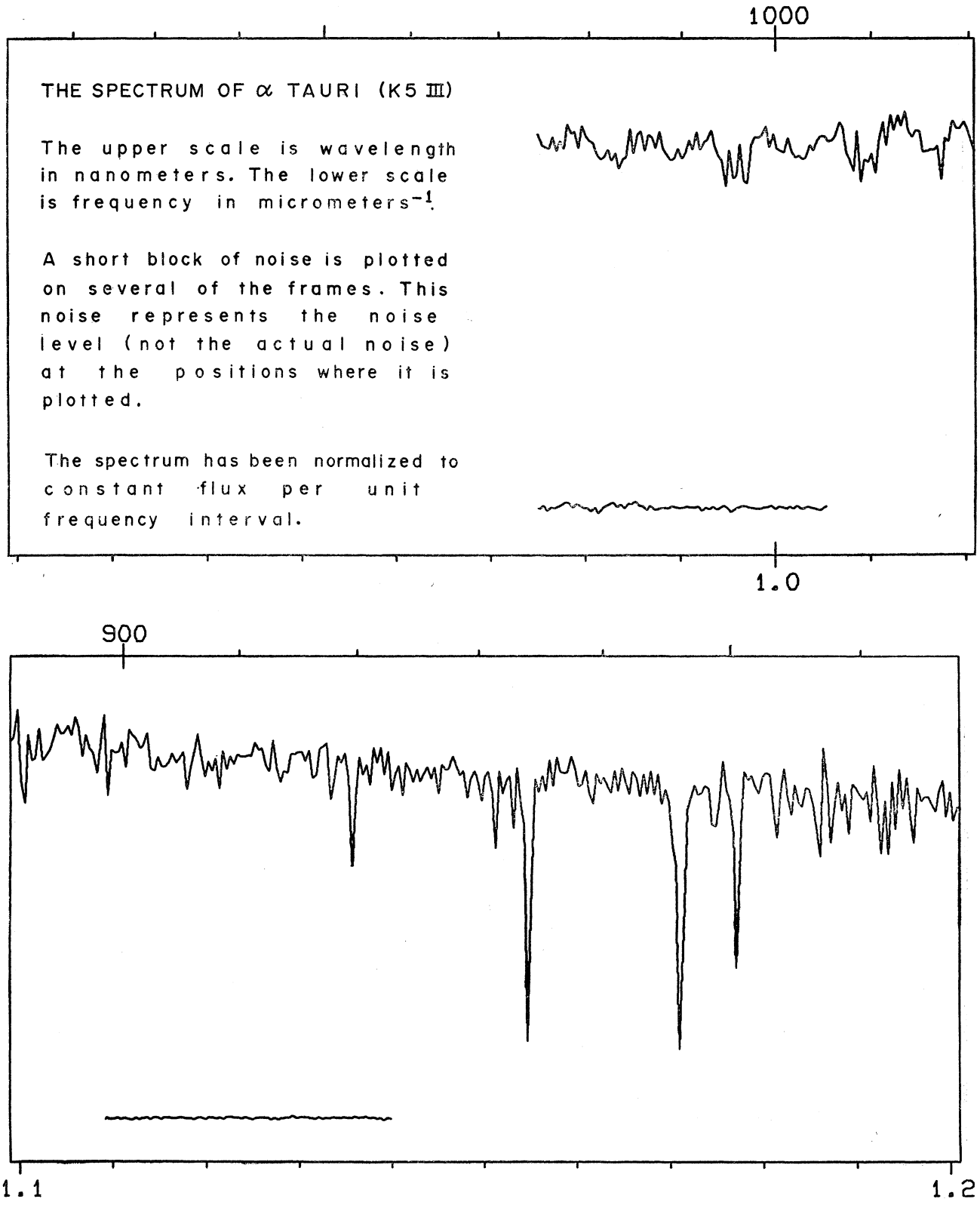

FIG. 10. The Spectrum of α Tauri (K5 III)

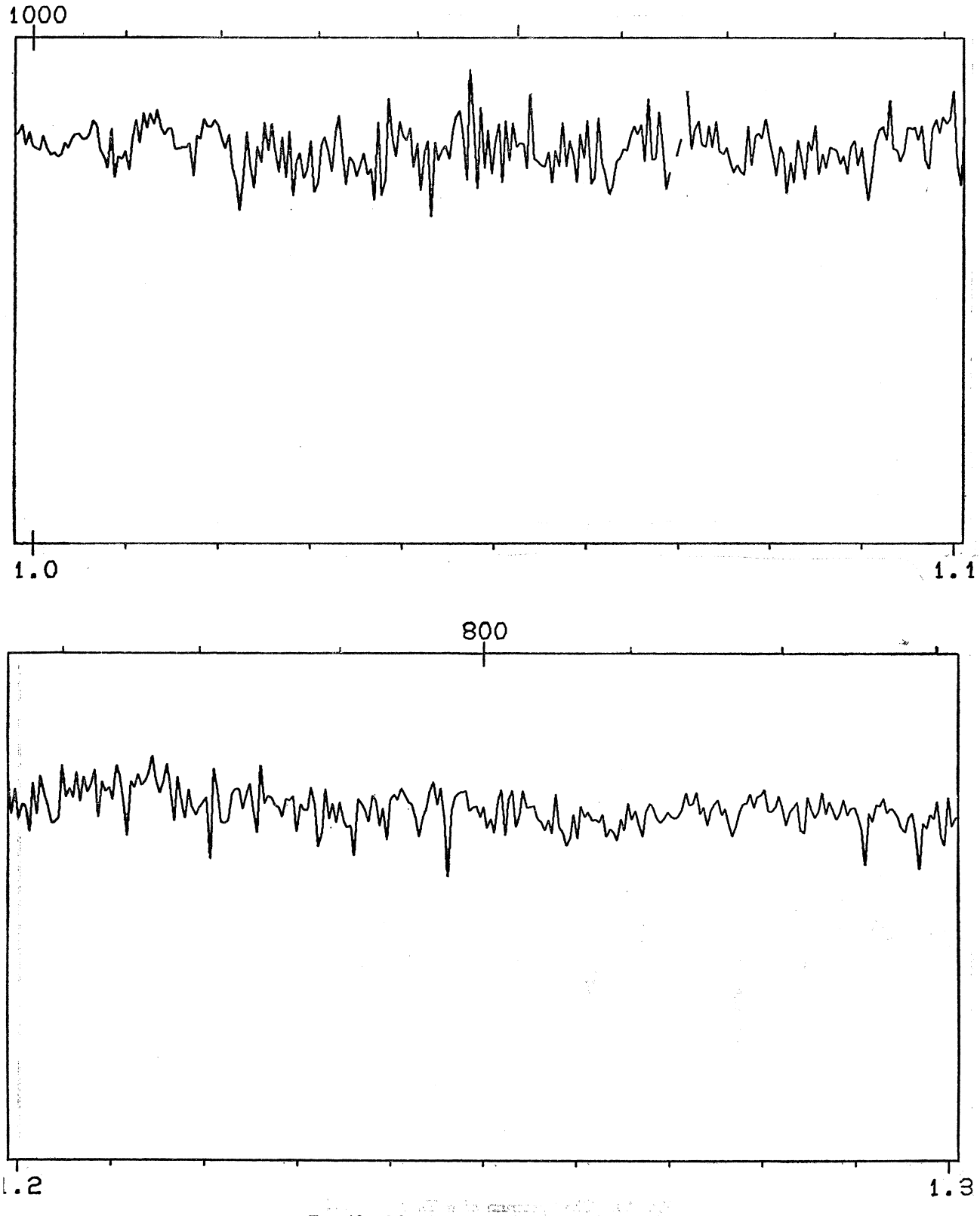

FIG. 10. The Spectrum of α Tauri (K5 III)

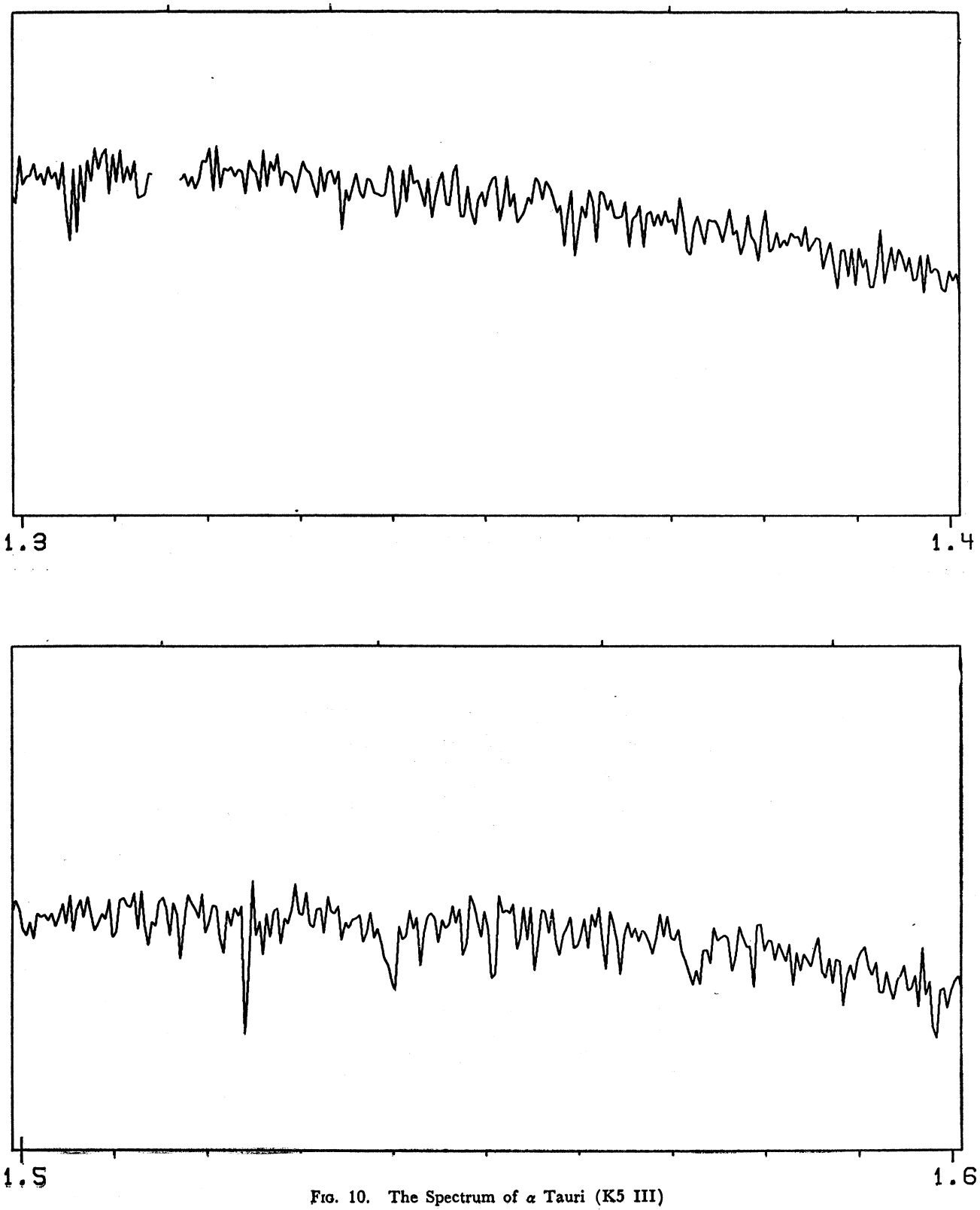

FIG. 10. The Spectrum of α Tauri (K5 III)

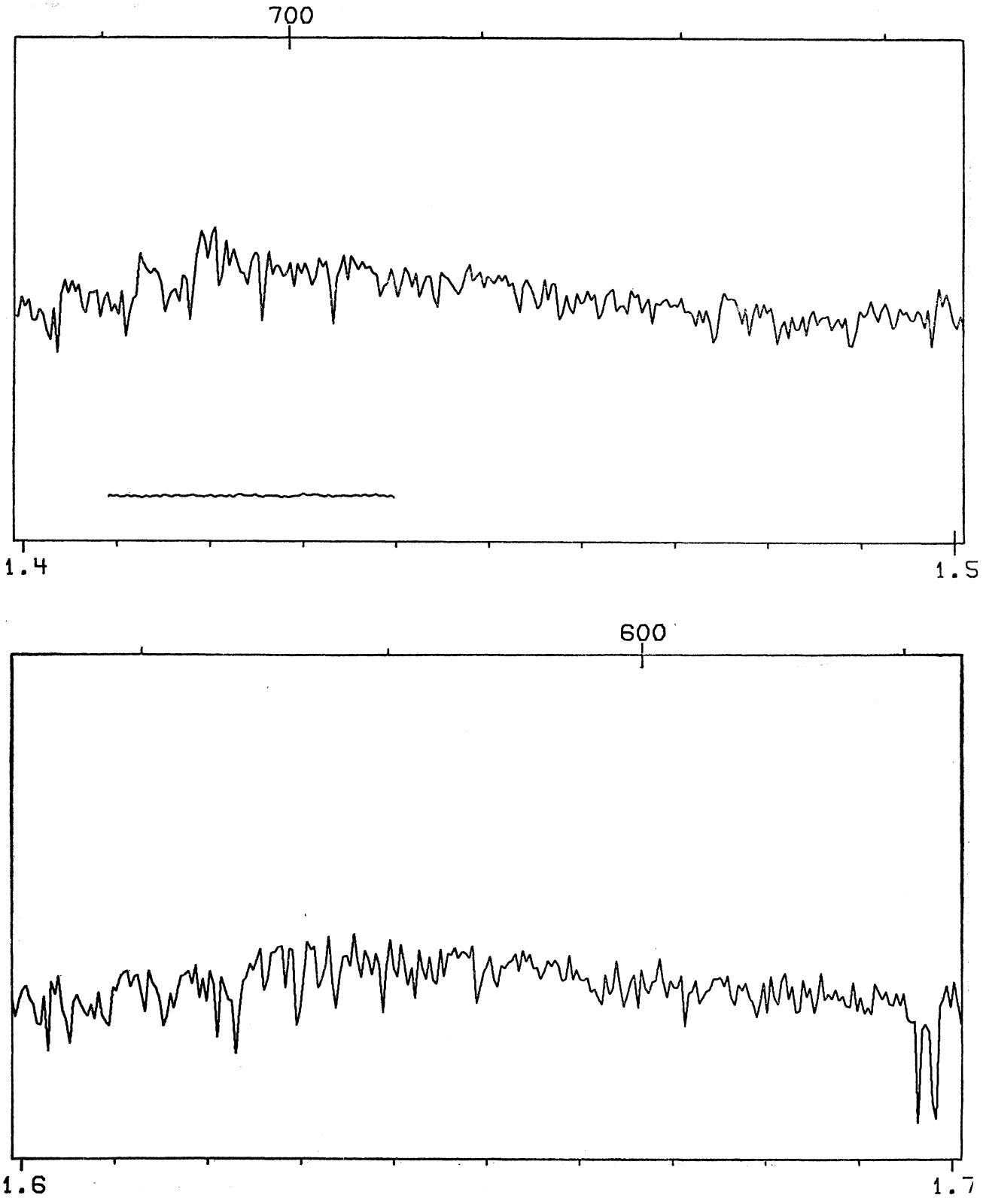

FIG. 10. The Spectrum of α Tauri (K5 III)

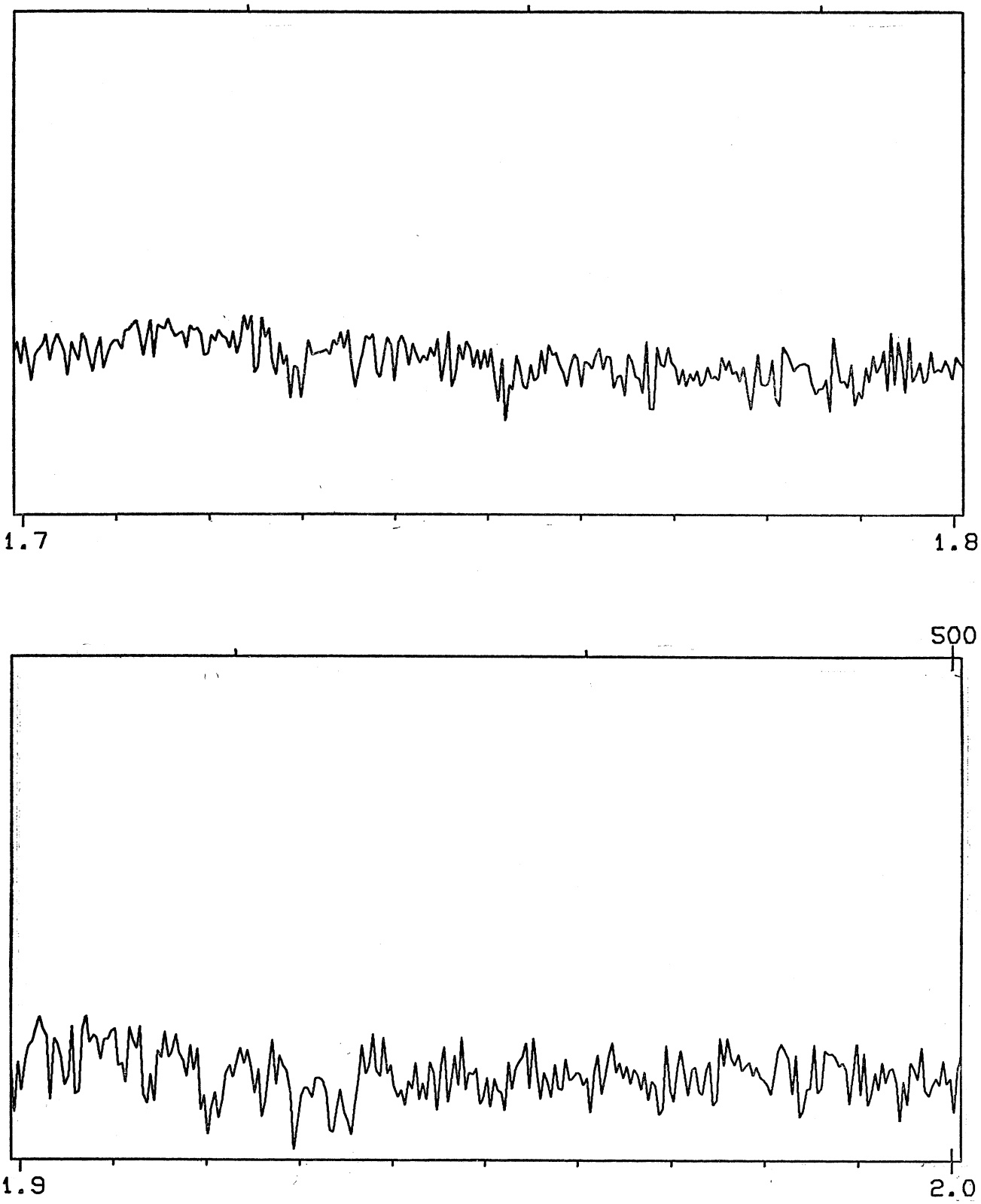

FIG. 10. The Spectrum of α Tauri (K5 III)

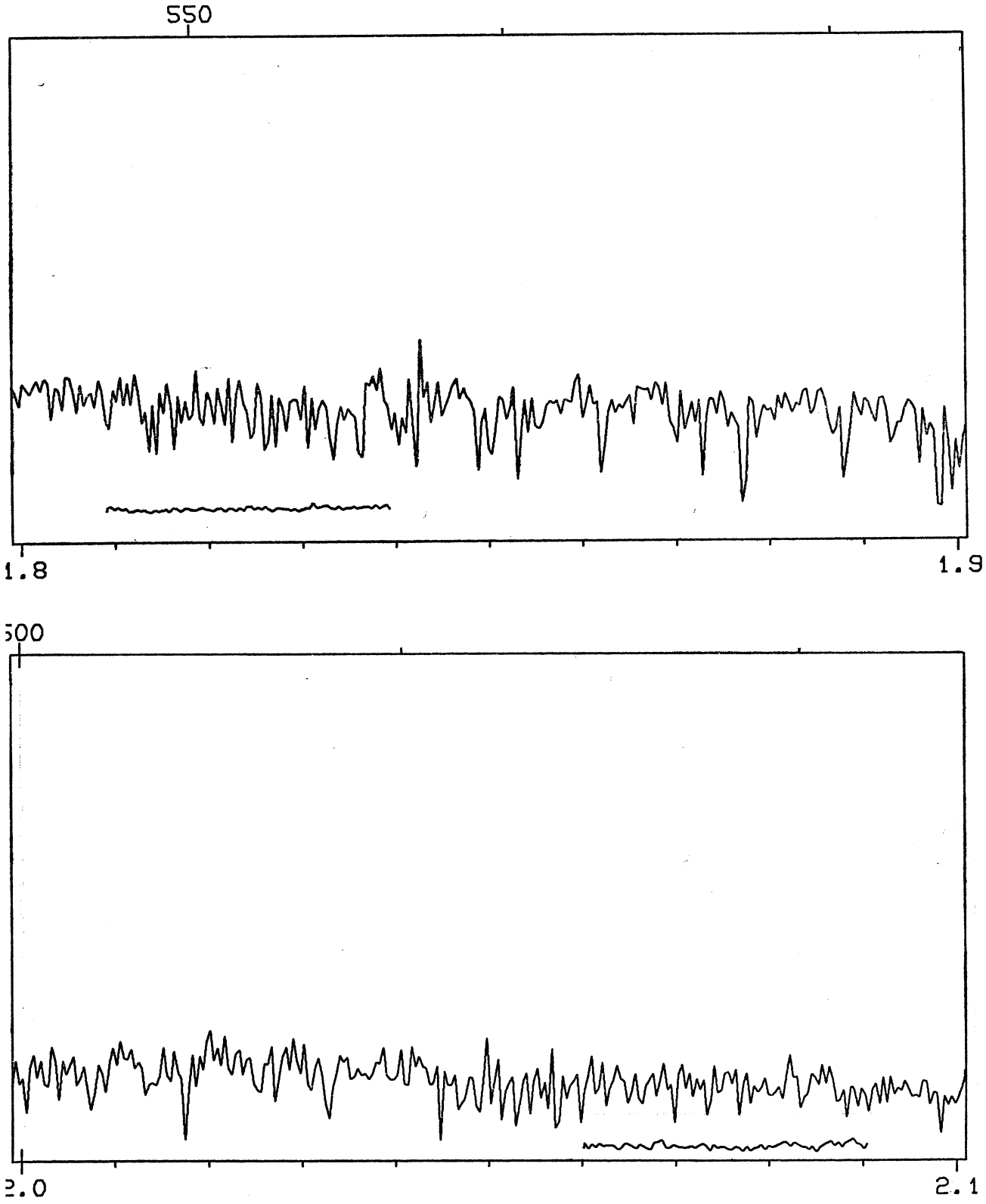

FIG. 10. The Spectrum of α Tauri (K5 III)

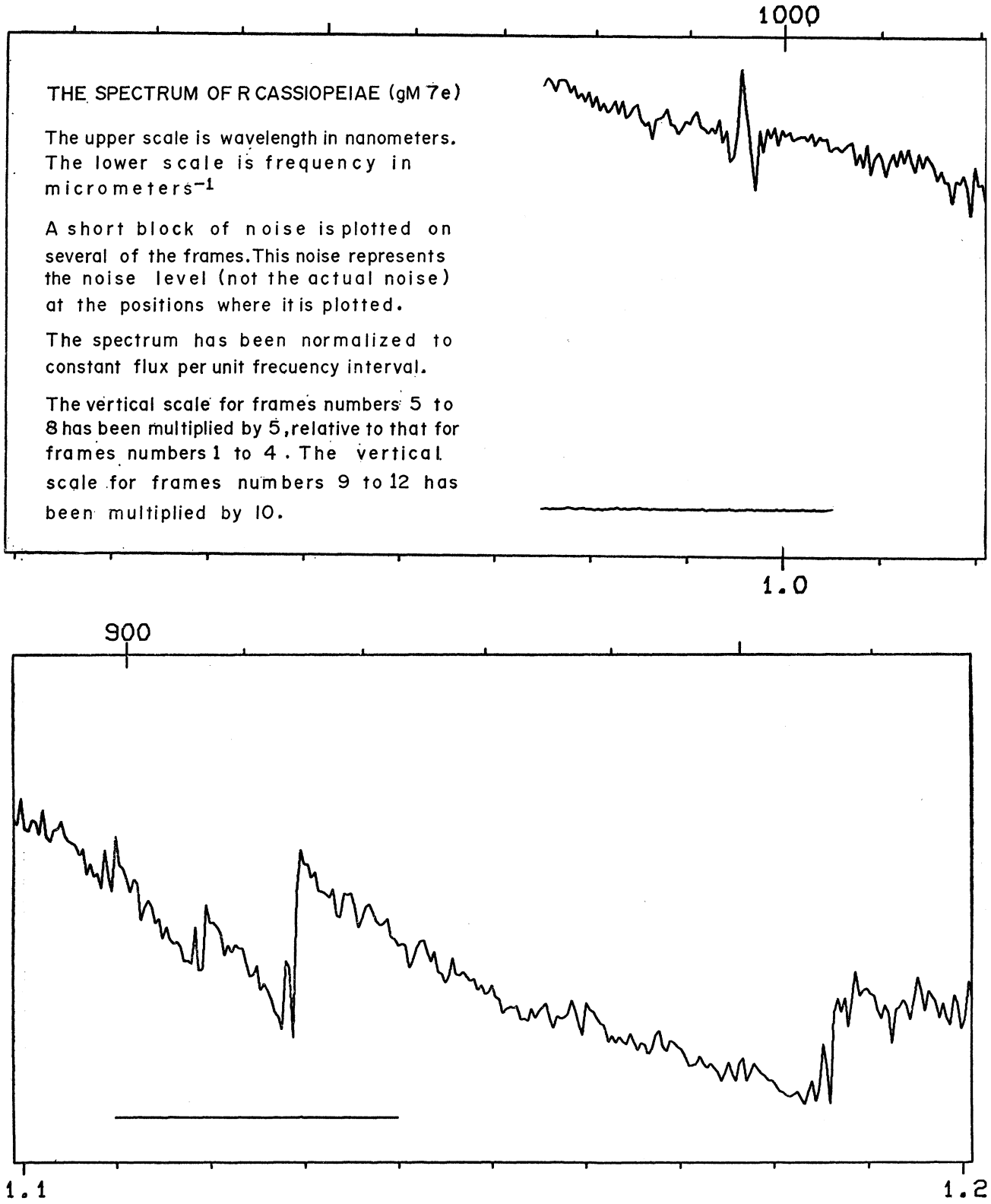

FIG. 11. The Spectrum of R Cassiopeiae (gM 7e)

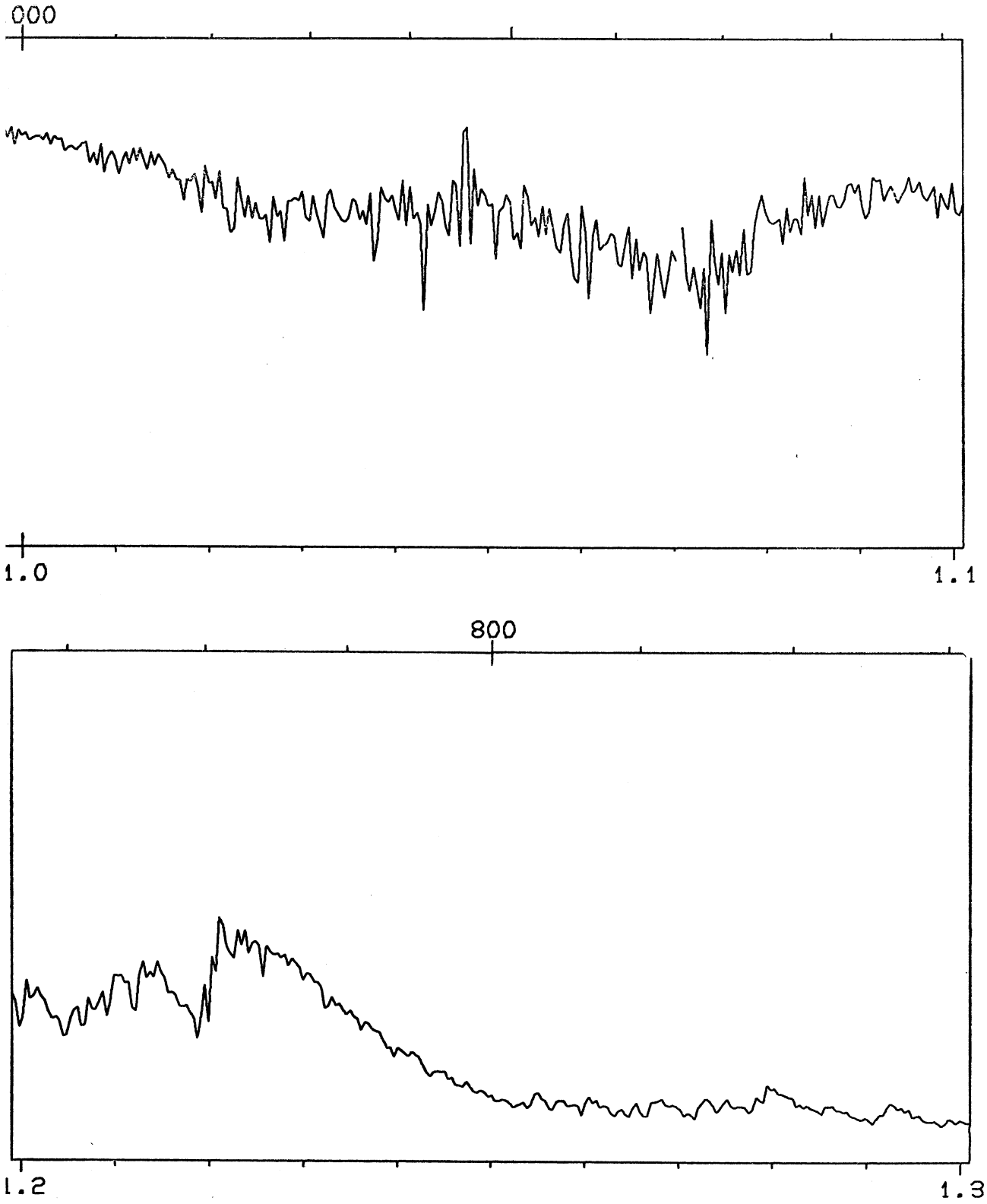

FIG. 11. The Spectrum of R Cassiopeiae (gM 7e)

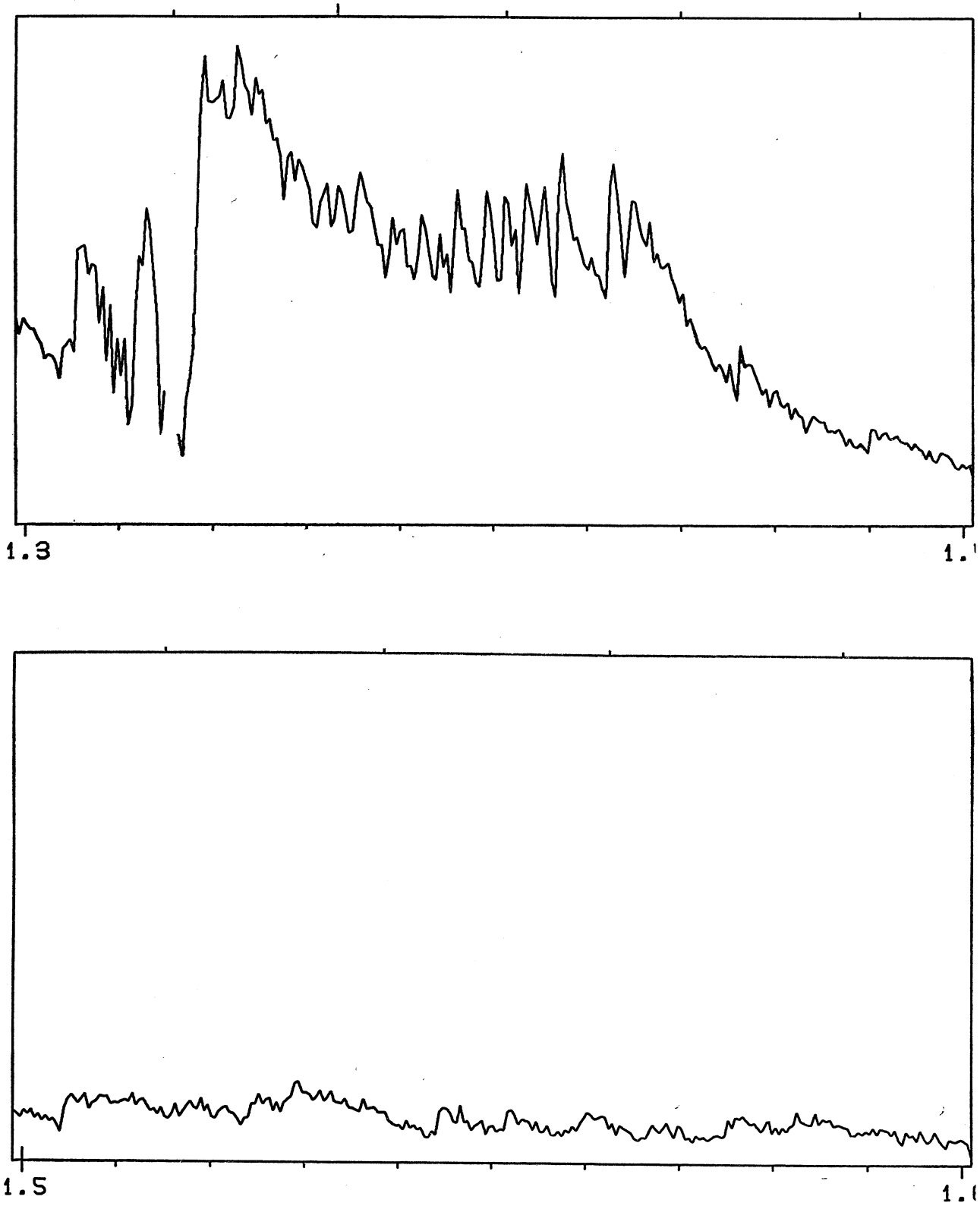

FIG. 11. The Spectrum of R Cassiopeiae (gM 7e)

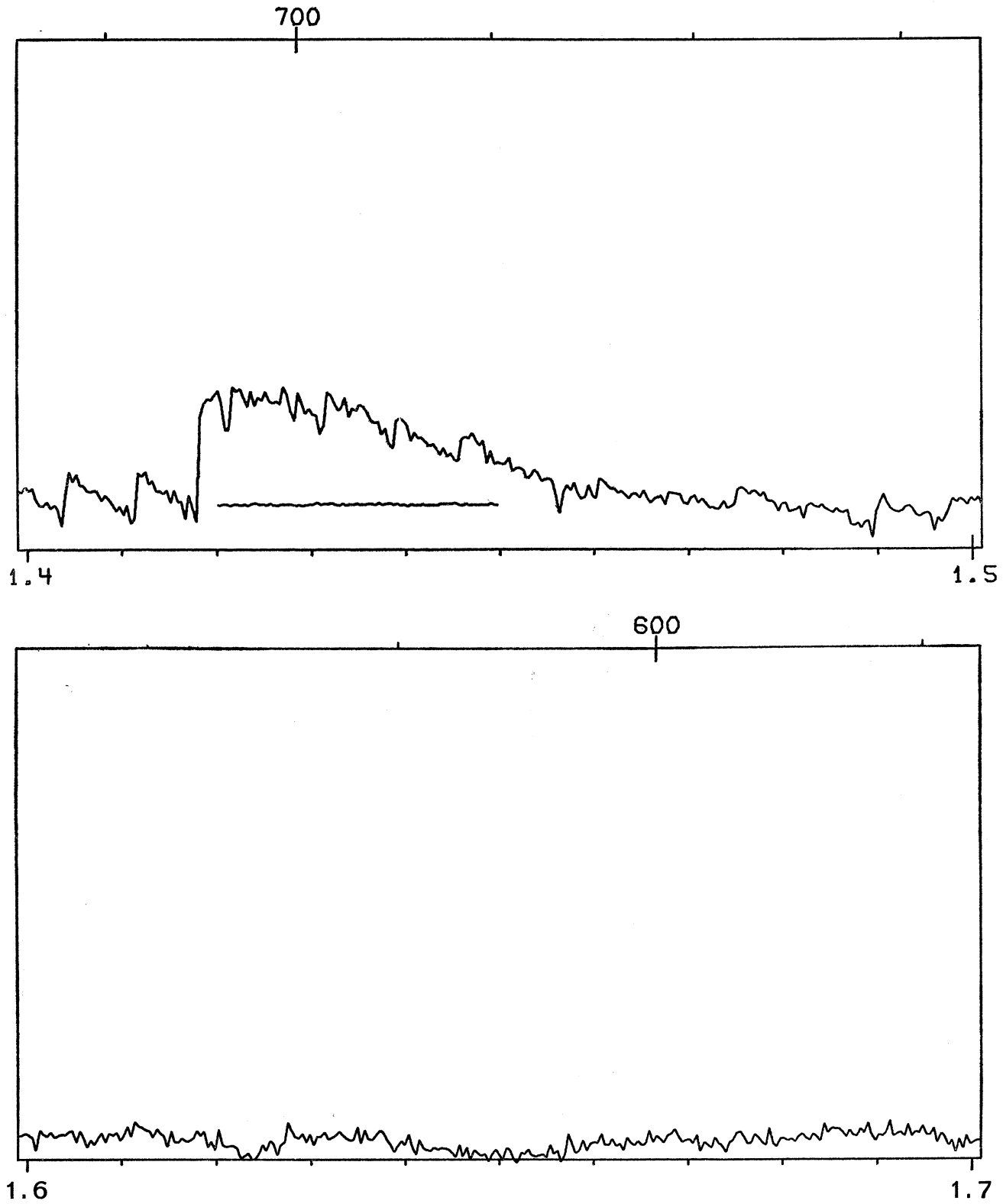

FIG. 11. The Spectrum of R Cassiopeiae (gM 7e)

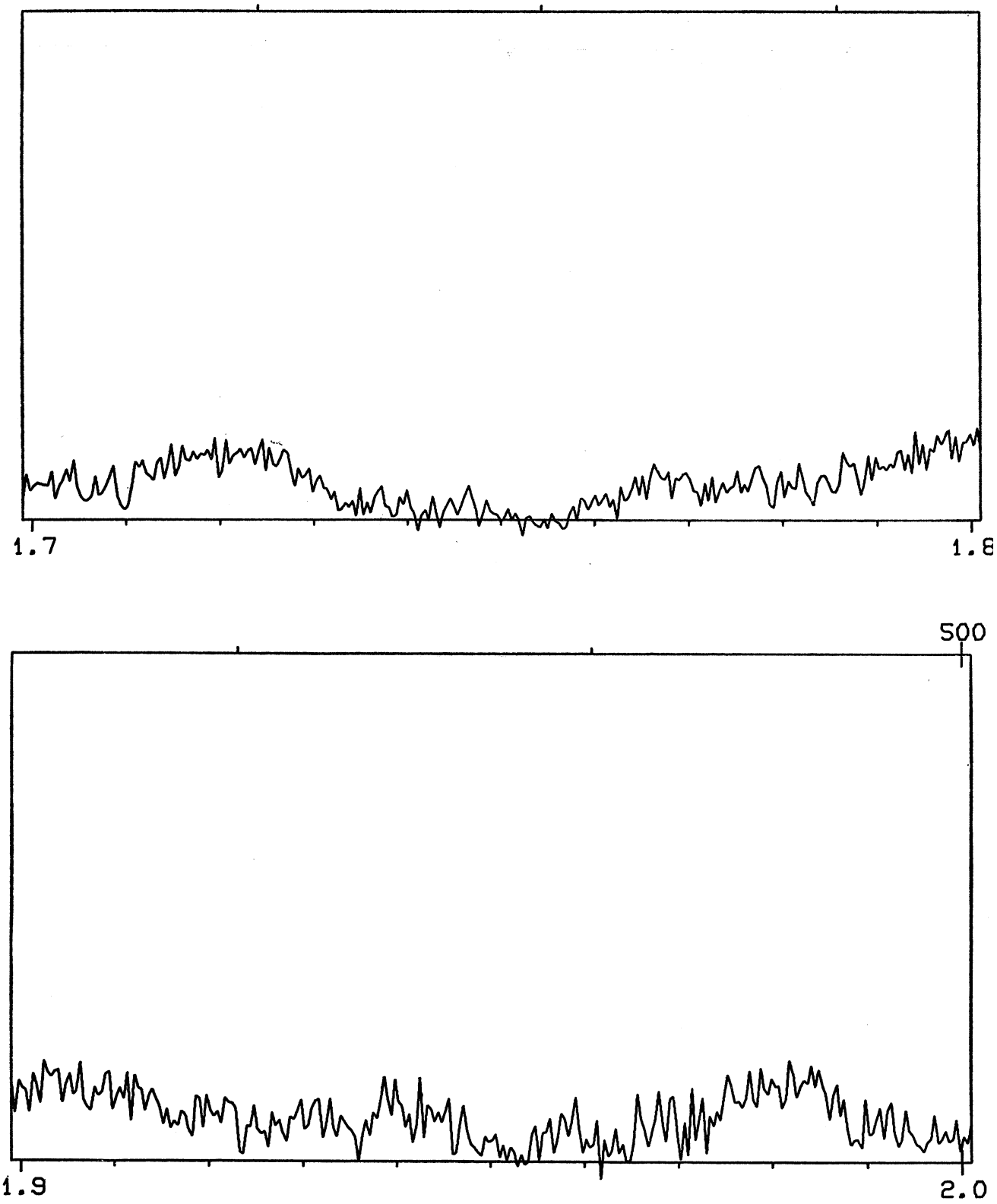

FIG. 11. The Spectrum of R Cassiopeiae (gM 7e)

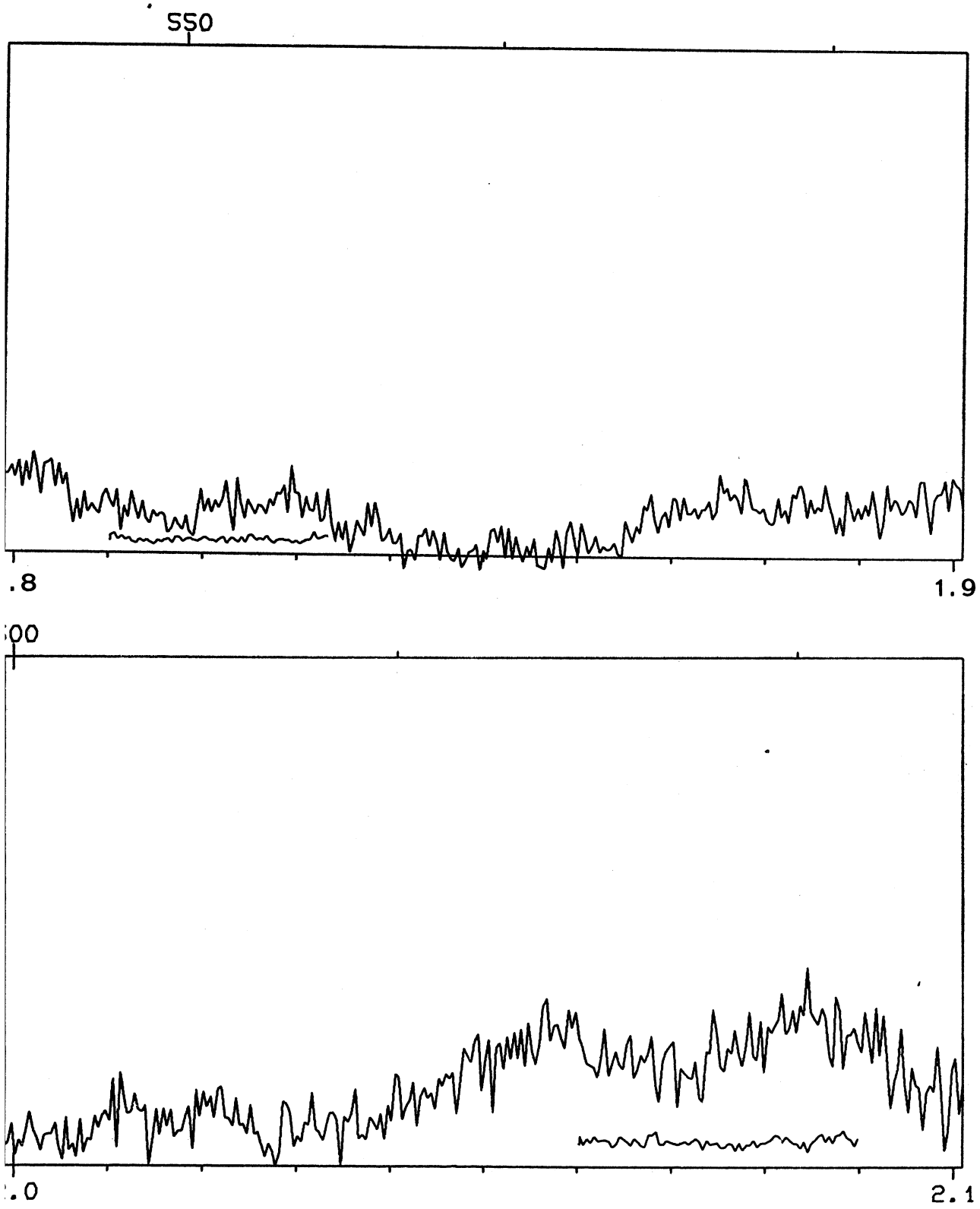

FIG. 11. The Spectrum of R Cassiopeiae (gM 7e)

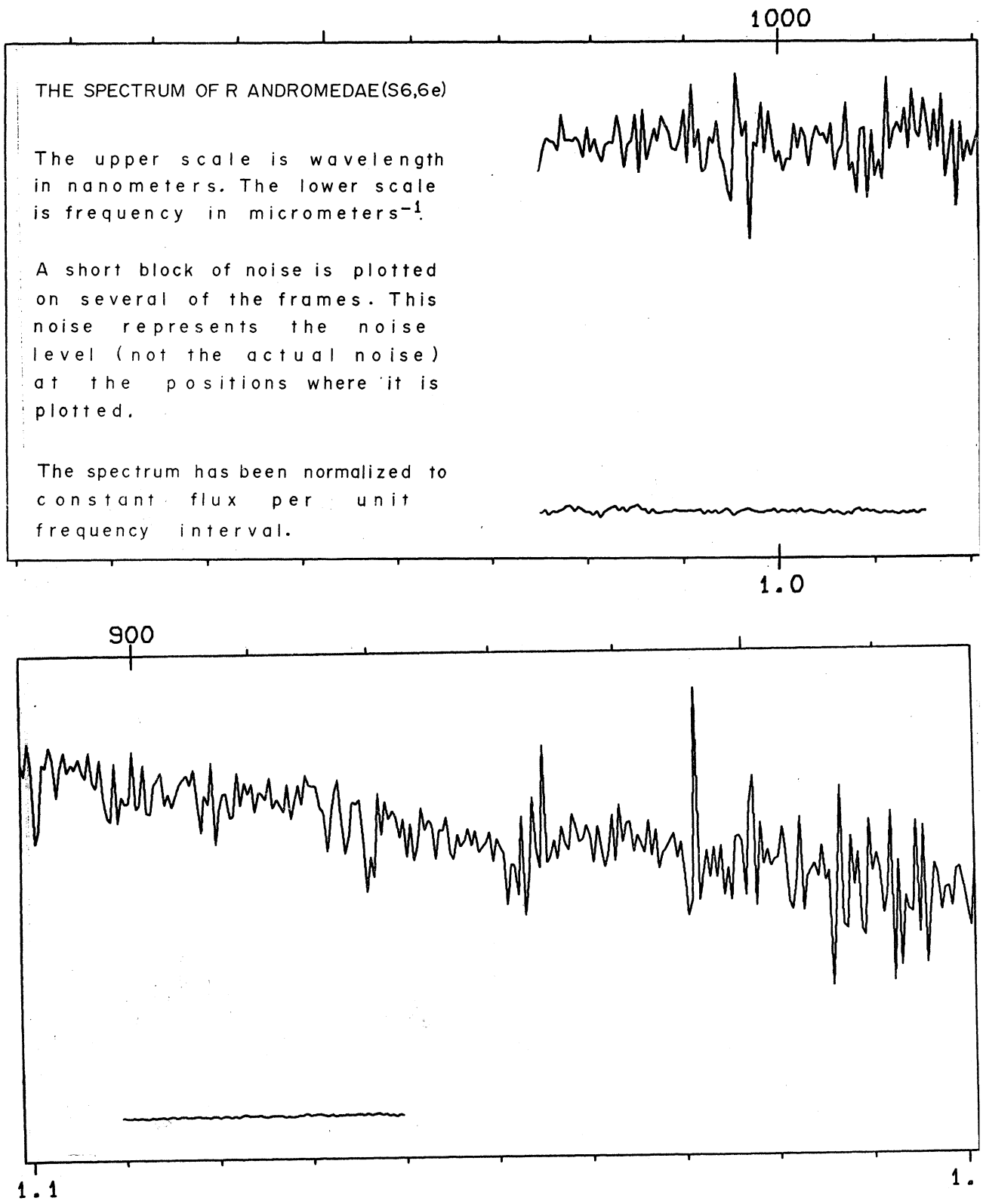

FIG. 12. The Spectrum of R Andromedae (S6,6e)

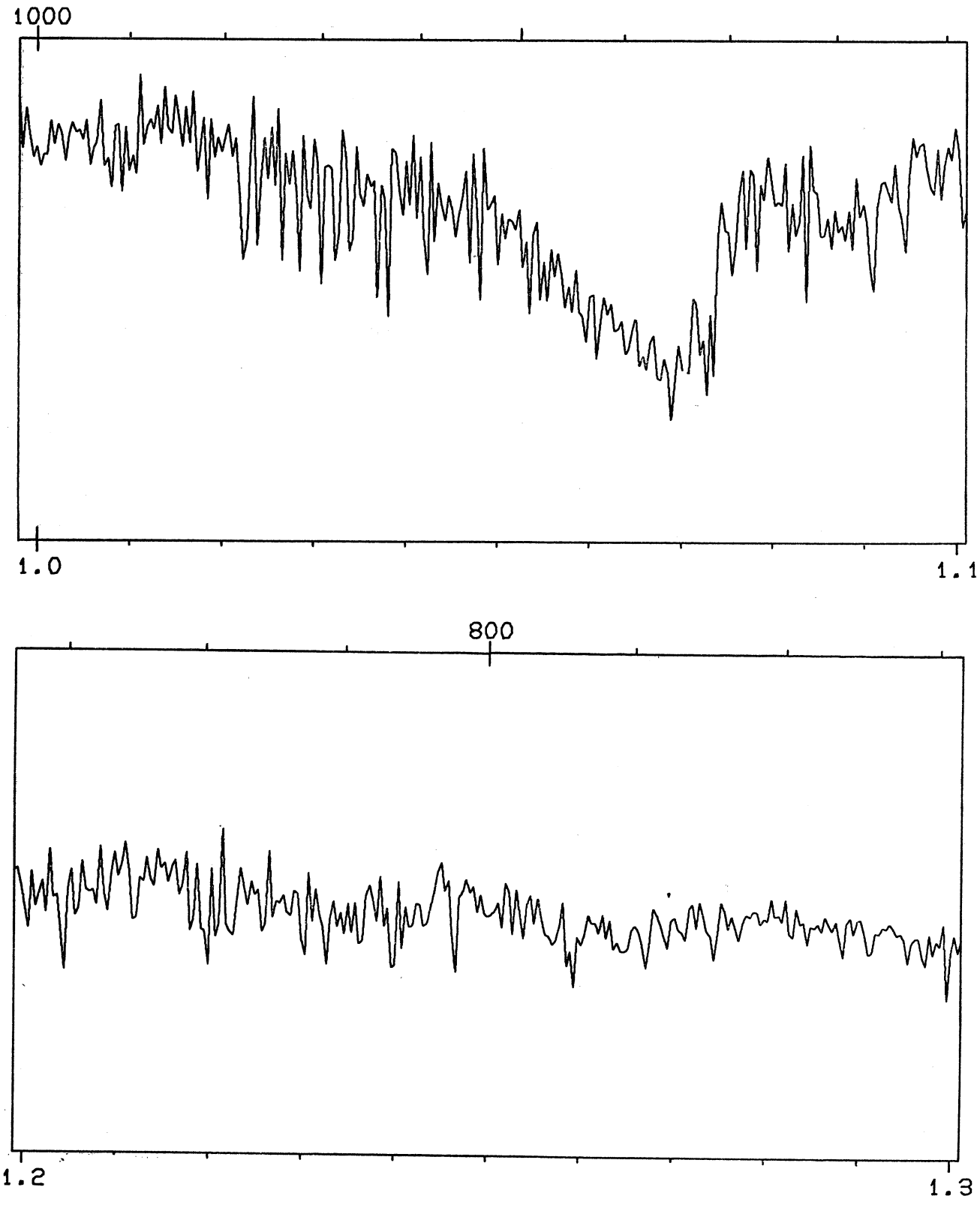

FIG. 12. The Spectrum of R Andromedae (S6,6e)

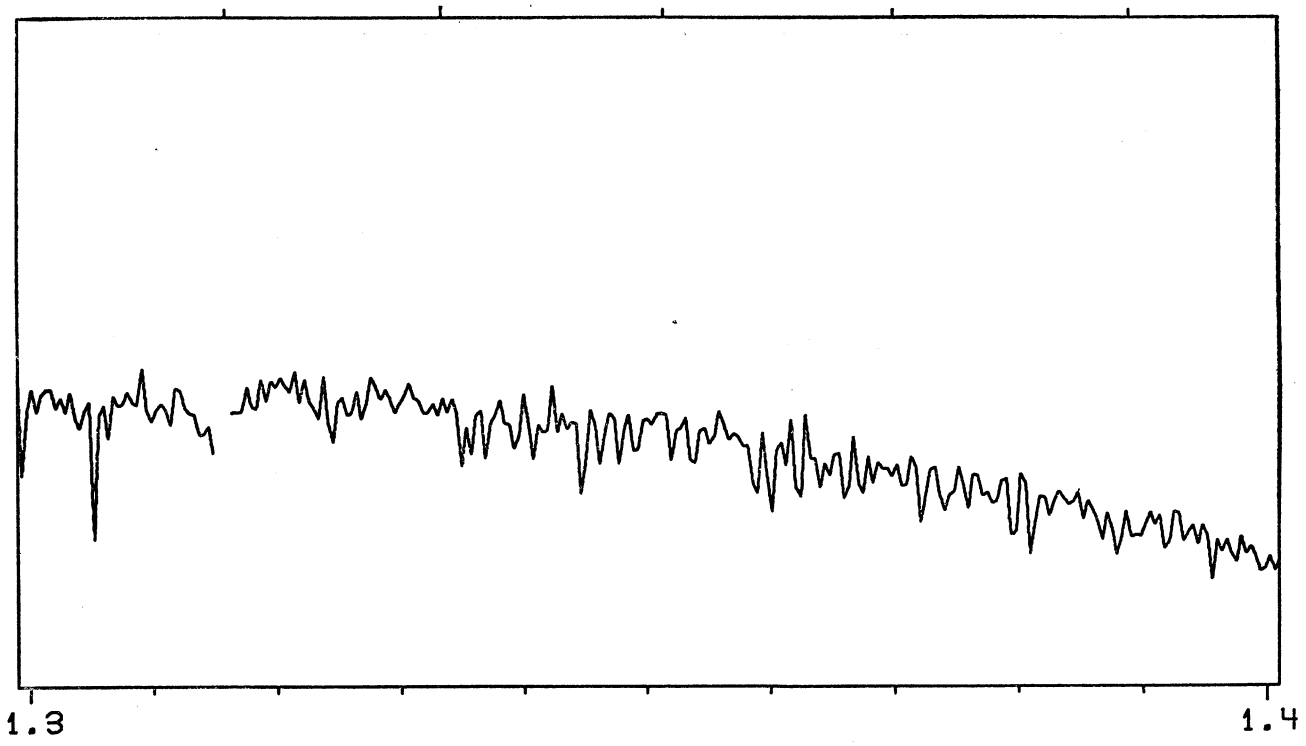

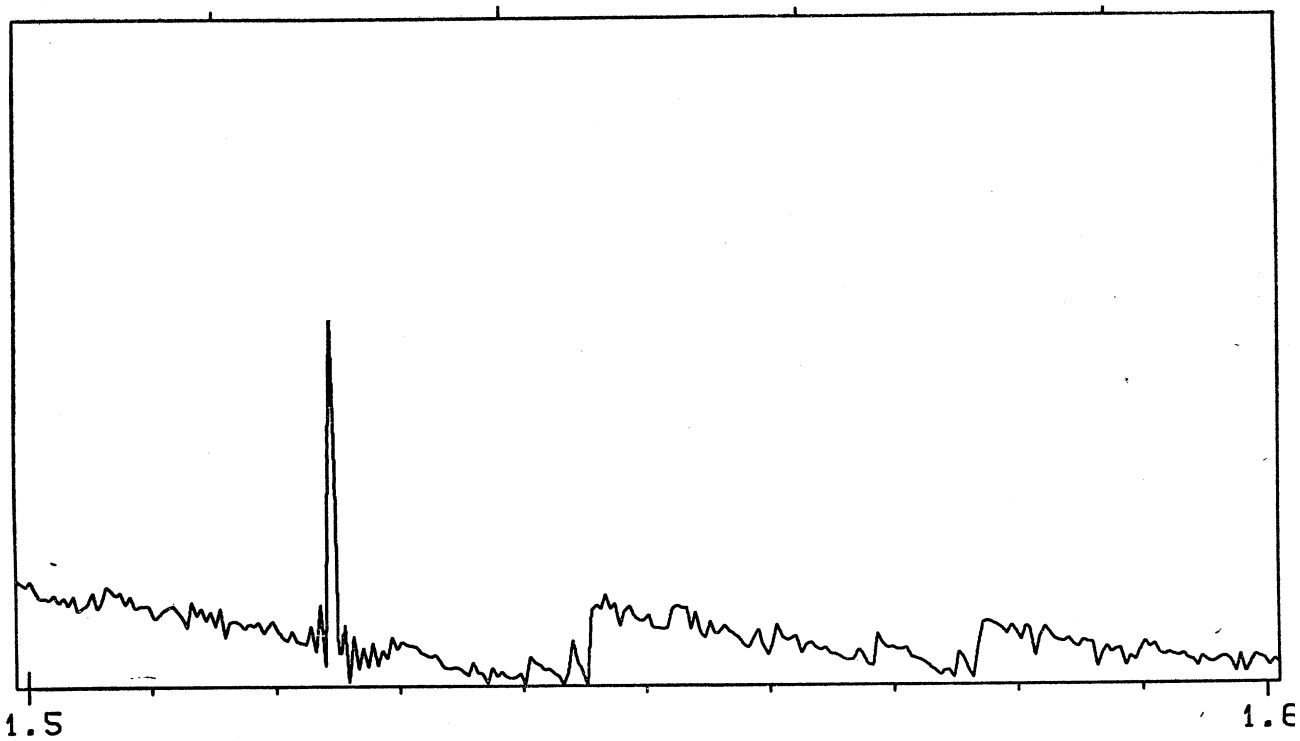

FIG. 12. The Spectrum of R Andromedae (S6,6e)

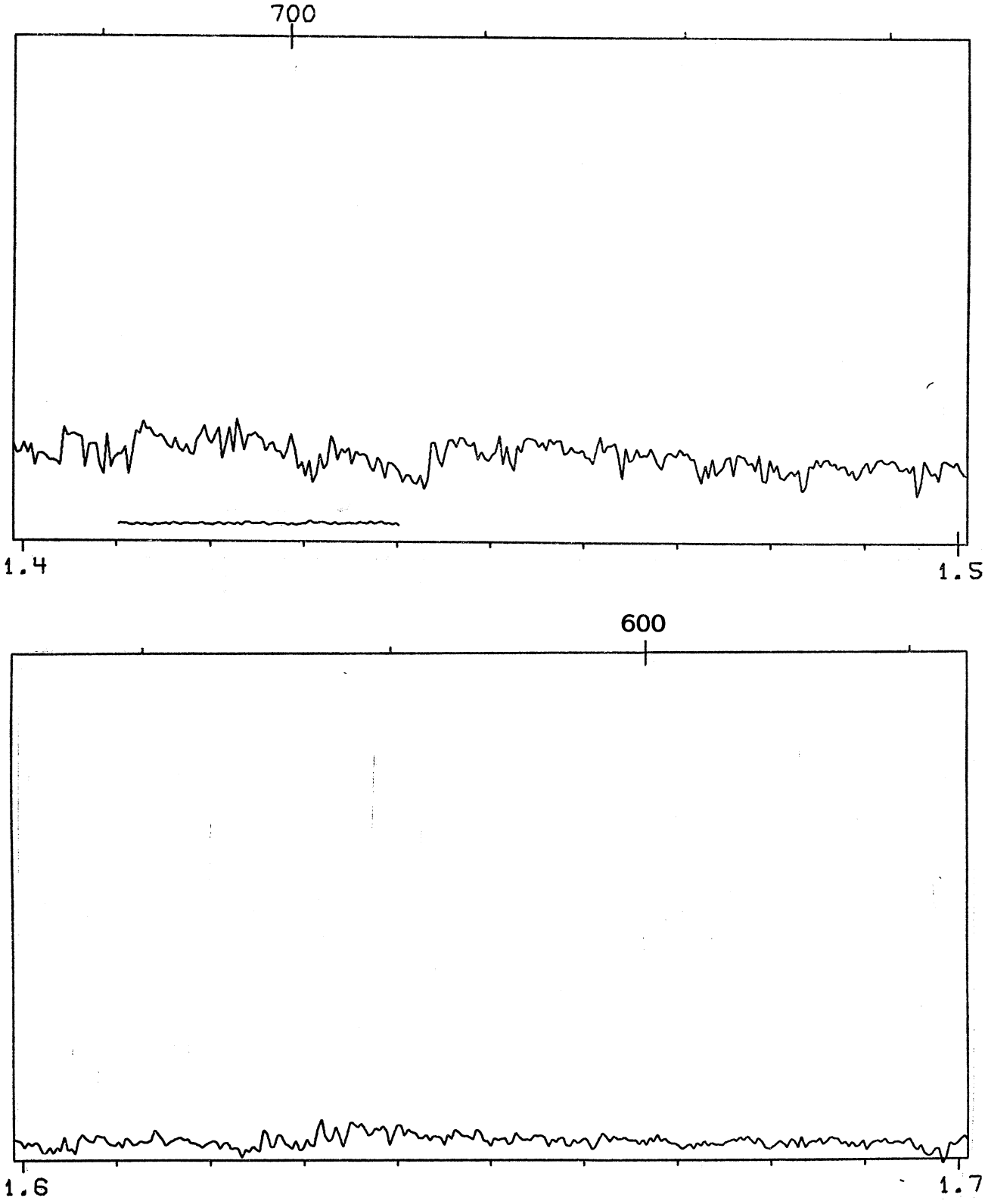

FIG. 12. The Spectrum of R Andromedae (S6,6e)

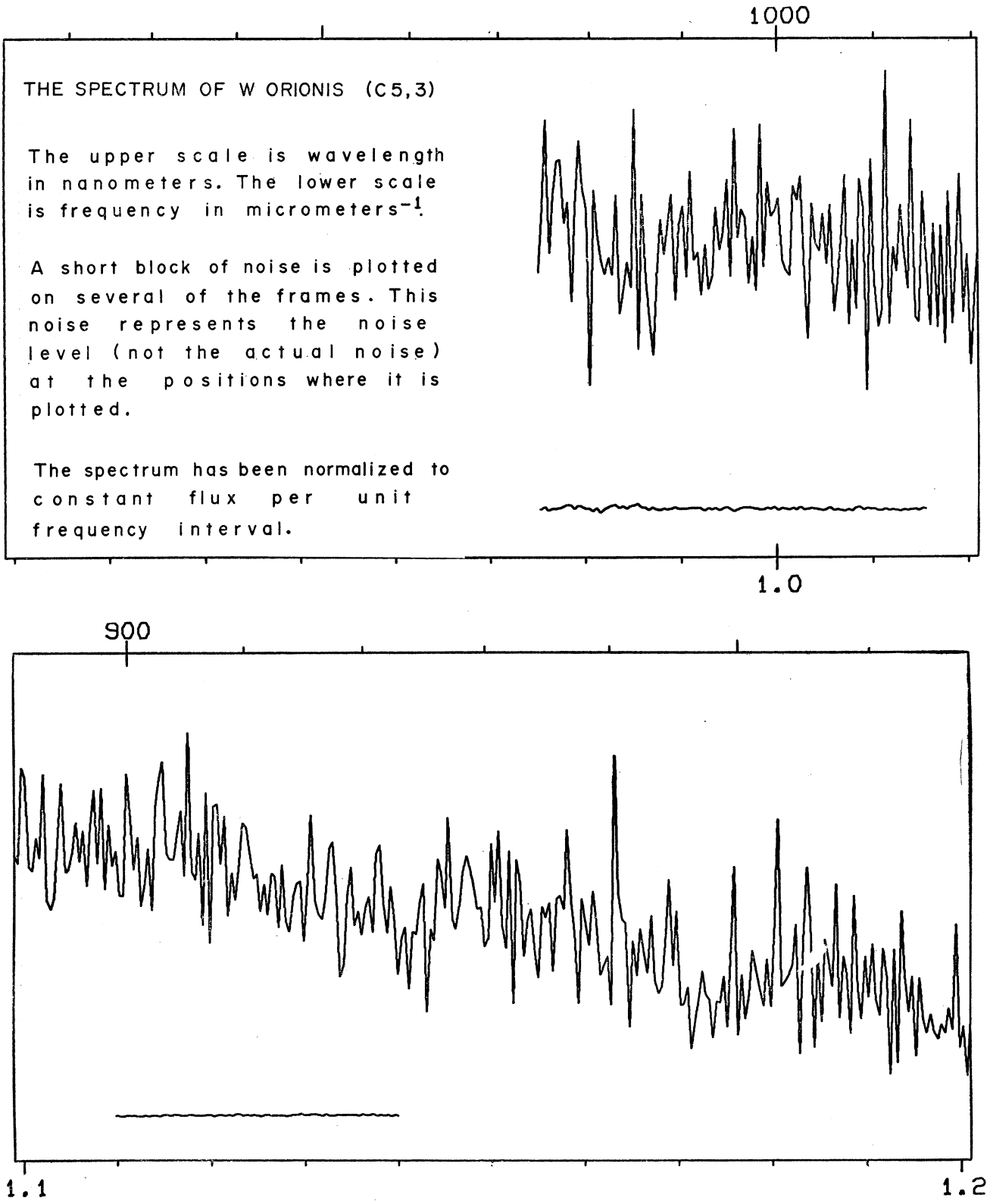

FIG. 13. The Spectrum of W Orionis (C5,3)

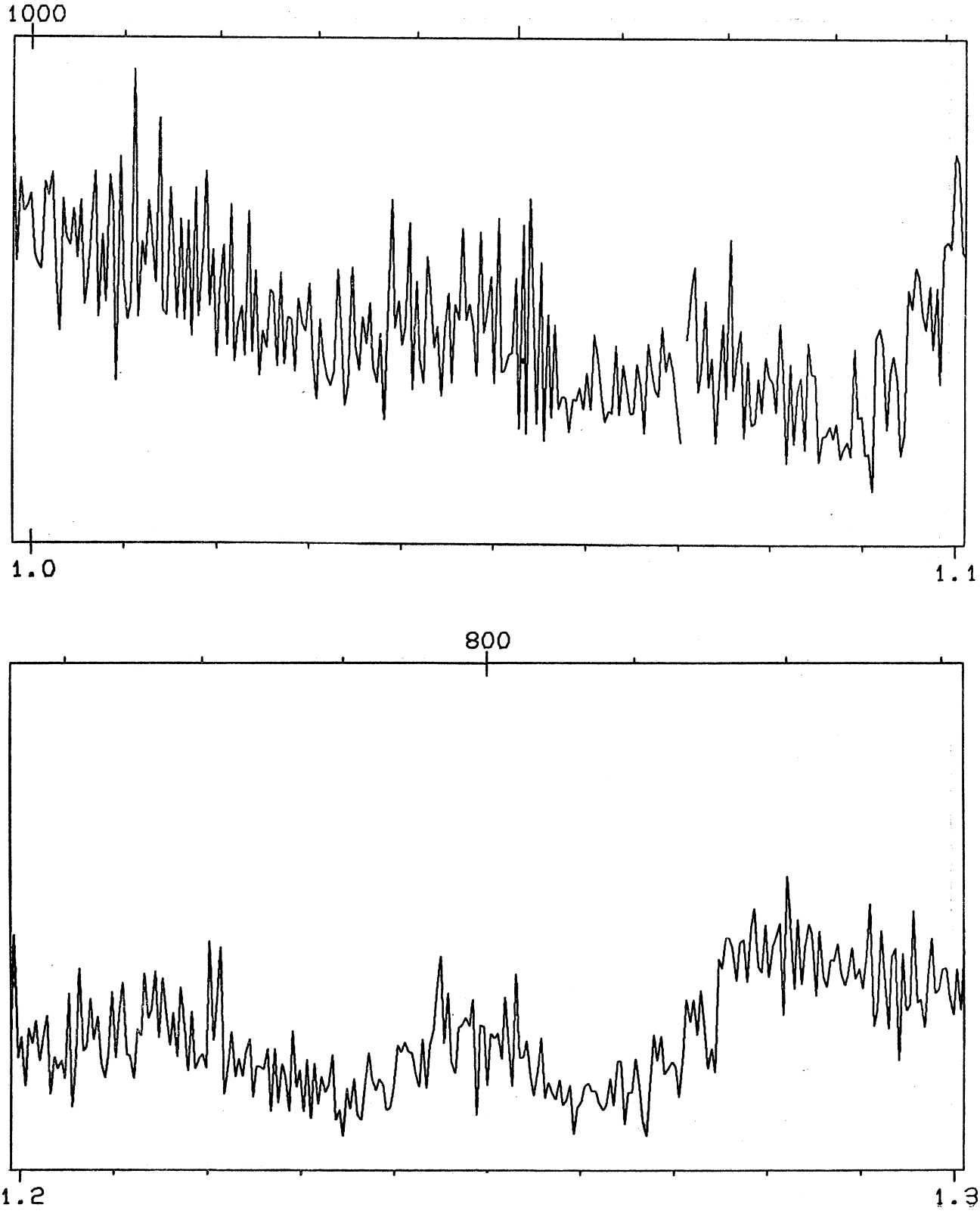

FIG. 13. The Spectrum of W Orionis (C5,3)

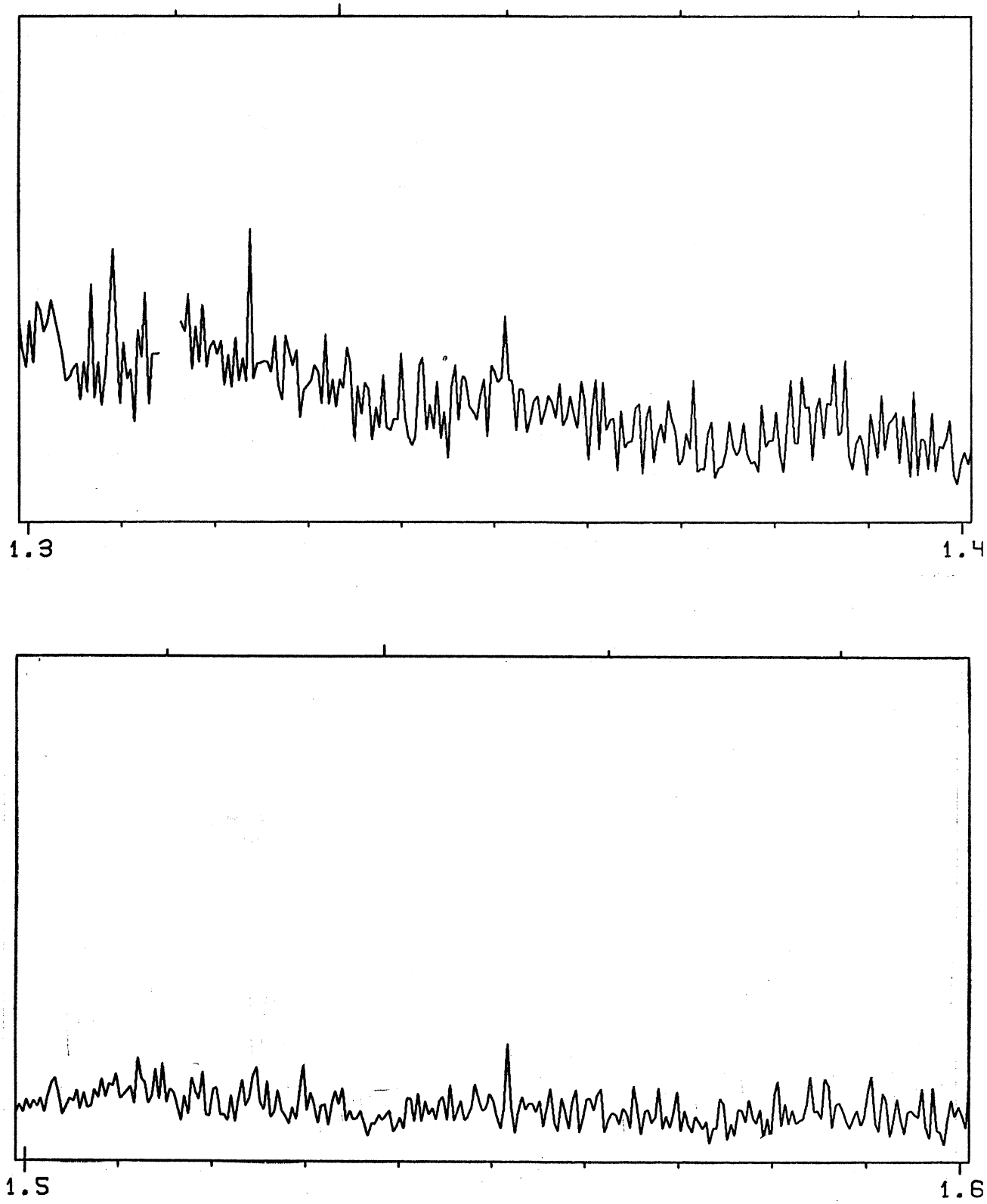

FIG. 13. The Spectrum of W Orionis (C5,3)

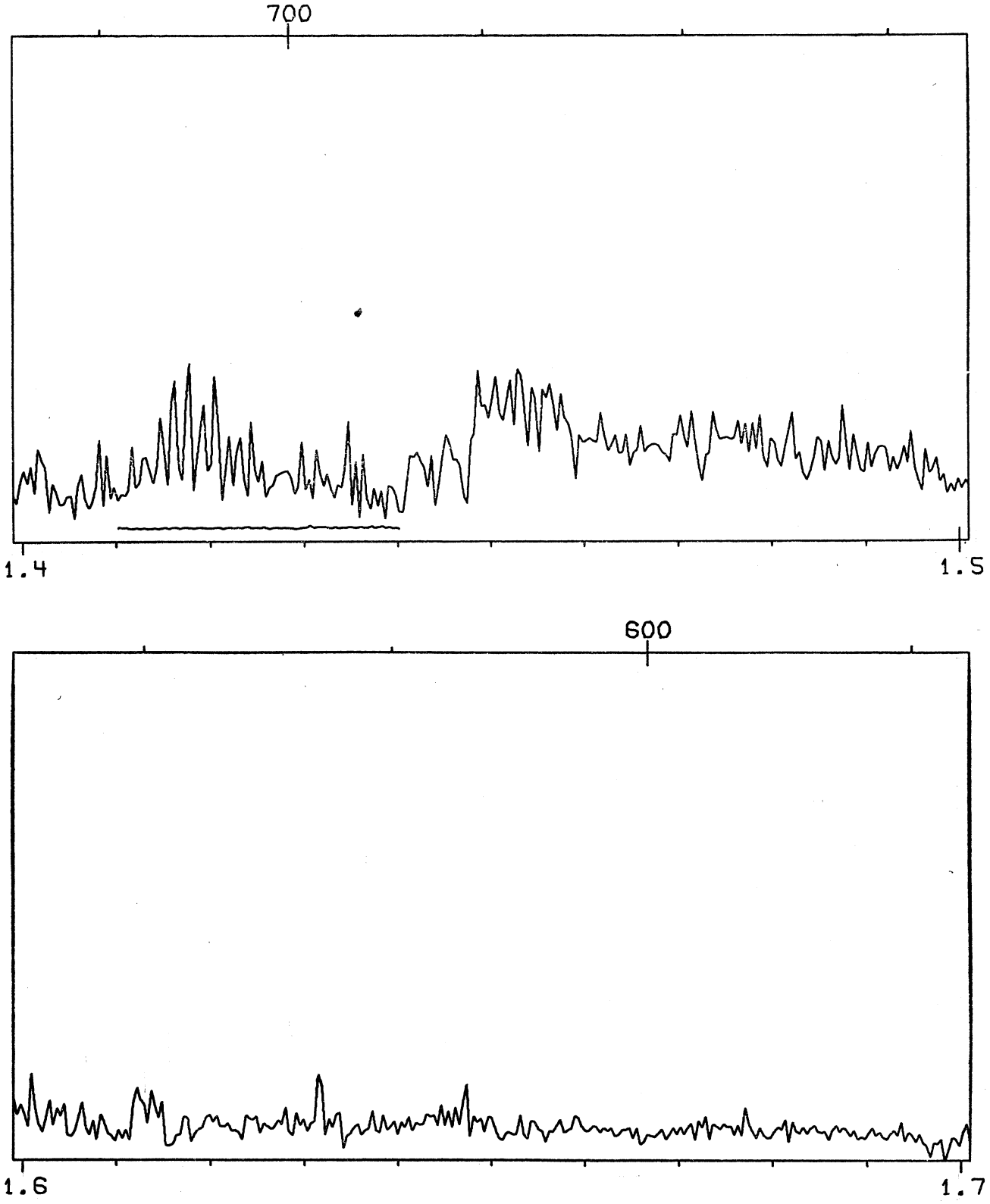

FIG. 13. The Spectrum of W Orionis (C5,3)

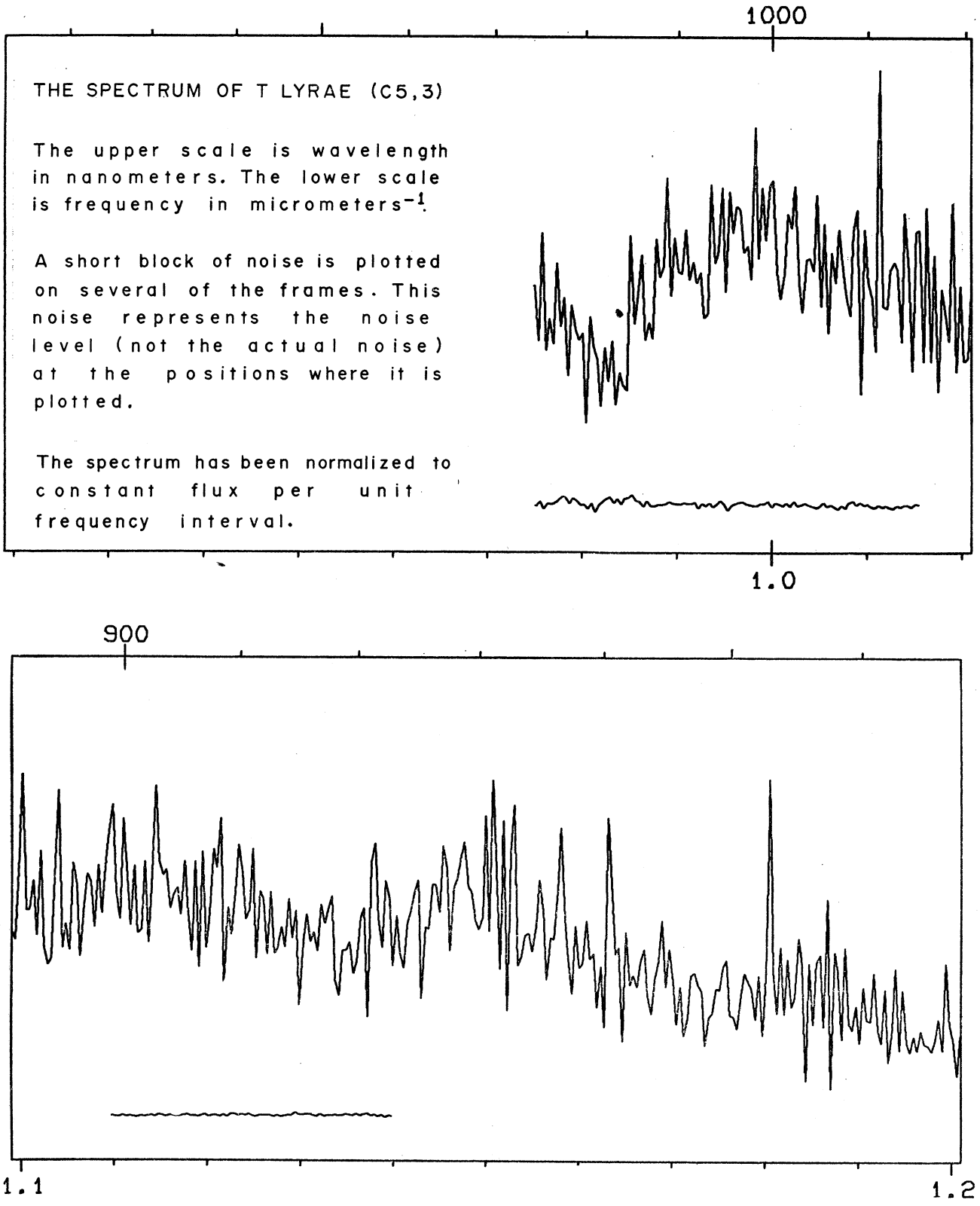

FIG. 14. The Spectrum of T Lyrae (C5,3)

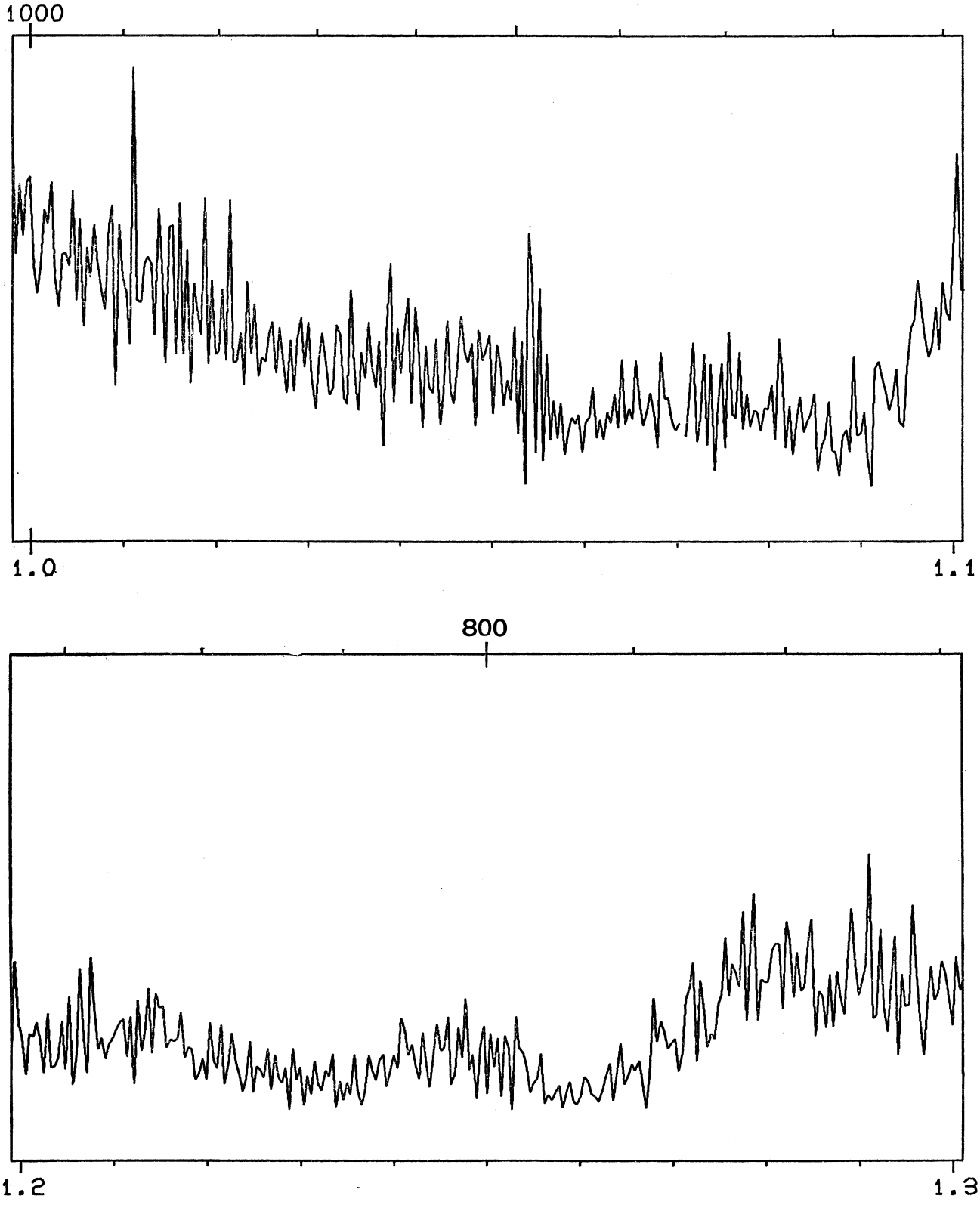

FIG. 14. The Spectrum of T Lyrae (C5,3)

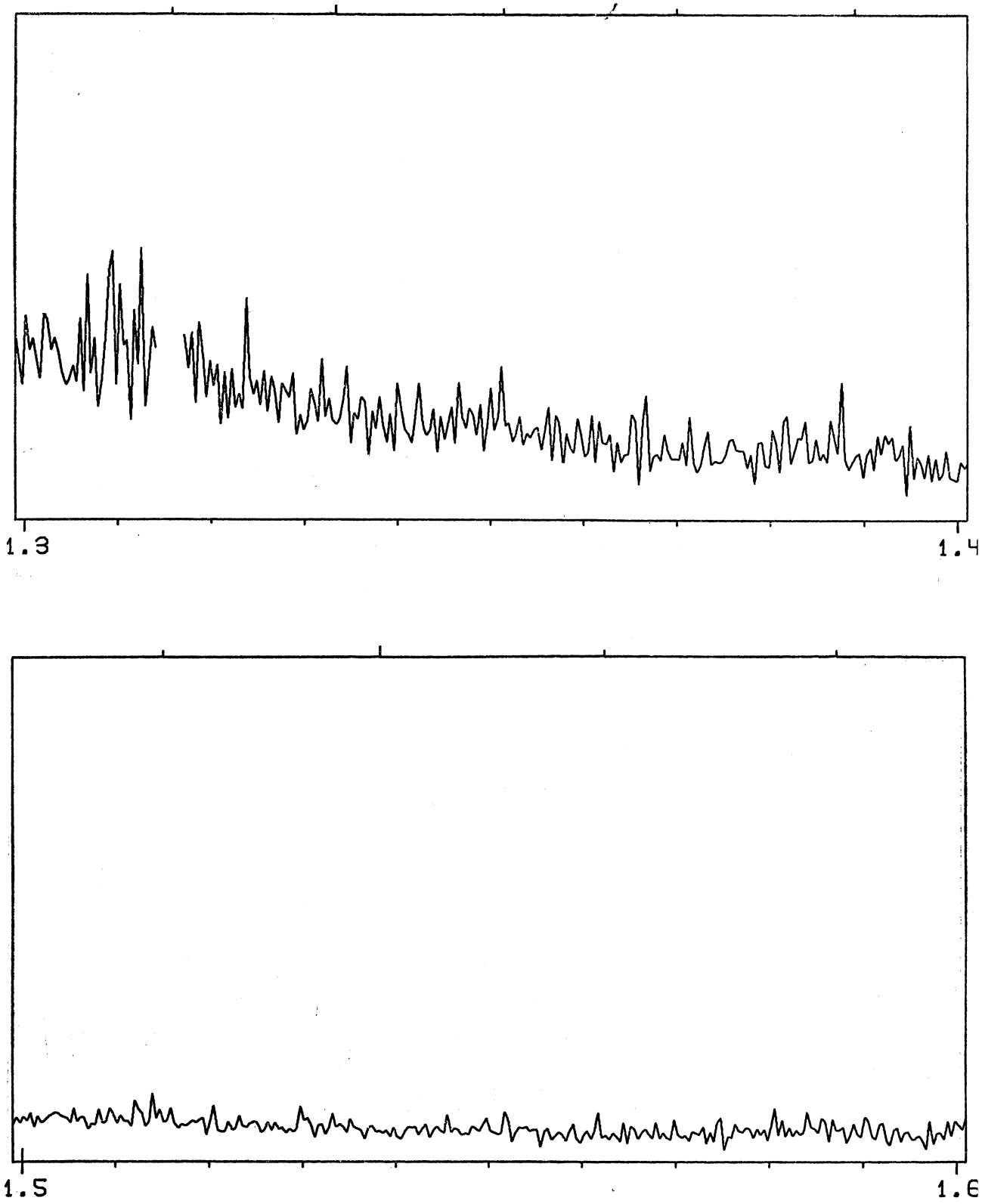

FIG. 14. The Spectrum of T Lyrae (C5,3)

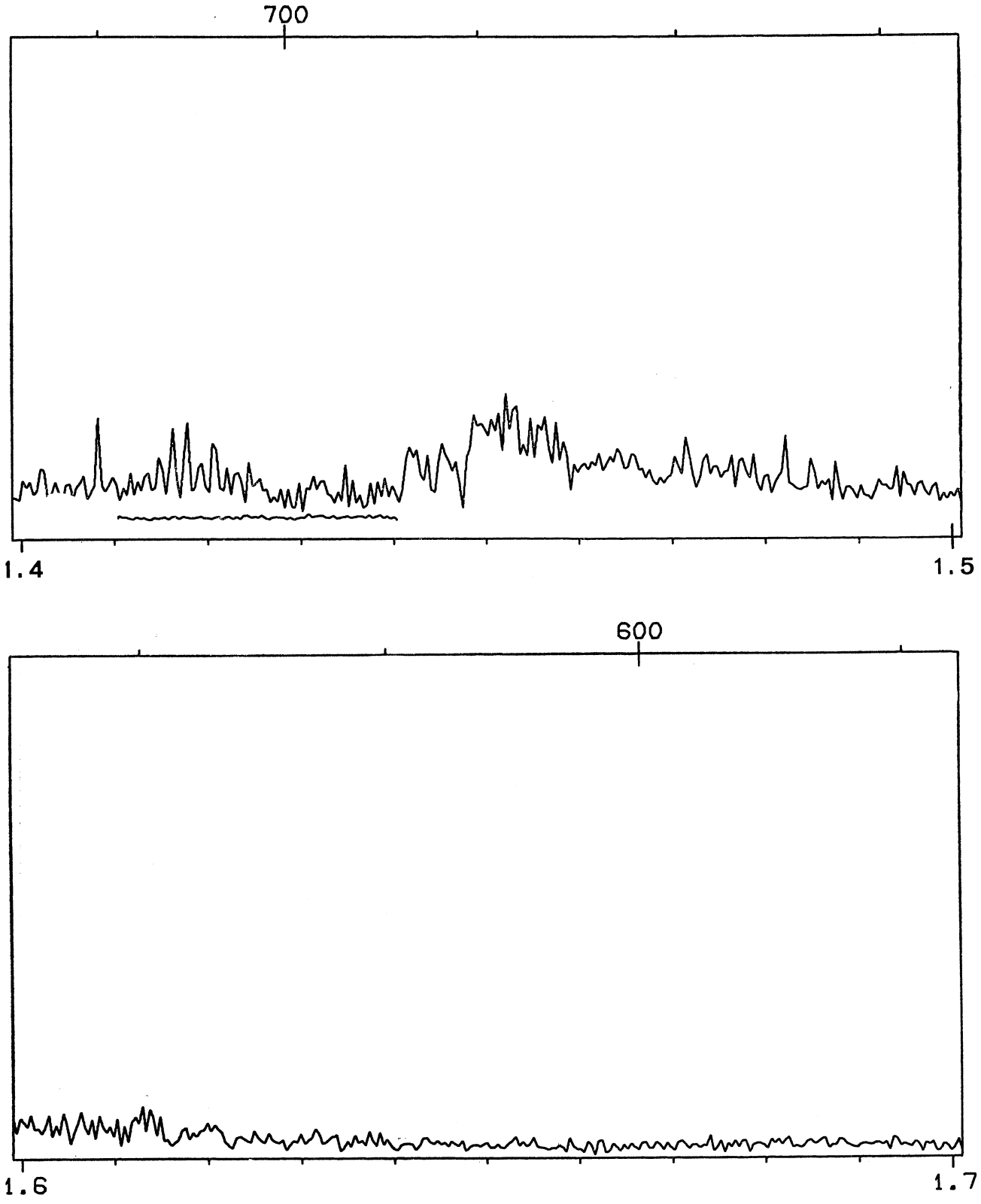

FIG. 14. The Spectrum of T Lyrae (C5,3)

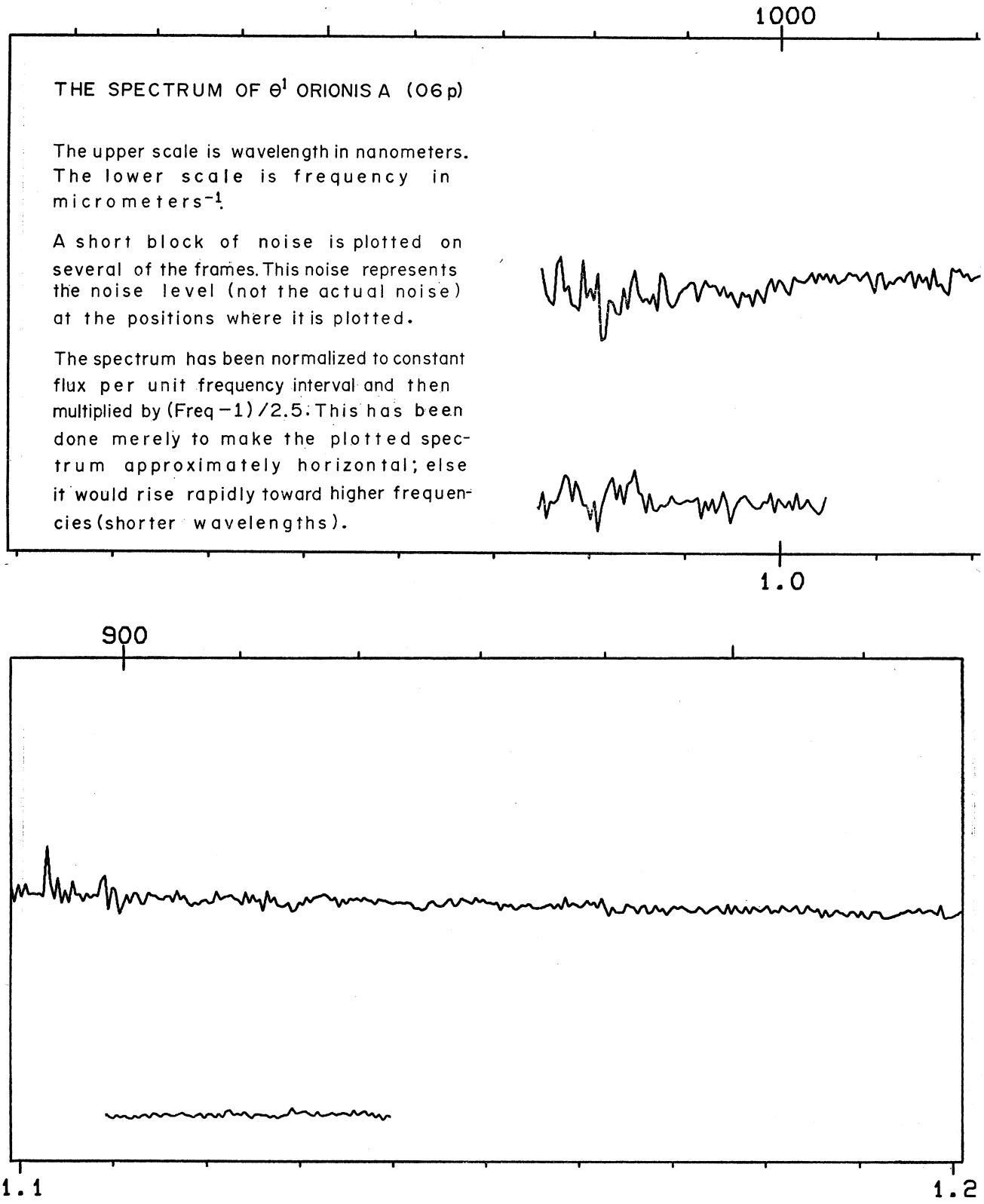

FIG. 15. The Spectrum of θ^1 Orionis A (O6 p)

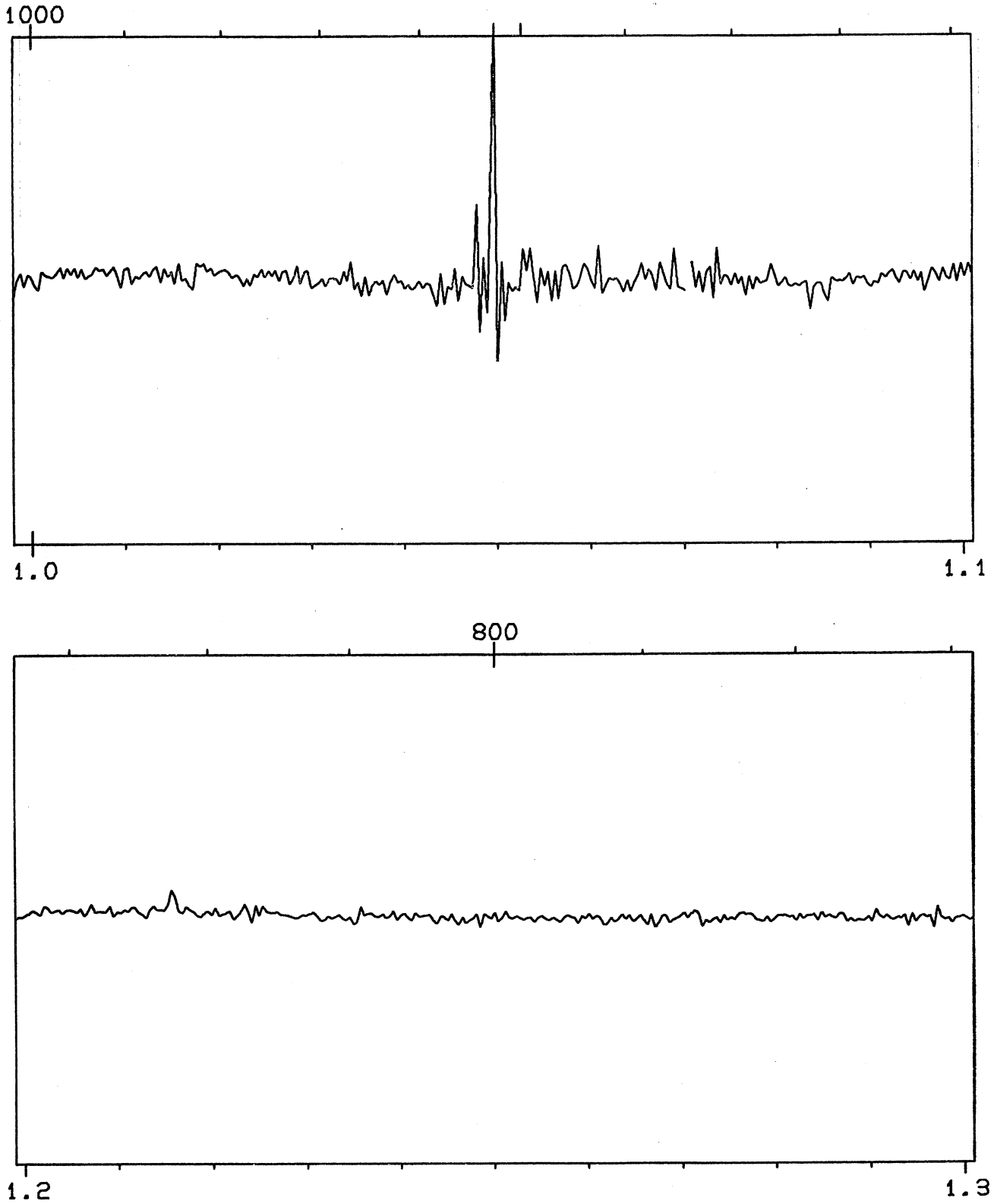

FIG. 15. The Spectrum of θ^1 Orionis A (O6 p)

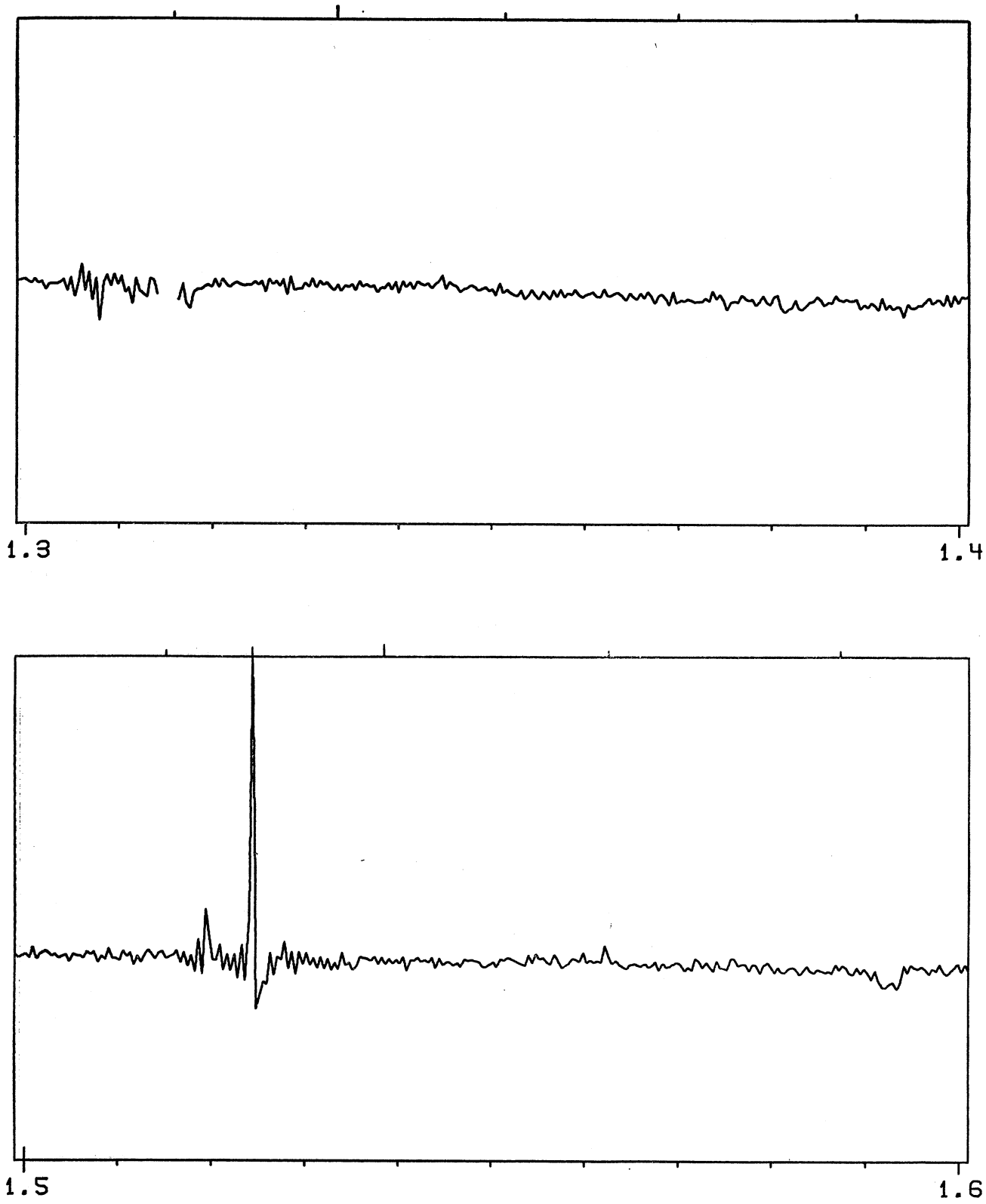

FIG. 15. The Spectrum of θ^1 Orionis A (O6 p)

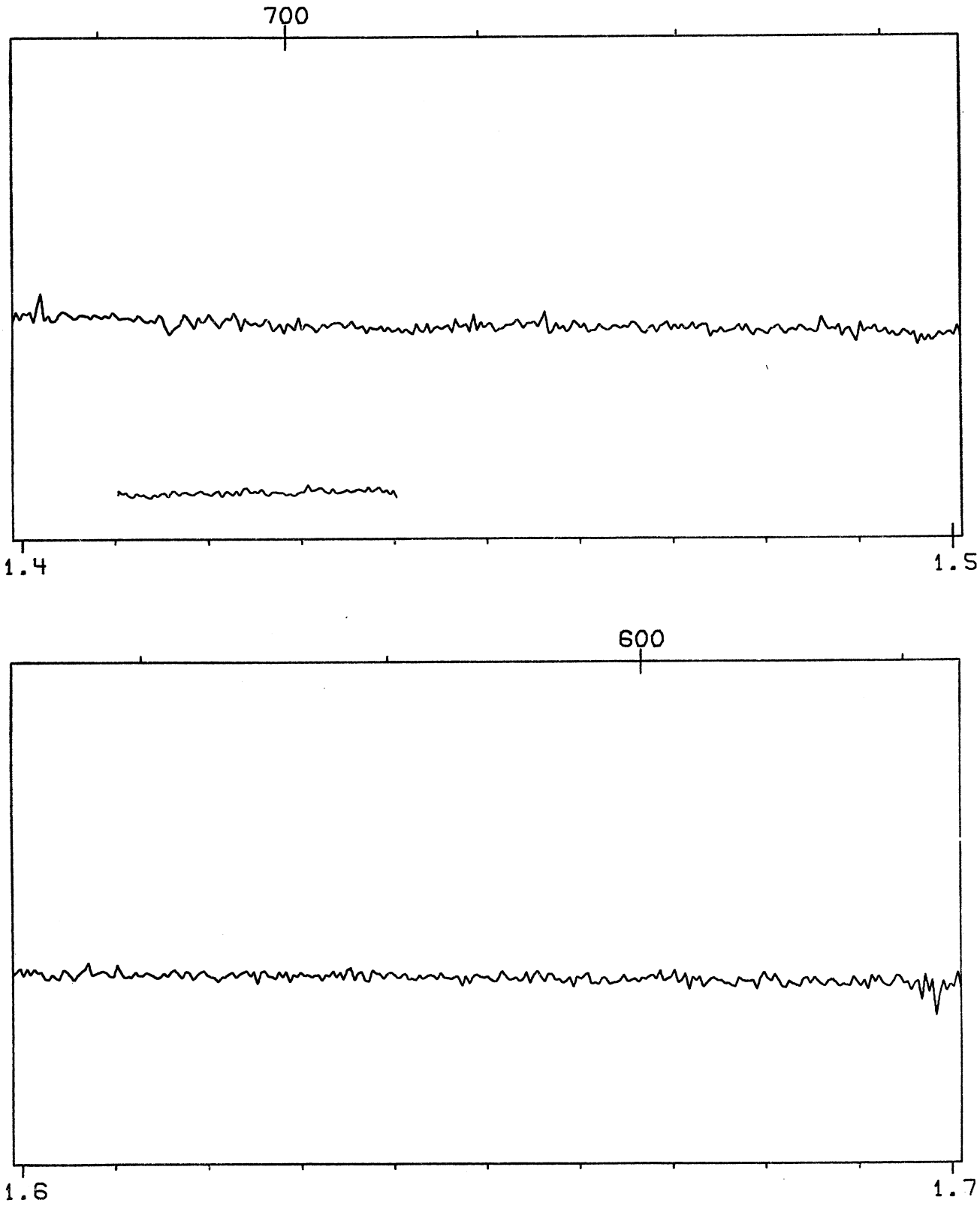

FIG. 15. The Spectrum of θ^1 Orionis A (O6 p)

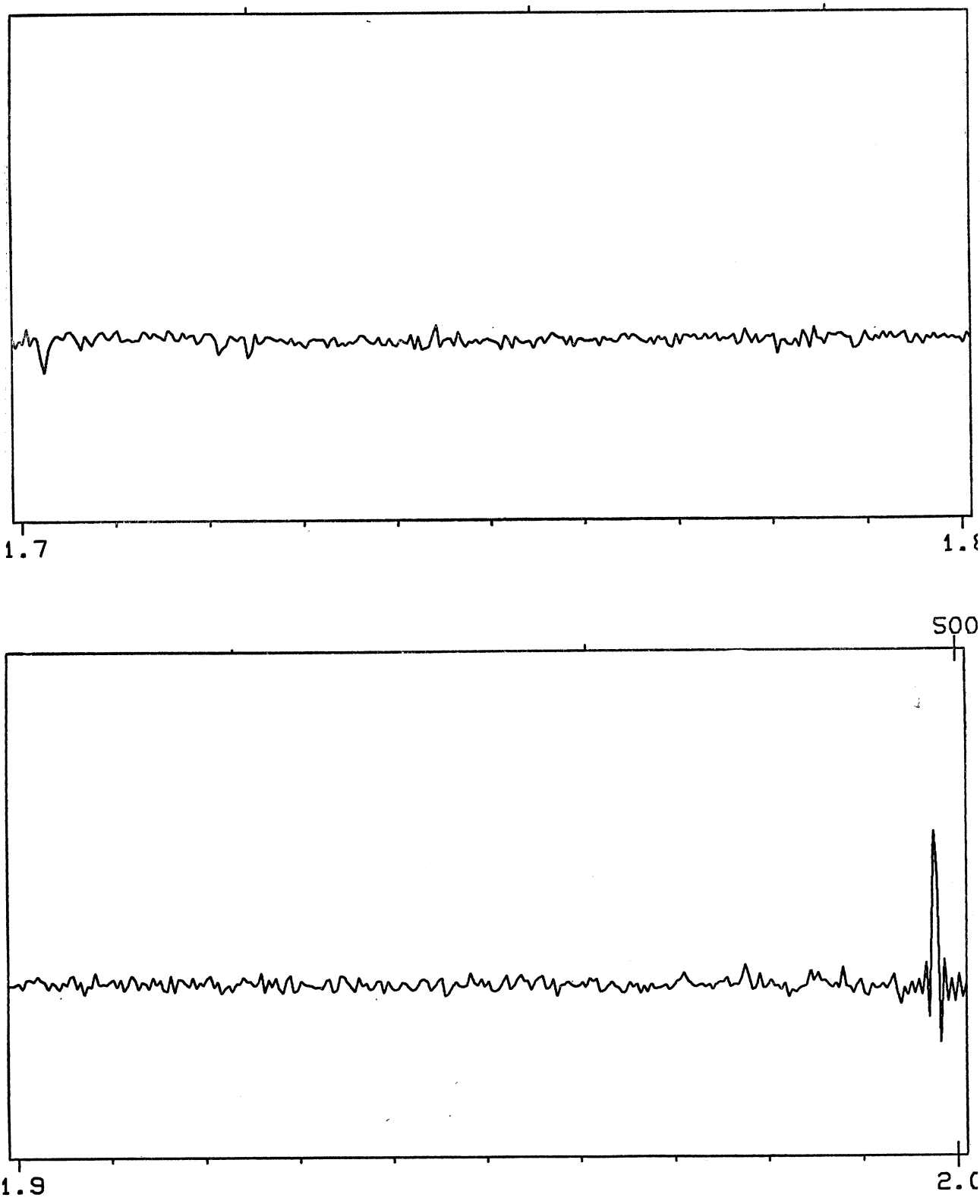

FIG. 15. The Spectrum of θ^1 Orionis A (O6 p)

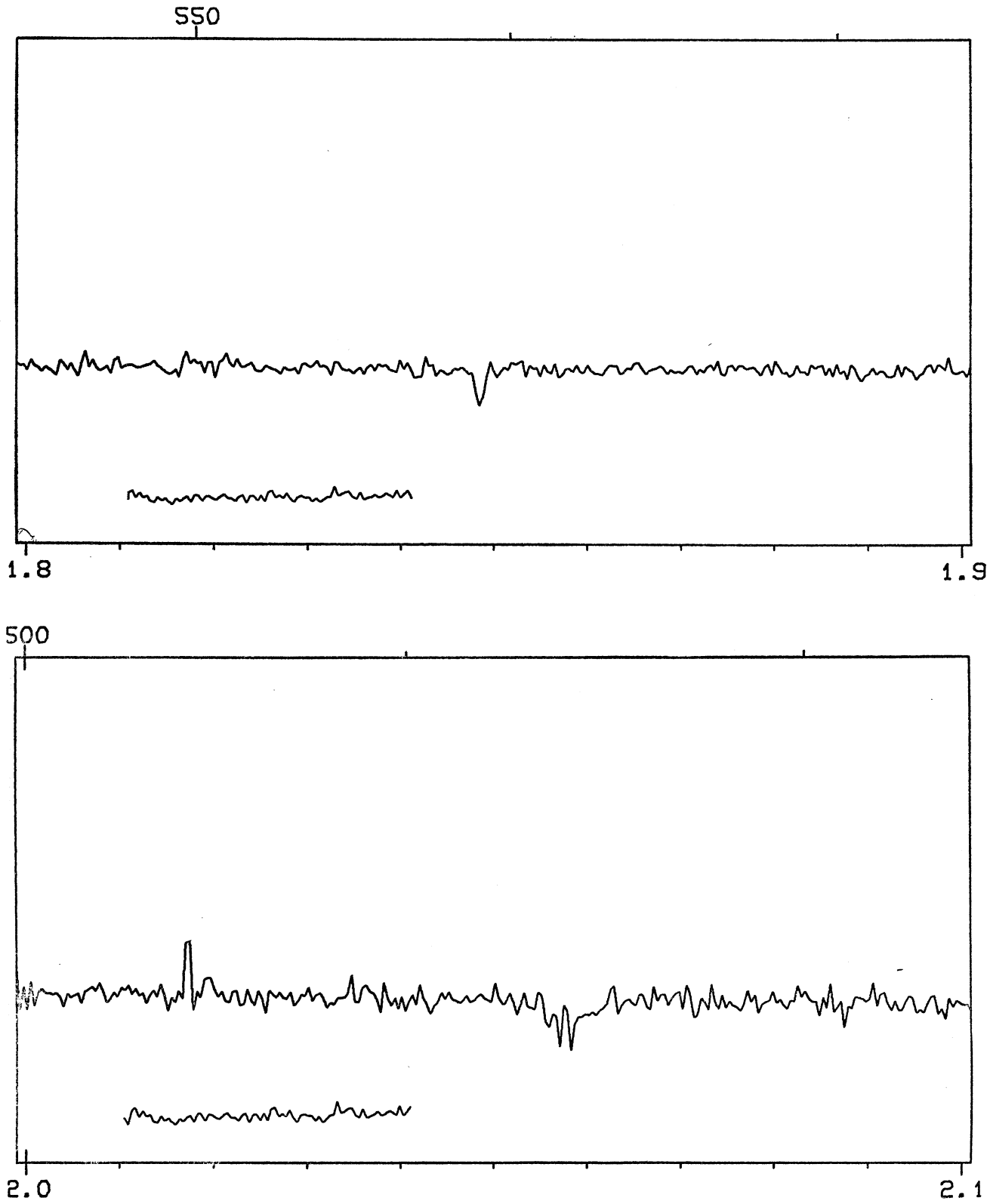

FIG. 15. The Spectrum of θ^1 Orionis A (O6 p)

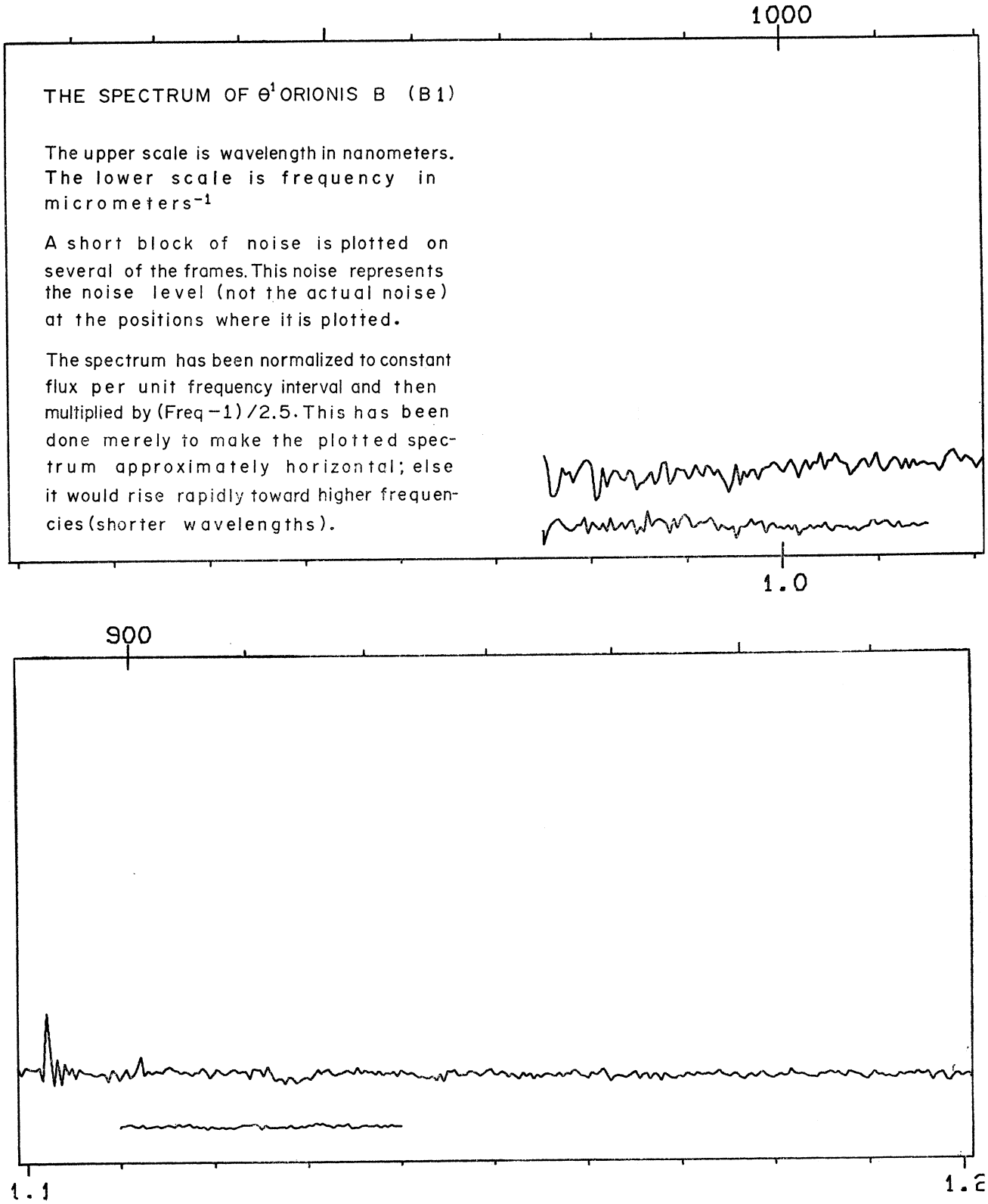

FIG. 16. The Spectrum of θ^1 Orionis B (B1)

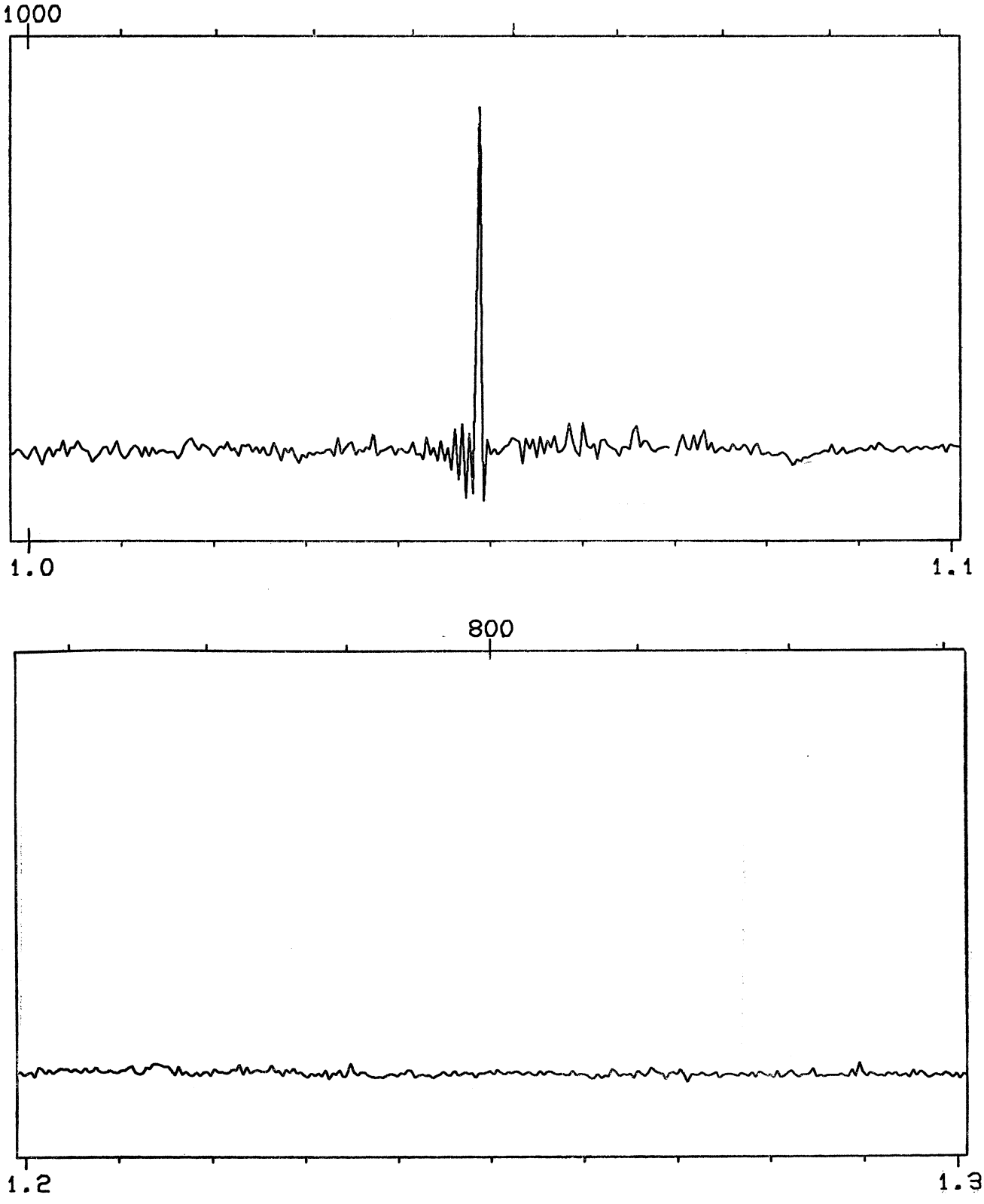

FIG. 16. The Spectrum of θ^1 Orionis B (B1)

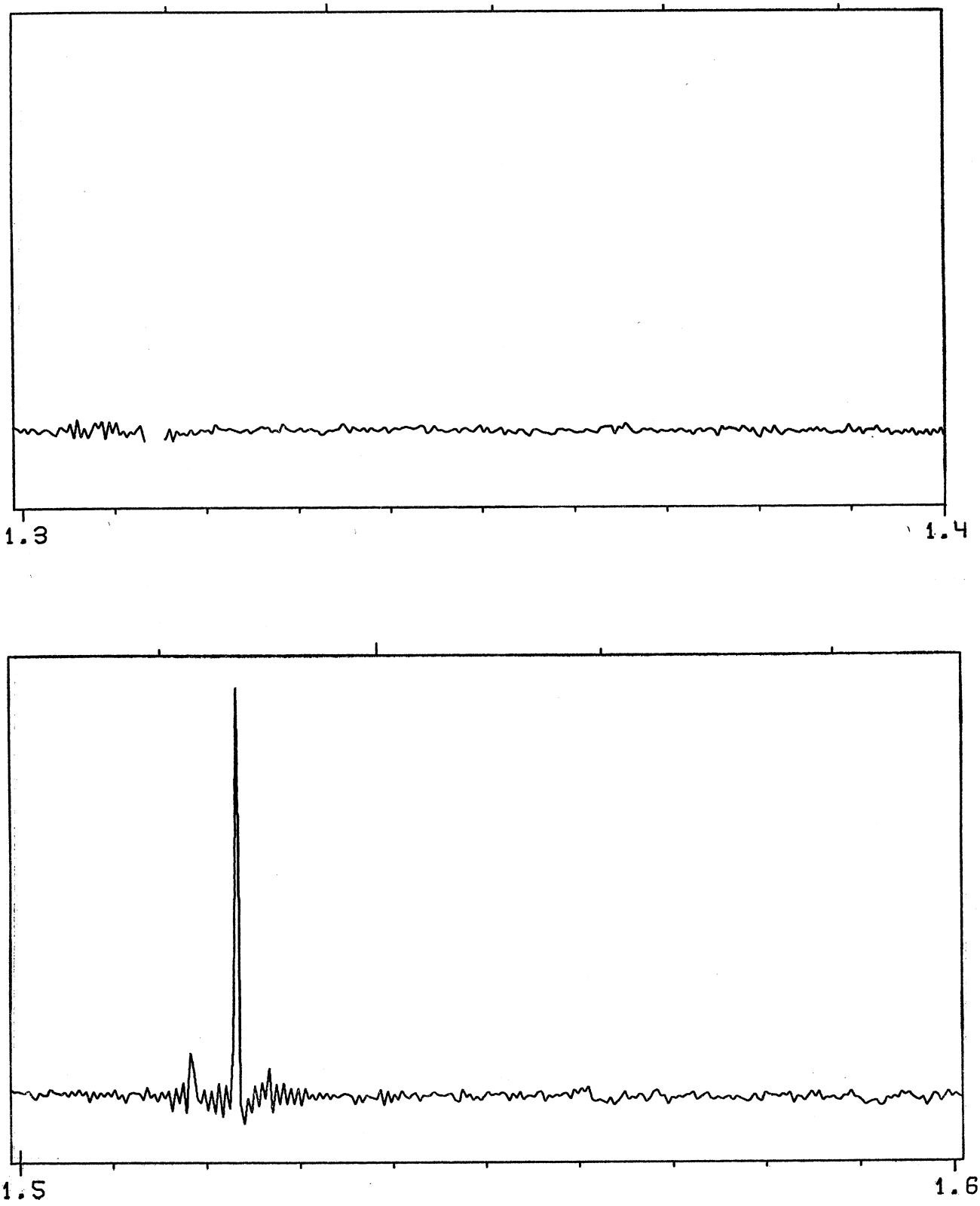

FIG. 16. The Spectrum of θ^1 Orionis B (B1)

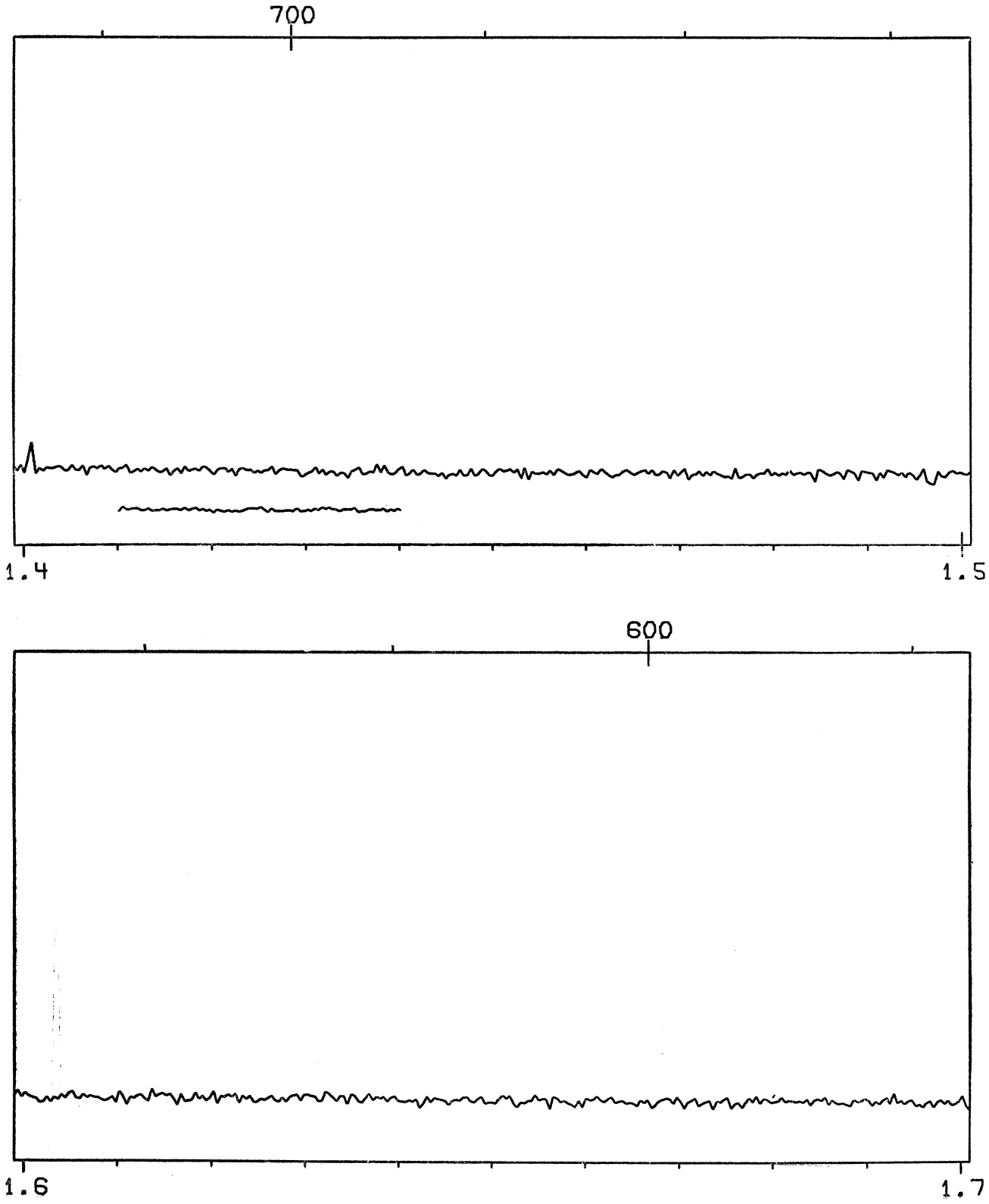

FIG. 16. The Spectrum of θ^1 Orionis B (B1)

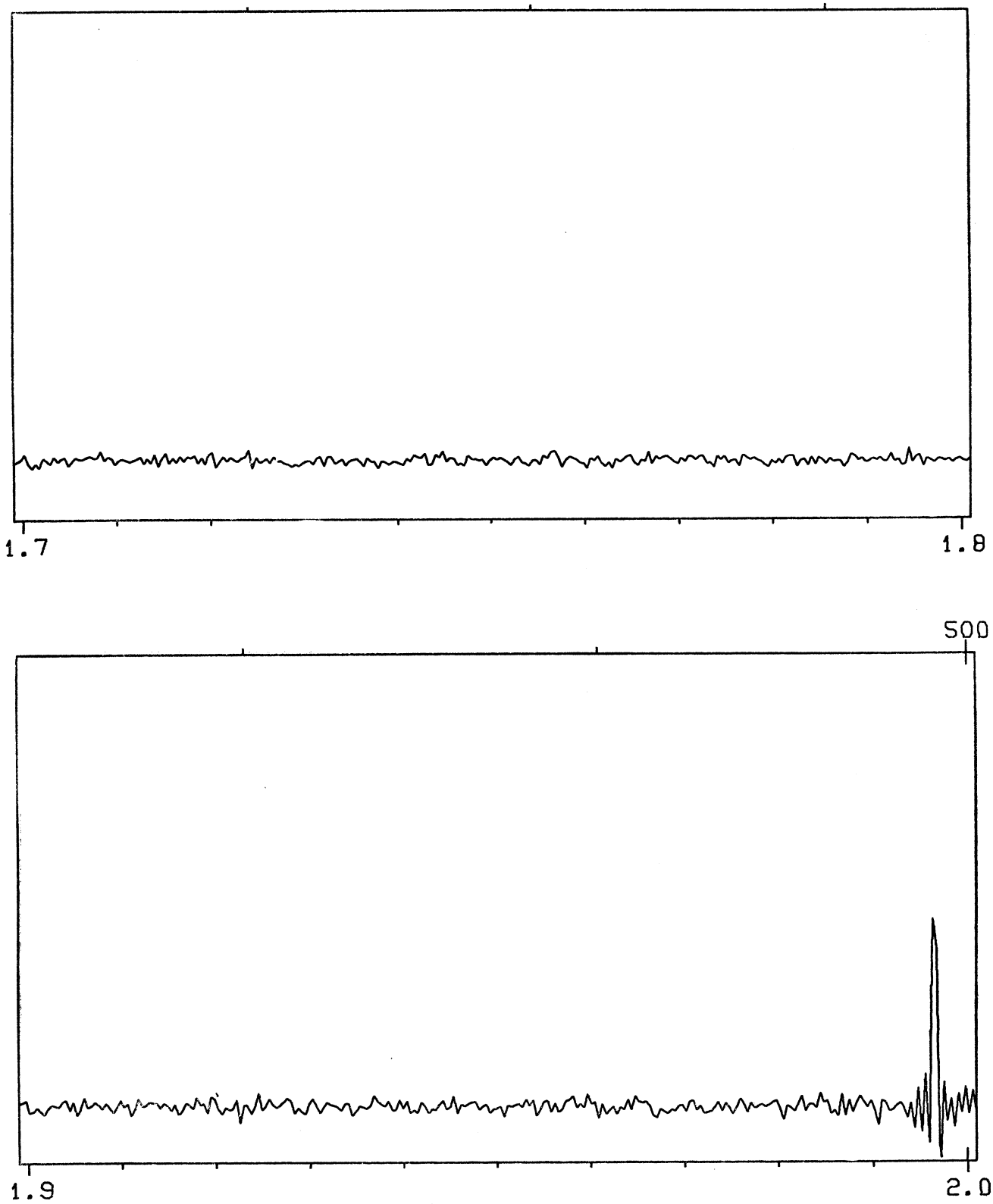

FIG. 16. The Spectrum of θ^1 Orionis B (B1)

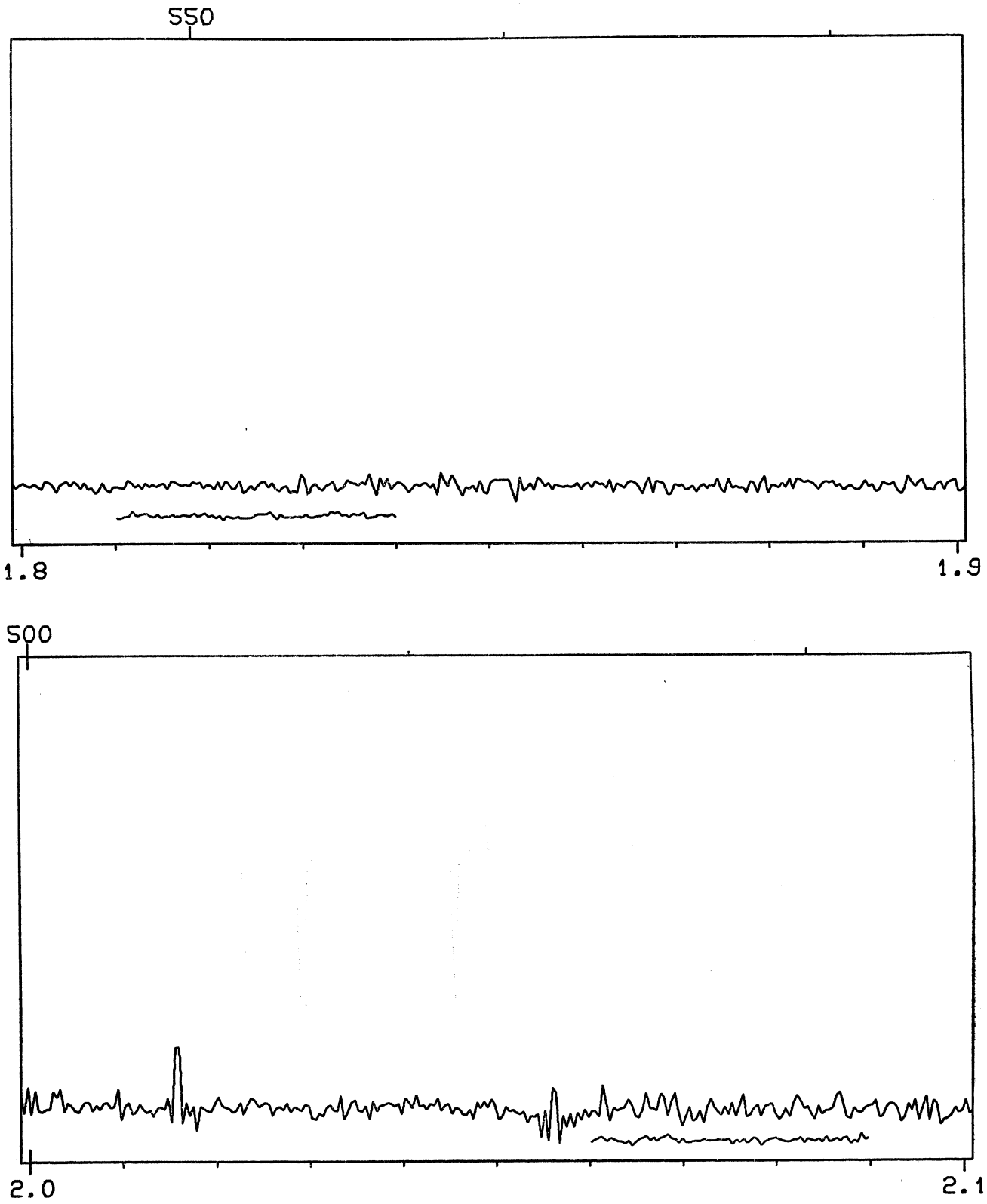

FIG. 16. The Spectrum of θ^1 Orionis B (B1)

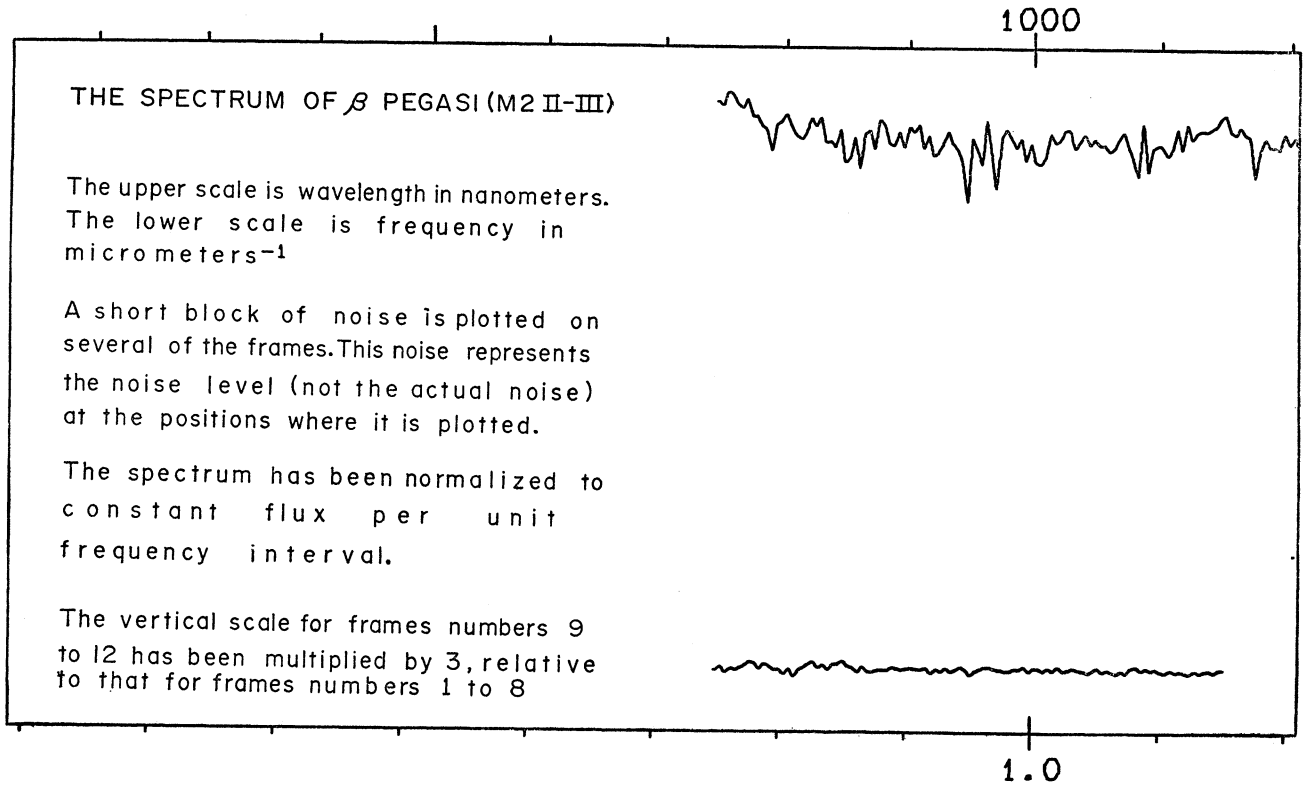

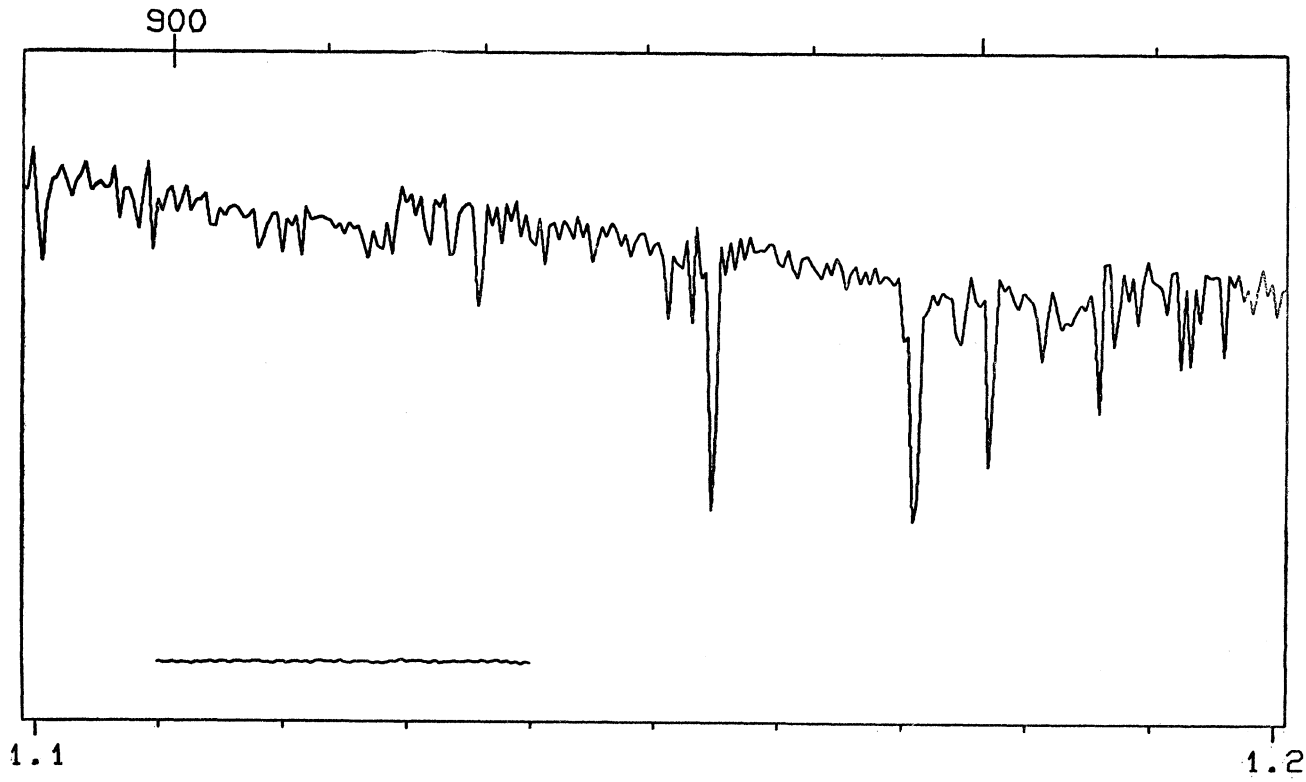

FIG. 17. The Spectrum of β Pegasi (M2 II-III)

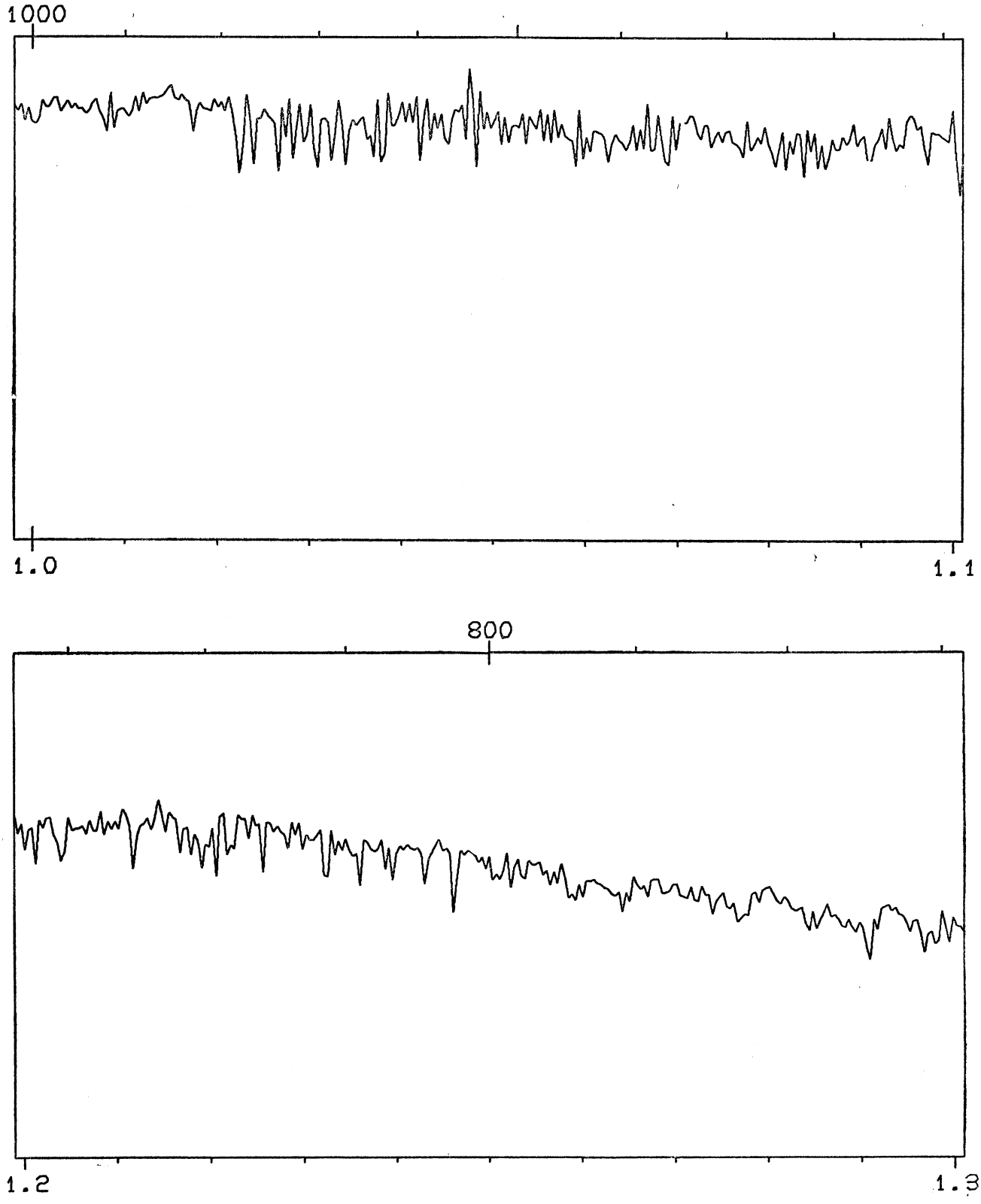

FIG. 17. The Spectrum of β Pegasi (M2 II-III)

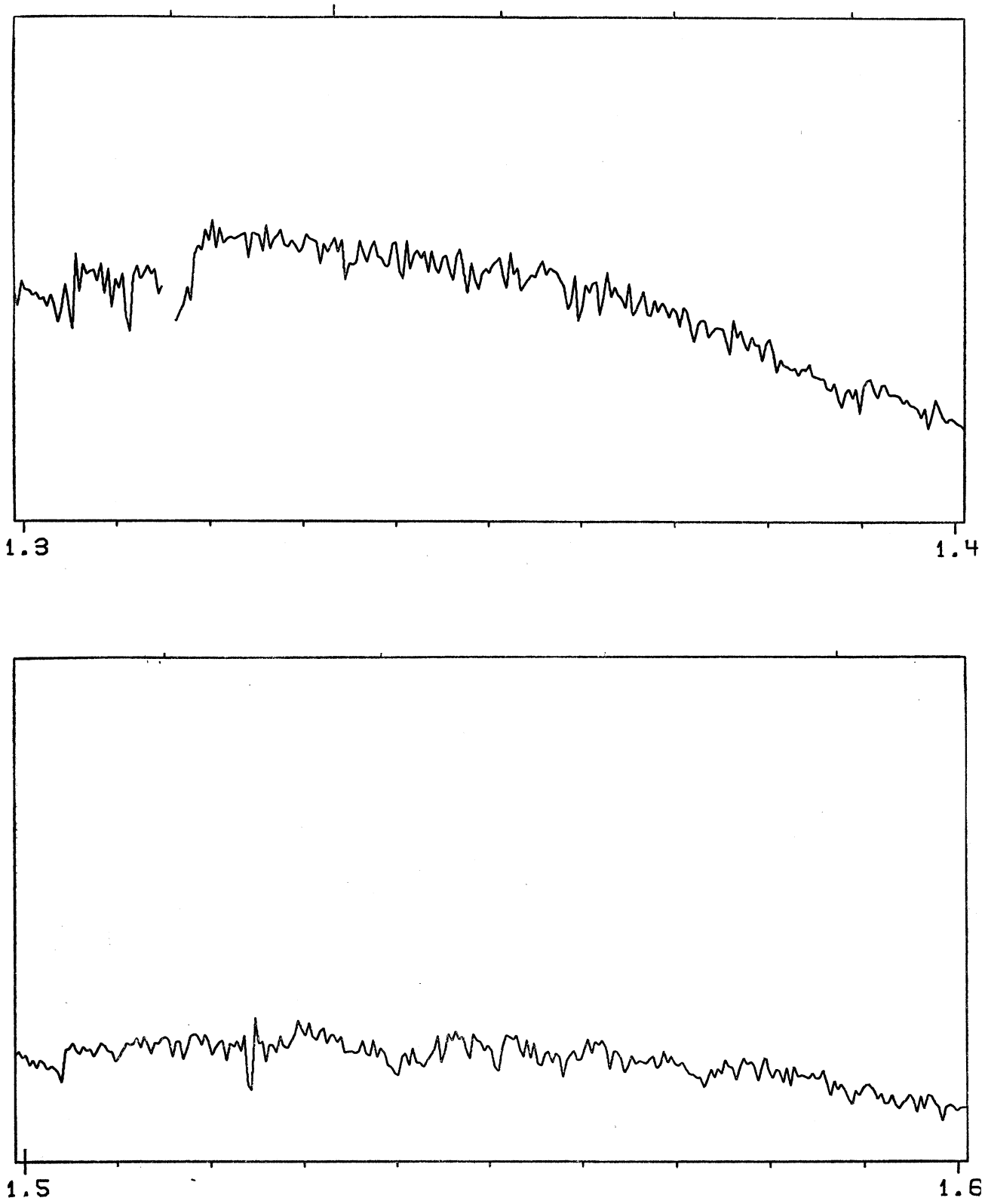

FIG. 17. The Spectrum of β Pegasi (M2 II-III)

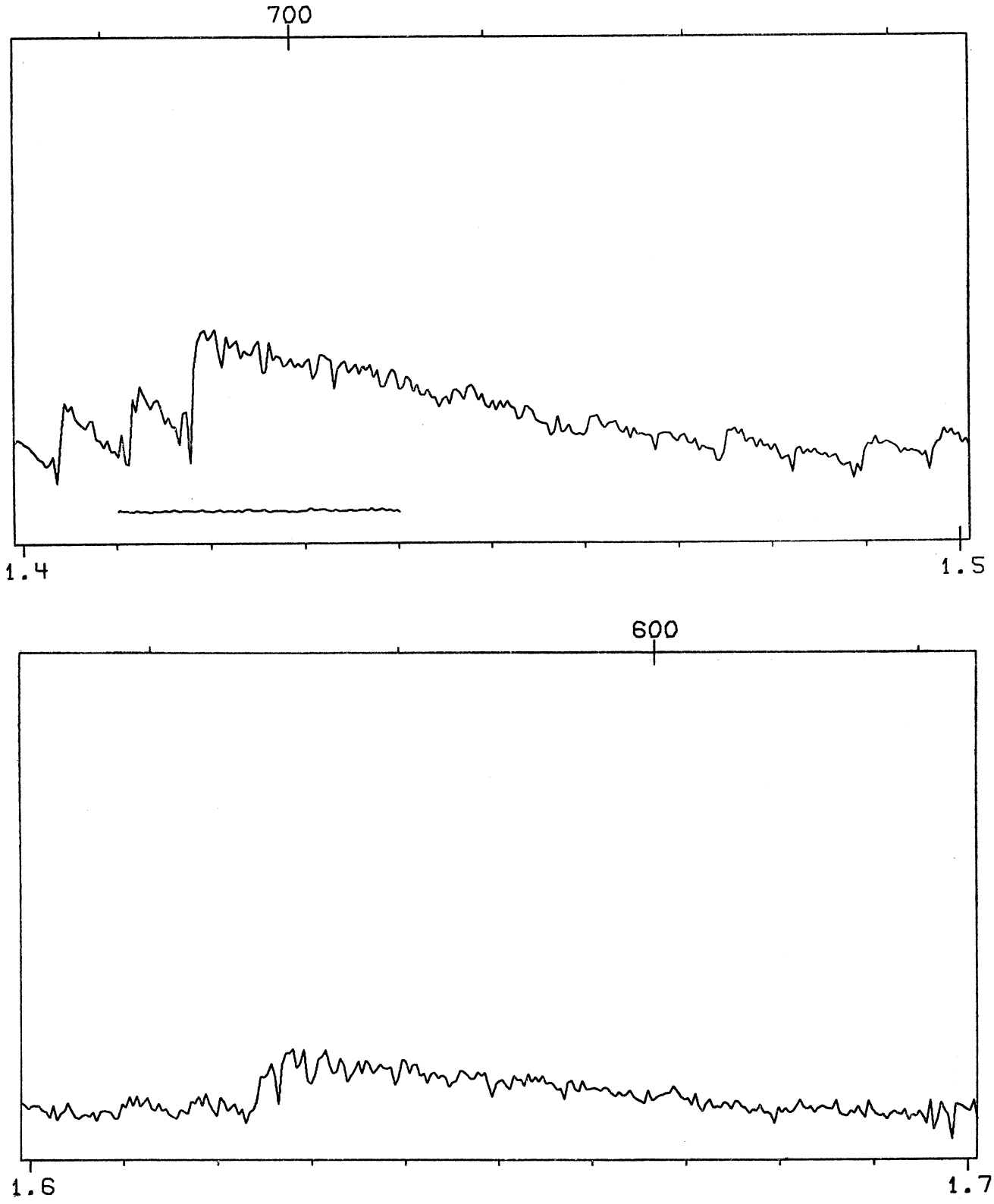

FIG. 17. The Spectrum of β Pegasi (M2 II-III)

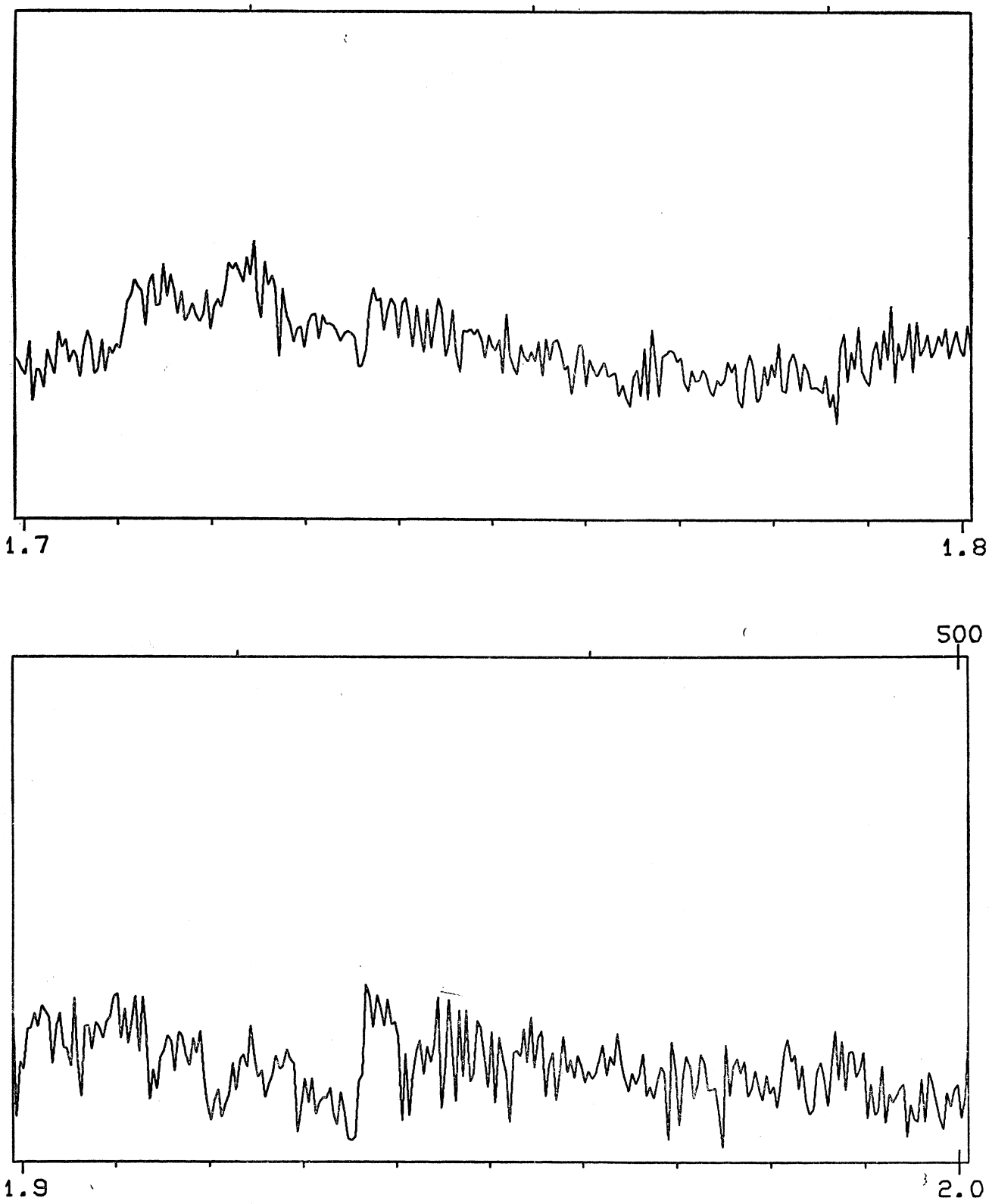

FIG. 17. The Spectrum of β Pegasi (M2 II-III)

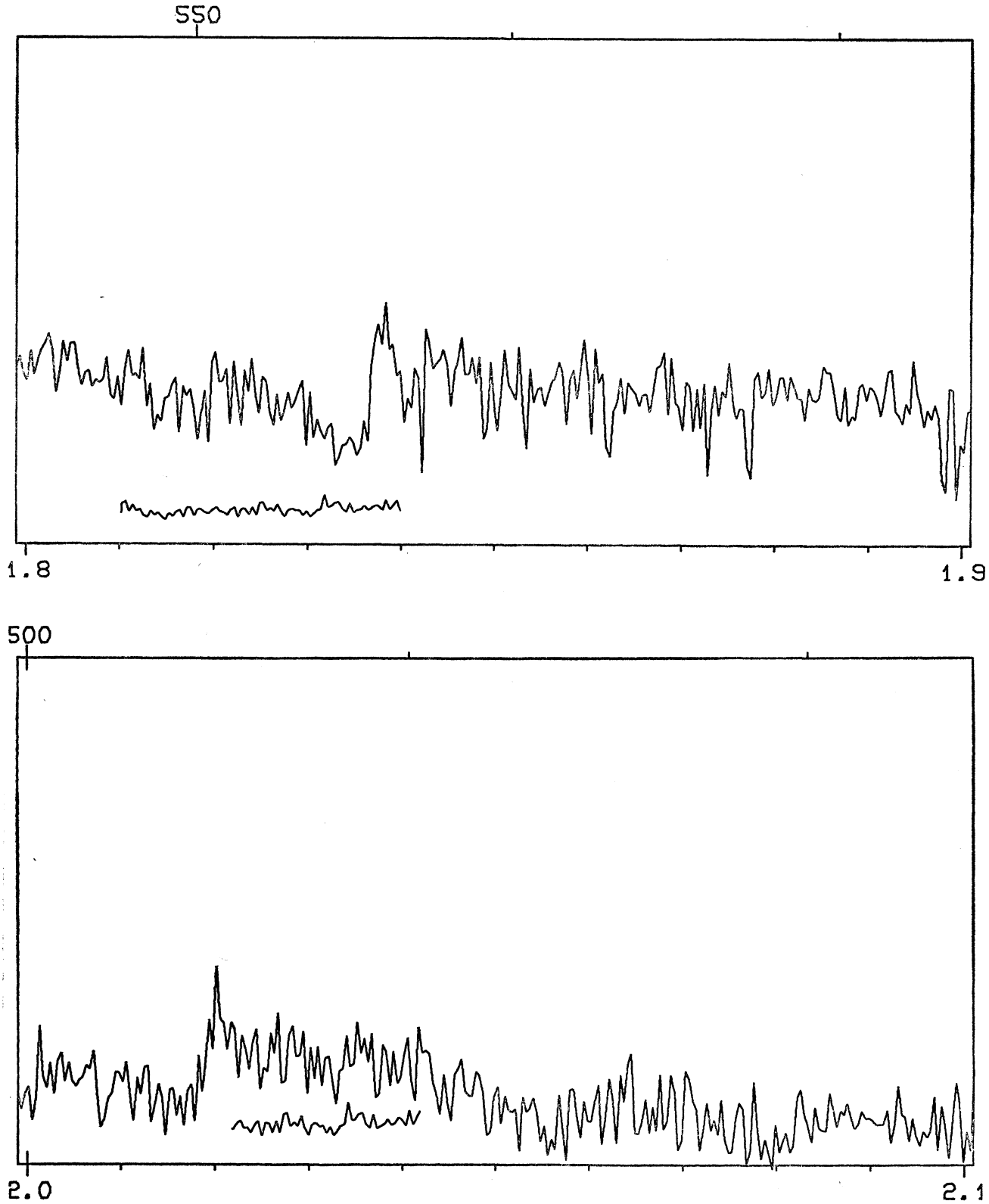

FIG. 17. The Spectrum of β Pegasi (M2 II-III)

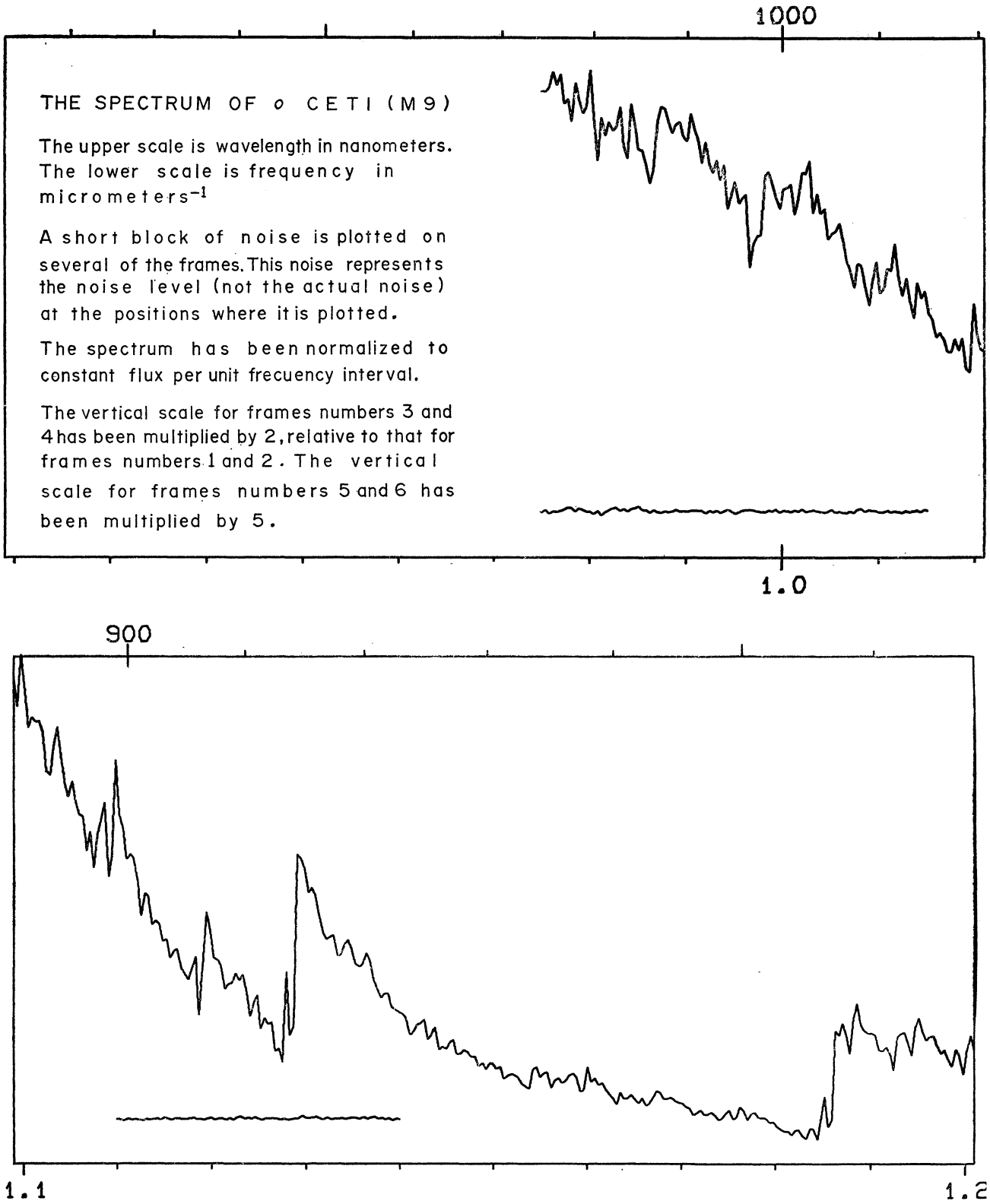

FIG. 18. The Spectrum of o Ceti (M9)

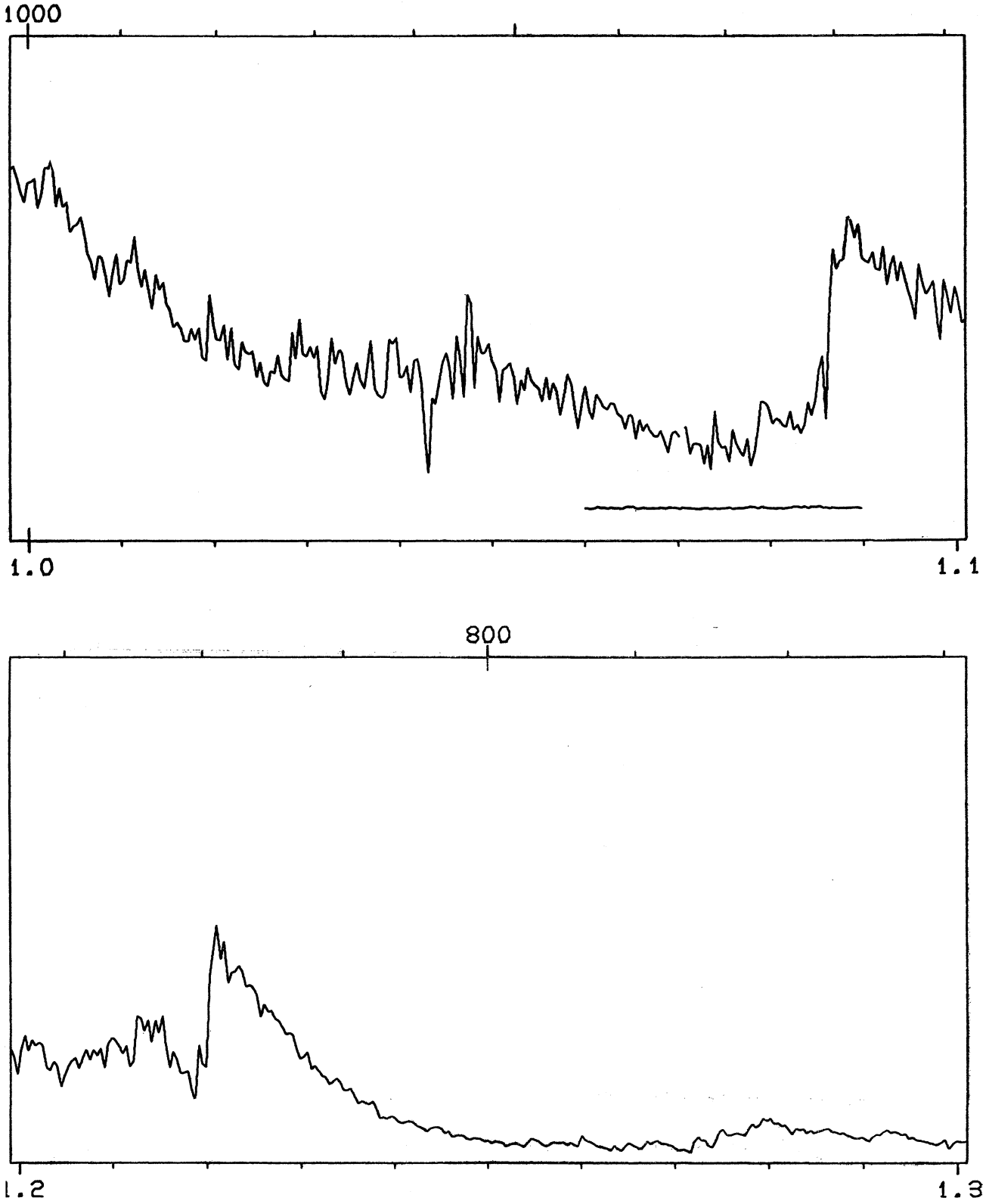

FIG. 18. The Spectrum of o Ceti (M9)

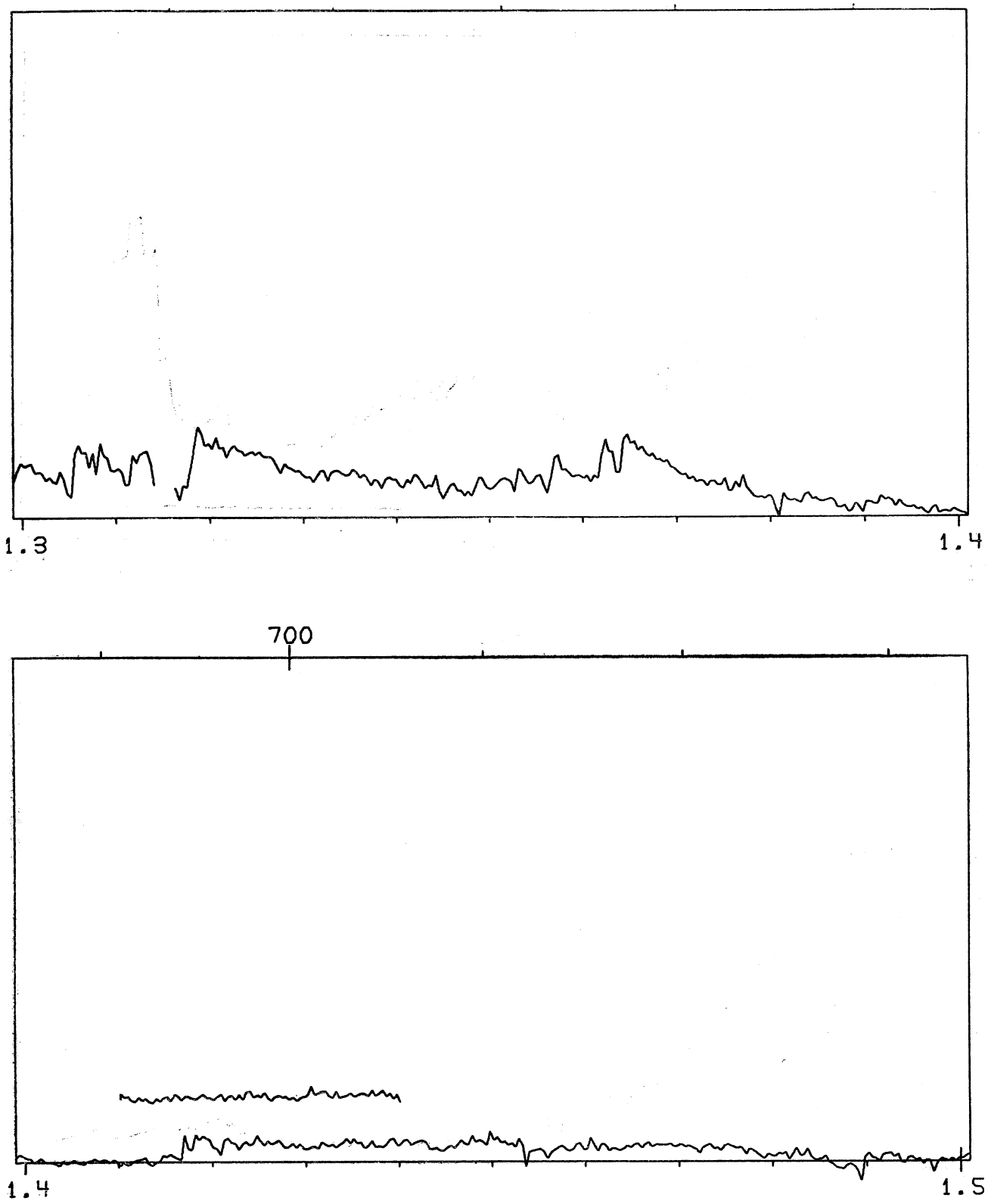

FIG. 18. The Spectrum of o Ceti (M9)